University of Ghana http://ugspace.ug.edu.gh

Dependence of Some Transmission Factors on Field Size and Treatment Depth in External Beam Radiation Therapy (EBRT) Using the Theratron Equinox 100 Cobalt 60 Machine

This thesis is submitted to the:

DEPARTMENT OF MEDICAL PHYSICS

SCHOOL OF NUCLEAR AND ALLIED SCIENCES

UNIVERSITY OF GHANA, LEGON

BY

PHILIP ODONKOR

10443046

BSc. (UCC), 2012

In partial fulfillment of the requirement for the award of:

MASTER OF PHILOSOPHY

IN

MEDICAL PHYSICS

JULY, 2015

University of Ghana http://ugspace.ug.edu.gh

DECLARATION

This thesis is the result of research work undertaken by Philip Odonkor in the Department of Medical Physics, School of Nuclear and Allied Sciences, University of Ghana, under the supervision of Prof. Cyril Schandorf, Prof. John H. Amuasi and Mr. Samuel N. A. Tagoe.

It is my conviction that, no part of this work has been presented in part or whole to any other university or institution for the award of a diploma, or degree at any level. Duly other works and/or researches done by other researchers cited in this work have been acknowledged under references.

……	……
PHILIP ODONKOR	PROF. CYRIL SCHANDORF
(STUDENT)	(PRINCIPAL SUPERVISOR)
Date……	Date……
……	……
PROF. JOHN. H AMUASI	MR. SAMUEL N. A. TAGOE
(CO-SUPERVISOR)	(CO-SUPERVISOR)
Date……	Date……..……

University of Ghana http://ugspace.ug.edu.gh

DEDICATION

This work is dedicated to my parents Mr. and Mrs. Odonkor, my siblings and to all my loved ones.

University of Ghana http://ugspace.ug.edu.gh

ACKNOWLEDGMENTS

My first and foremost thanks and appreciation goes to God Almighty for protecting and guiding me, giving me the sound health, wisdom, knowledge and providing me with all that I needed throughout this research work. May His sovereign name be praised now and forever more.

With all maximum respect and a standing ovation, I sincerely salute my able and indefatigable supervisors, Prof. Cyril Schandorf, Prof. John H. Amuasi and Mr. Samuel N. A. Tagoe for working tirelessly day and night, painstakingly going through my write up and guiding me through my data collection. Actually, their constructive criticism, corrections, encouragement and pieces of advice they bestowed on me have contributed immensely in coming up to this far. Over the hill, posterity shall record their names in golden capital letters.

My special thanks also goes to my Head of Department Prof. Augustine W. K. Kyere and Mr. Patrick K. Mensah-Amoah, Physics Lecturer, UCC for their continues encouragement and motivation. Also my heart felt gratitude goes to Mr. Evans Sasu (medical physicist) and Mr. Solomon Nartey (radiotherapist) both of Korle Bu Teaching Hospital for their immense assistance during my data collection. Not forgetting Mr. George Felix Acquah of Sweden Ghana Medical Centre who was always there to assist and provide me with any material/equipment I needed for my work.

Finally, my profound gratitude goes to my parents, sisters and colleagues (most especially Ainadine Momade, Jerome Kambuwa and Yaa Akomah Asenso); not forgetting my friends (especially Maruf Abubakar, Baraka Benson, John Gyamfi and Charles Ansre); who encouraged me and lifted up my spirit at a point when I was downhearted and nearly threw my hands up in despair. May God be gracious unto them and lift His light of countenance upon them all and may they be a blessing to this present and future generations.

University of Ghana http://ugspace.ug.edu.gh

TABLE OF CONTENTS

University of Ghana http://ugspace.ug.edu.gh

University of Ghana http://ugspace.ug.edu.gh

University of Ghana http://ugspace.ug.edu.gh

INTEGRI PROCEDAMUS

University of Ghana http://ugspace.ug.edu.gh

LIST OF FIGURES

Page

University of Ghana http://ugspace.ug.edu.gh

University of Ghana http://ugspace.ug.edu.gh

LIST OF TABLES

University of Ghana http://ugspace.ug.edu.gh

ABBREVIATIONS

RT	Radiation therapy/Radiotherapy
EBRT	External Beam Radiation Therapy
Co-60	Cobalt 60
NCRNM	National Center of Radiotherapy and Nuclear Medicine
KBTH	Korle Bu Teaching Hospital
LINACs	Linear Accelerators
TF	Transmission Factor
FS	Field size
d	Treatment depth
SAD	Source to Axis Distance
SSD	Source to Surface Distance
TPD	Tray to Phantom Distance
NTF	Normalized Transmission Factor
FS_{ref}	Reference Field size
FS_{nor}	Normalized Field size
d_{ref}	Reference depth
d_{nor}	Normalized depth
d_{max}	Depth of maximum dose (0.5cm for cobalt)
ISL	Inverse Square Law
MUs	Monitor units
OAR	Off-Axis Ratio
RDD	Relative Depth Dose
PDD	Percentage Depth Dose

University of Ghana http://ugspace.ug.edu.gh

ABSTRACT

The use of beam modifiers in today's radiotherapy is very important as it attenuates the beam and reduces the dose to the patient; therefore the need to know the amount of attenuation (in terms of a transmission factor) they provide during treatment. The purpose of this research work is to evaluate the variation (or dependence) of the transmission factors (TFs) of block tray and physical wedges (of different angles) as a function of treatment depth and field size using both iso-centric setups, SAD and SSD; and thus compare the results from the two setup techniques. Wedge and tray TF measurements were performed in a full scatter, large water phantom using a 0.04cc ionization chamber and an average photon energy of 1.25MV from a cobalt-60 unit at an SAD/SSD of 100cm at various depths and field sizes with gantry and collimator angles fixed at 0^{o}. From the measurements carried out, the wedge TF of the 15^{o}, 30^{o}, 45^{o}, and 60^{o} wedges were found to be 0.775±0.005, 0.650±0.010, 0.505±0.015, and 0.280±0.015 respectively; and the tray TF was found to be 0.960±0.003. Also, the results obtained showed that both the wedge TF and the tray TF has a strong linear dependence on treatment depth; however, the variation of the 15^{o} wedge TF and the tray TF with depth is less significant (less than 2%). Maximum percentage variation for the 15^{o} wedge for the SAD setup was 1.1% and 1.59% for the SSD setup; and that for the tray was 0.60% for the SAD setup and 0.12% for the SSD setup. Also, the variation of the 15^{o}, 30^{o} and 45^{o} wedge TF with field size was less significant (less than 2%); and a weaker dependence was observed with field size as compared to the treatment depth. However, the 60^{o} wedge showed a significant variation (maximum of 2.22% and 2.88% for the

University of Ghana http://ugspace.ug.edu.gh

SAD and SSD setups respectively) as an increase in field size was accompanied by an increase in its wedge TF. Also though the tray TF graphically showed a strong linear dependence on field size the percentage variation was far less significant (maximum of 0.29% for the SAD setup and 0.18% for the SSD setup). It can therefore be concluded from this study that the wedge TF depends strongly on treatment depth and must be taken into account during treatment planning and/or manual dose calculations, whilst a single tray TF can be used for any field size and at any treatment depth.

University of Ghana http://ugspace.ug.edu.gh

CHAPTER ONE

INTRODUCTION

1.1 BACKGROUND

Radiation therapy (RT) is a treatment modality that is employed in managing approximately 50% of cancer patients worldwide. It involves the use of high energy photon beams and it requires careful consideration as it produces inhomogeneous doses in the surface region which in turn causes damage to the skin and normal tissue that is attributed to skin-sparing effect [1, 2]. The use of physical wedge filters absorbs low-energy scattered photons and thus produces lower surface doses and higher skin-sparing effects, thus decreasing skin damage [3, 4]. Apart from advances in the so-called physical treatment planning, which refers to techniques used for improving radiation dosimetry and dose distribution, it is now widely recognized that further improvements in radiotherapy treatment will most probably require increasing grounding in fundamental radiobiological mechanisms [5].

Radiotherapy procedures fall into two main categories: external beam radiation therapy (EBRT also known as teletherapy) and brachytherapy. In EBRT, the radiation source is at a certain distance from the patient and the target within the patient is irradiated with an external radiation beam. In brachytherapy radiation sources are placed directly into the target volume (intracavitary or interstitial brachytherapy) or on to a target (surface mould or intraoperative radiotherapy). Most EBRT is carried out with photon beams, some with electron beams and a very small fraction with more exotic particles such as protons, heavier ions or neutrons [6]. It is usually carried out with more than one radiation beam in order to achieve a uniform dose distribution inside the target volume and an as low as

University of Ghana http://ugspace.ug.edu.gh

possible a dose in healthy tissues surrounding the target. ICRU Report No. 50 [7] recommends a target dose uniformity within +7% and –5% of the dose delivered to a well-defined prescription point within the target. Modern EBRT is carried out with a variety of beam energies and field sizes under one of two set-up conventions: a constant source to surface distance (SSD) for all beams or an iso-centric set-up with a constant source to axis distance (SAD) [6, 8]. This seeks to destroy the cancerous tissue whilst minimizing the dose to normal tissues and/or critical organs to as low as reasonably achievable in the region.

EBRT with photon beams is carried out with three types of treatment machine: x ray units, isotope teletherapy units (mainly cobalt-60 units) and linear accelerators (LINACs). These machines allow radiation to be delivered from any angle and shapes radiation beams to the contour of the tumor. In the use of EBRT, consideration is given to certain physical parameters such as patient setup, design of patient couch top, and use of beam modifiers (such as block tray, wedges and head rest) [1, 4, 8]. In RT, any device that is placed in the path of the treatment field attenuates the beam and reduces the dose to the patient. Beam modifying devices such as wedge filters, compensators and blocking tray(s) among others are utilized in order to control the amount of radiation dose to the treatment area modifying isodose curves and optimizing the target dose distribution.

When preparing radiation treatment, the prescribed dose and irradiation geometry must be translated into physical machine parameters known as treatment (or beam) parameters. As the electron or photon beam is incident, the absorbed dose in the patient or phantom varies with depth and depends on the following treatment parameters [6, 8]:

University of Ghana http://ugspace.ug.edu.gh

- Beam energy
- field size
- Beam collimation system.
- Source to surface distances (SSD) or source to axis distance (SAD)

1.1.1 Transmission Factors used in EBRT

A transmission factor (TF) is a measure of the degree of shielding afforded by a structure or a set of specified shielding conditions. It is also that fraction of the outside dose or dose rate which is received inside the enclosure providing the shielding. Mathematically, TF is expressed as the ratio of the radiation dose with a beam modifier to the radiation dose without the beam modifier and it accounts for the material in the beams path. TFs are therefore used to determine the proportional reduction in the dose received when patients are protected from radiation. There are several TFs used in radiotherapy, however the ones considered in this work are the tray TF and the wedge TF.

1.1.1.1 Tray transmission factor

This defines how much of the radiation is transmitted through a (block) tray. It is defined as the ratio of the central axis dose rate for a given field with and without a blocking tray [9, 10, 13]. It can also be defined as the ratio of the dose measured at the reference depth (d_{ref}), with or without the tray in the beam for the same number of monitor units [11].

When the photons from the treatment machine interact with the tray material, there is attenuation in the energy fluence of the primary radiation in the beam and so it can be expected that the tray TF will vary with the collimator setting

University of Ghana http://ugspace.ug.edu.gh

(field size), the source to surface distance (SSD) and with the distance from the tray to the measuring point [6]. However, according to Gibbon et al [13], the tray TF is almost independent of field size, depth, and SSD, and a constant value is sufficient in most cases. The presence of the tray will affect the dose in the build-up region through the production of secondary electrons as well as the absorption of secondary electrons produced upstream of the tray. Thus, it is recommended that this factor be measured at a depth well beyond the maximum range of electron contamination [11, 13]; such as a10cm depth [10]. The tray TF may also be used to account for attenuation due to other devices, such as additional trays, beam spoilers, compensators, or special patient support devices.

1.1.1.2 Wedge Transmission Factor

The wedge TF is defined as the ratio of the dose per monitor unit (MU) measured with and without the wedge in the beam [11-13]. This definition is given here only for the reference depth (d_{ref}) and with the practical use of the wedge TF. It is also concluded from this definition that the possible depth of wedge TF is taken into account by the different relative depth doses (RDDs) of the wedged and open beam [11].

Also the wedge factor can be defined as the ratio of dose at a specified depth (usually d_{max}) on the central axis with the wedge in the beam to the dose under the same conditions without the wedge [6]. This factor is used in monitor unit calculations to compensate for the reduction in beam transmission produced by the wedge.

University of Ghana http://ugspace.ug.edu.gh

The wedge TF is therefore used as a measure of the wedge-induced change in the energy fluence per monitor units (MU) measured at the point of interest (at the reference depth) in the beam [12]; hence it can be said that, the influence of the wedge varies with collimator setting and with SSD [11]. Also, depending on the type and angle of the wedge, wedge TF may depend on the wedge angle, field size, depth, and off-axis distance [6, 13].

1.2 STATEMENT OF THE PROBLEM

When preparing radiation treatment, the prescribed dose and irradiation geometry must be translated into physical machine and beam parameters. An error in the calculations or machine settings can negatively affect the intended treatment outcome. While most of the efforts to optimize radiotherapy have aimed to improve treatment from the physical and technological standpoint such as precision in dose delivery, optimization of treatment plans, etc., less progress has been made to include certain relevant transmission factors (TFs) as well as their variation with some treatment parameters into treatment planning. Also, the Radiological Physics Center (in USA) through its dosimetry review visits to various radiotherapy centers is aware that many centers ignore the field-size and depth dependency of most transmission factors. This 'ignorance' may result in significant tumor-dose discrepancies to patients and can lead to over dose or under dose.

There is therefore the need to investigate into the dependence of some of these TFs used in EBRT on certain treatment parameters (such as beam energy, depth, field size and SSD) and that is what this work seeks to do.

University of Ghana http://ugspace.ug.edu.gh

1.3 OBJECTIVES

The principal objective of this research is to evaluate the variation of block tray and wedges as a function of treatment depth and field size for both iso-centric setups, SAD and SSD, keeping the primary beam energy at 1.25MV

The specific objectives of this research work are:

- To determine the wedge TF for different wedge angles (15^o, 30^o, 45^o, and 60^o) at different treatment depths and field sizes using both SAD and SSD setups.
- To determine the tray TF at different treatment depths and field sizes using both SAD and SSD setups.
- To compare the two setup techniques to see if there is any variation in the results.
- To make appropriate recommendation to address any discrepancies in dose delivery during cancer treatment at the National Center of Radiotherapy and Nuclear Medicine (NCRNM) at the Korle Bu Teaching Hospital (KBTH) by including relevant TFs in treatment planning.

1.4 RELEVANCE AND JUSTIFICATIONS

The aim of external radiation treatment is to give maximum dose to the tumor whilst reducing dose as much as possible to the normal surrounding tissues and thus the dosimetric effect of certain treatment parameters is non negligible in today's RT. The calculated dose may vary from the dose delivered to the patient

University of Ghana http://ugspace.ug.edu.gh

during treatment due to the changes in treatment parameters which might affect certain transmission factors.

Most of the time a single TF is used for the treatment time/monitor units (MUs) calculation of the patients, which is usually measured for a reference field size of $10\times10cm^2$ and a reference depth of. d_{max} (0.5cm) or d_{10} (10cm). If the depth, beam energy, SAD/SSD and field size dependency of various or different TFs are not taken into account in dose calculations, it may result in significant tumor-dose discrepancies for the patients which can lead to over dose or under dose. It is therefore important to specify any changes to transmission values resulting from these treatment (or beam) parameters and incorporate them into the treatment planning process.

1. 5 SCOPE OF STUDY

This study is being undertaken to develop and implement protocols for optimisation of patients' treatment and protection at the National Radiotherapy centre of the Korle Bu Teaching Hospital (KBTH) in Accra, Ghana, by including the wedge and tray transmission factors at various treatment depths and field sizes in their treatment planning system using a Co-60 Teletherapy machine. The measurements will be collected from a Co-60 tele therapy or EBRT machine at KBTH using a locally manufactured large water phantom (which will mimic the human tissue) within a period of four weekends (Saturday and Sunday per weekend). Measurements will be taken separately for open field, wedge (of angles 15^o, 30^o, 45^o, and 60^o) in beam path and a block tray (6mm thick) in beam path for different treatment depths which include d_{max} (0.5cm), TG-21 calibration depth (5cm or 6cm), ICRU wedge angle defining depth (10cm), 15 cm and 20cm) as well as for various square field sizes (2cmx2cm to 30cmx30cm).

University of Ghana http://ugspace.ug.edu.gh

CHAPTER TWO

LITERATURE REVIEW

2.1 GENERAL OVERVIEW

This chapter seeks to review the literature on the transmission and tray factors (TFs) with respect to cobalt-60 machine and linear accelerator (linac); and also their effects on delivered doses as well as possible dependence on various treatment parameters which have been reported by various researchers.

2.2 THE COBALT-60 MACHINE

2.2.1 Background

Teletherapy cobalt-60 units were first used for patient treatment in 1951 in Canada [5]. Although megavoltage x-ray units had been available for some years prior to this date, they were not in widespread use, whereas, cobalt units became the mainstay of external beam therapy for the next 30 years or so world-wide. Cobalt-60 is manufactured by irradiating cobalt-59 in a high neutron flux nuclear reactor. The main reasons for its suitability for teletherapy are the availability of relatively small, high specific activity sources that minimizes the beam penumbra and has a relatively long half-life of 5.27 years. It is also the most monochromatic high-energy photon emission element of energies 1.173MV and 1.333MV in equal quantity [5, 14].

Compared to modern linear accelerators, cobalt units offer poorer geometrical precision in treatment because of a larger penumbra and greater mechanical inaccuracy [5]. Cobalt can no longer provide the basis for contemporary

University of Ghana http://ugspace.ug.edu.gh

sophisticated radiation therapy. This is because cobalt beams are less penetrating than those from linacs and they also lack the flexibility in the control of the radiation output offered by linacs. However, commercially available cobalt units may be quite adequate for many non-radical treatments, and there are even some applications where cobalt sources have been used in specially designed equipment to give a performance that could be argued to be superior to that obtainable from a conventional linac [5].

Cobalt-60 therapy is the most appropriate choice for radiotherapy in countries where facilities for the maintenance of linear accelerators (LINACs) are lacking [5]. Many of the major techniques and advances in the physics of external beam therapy were developed on cobalt units. These include arc therapy, conformal therapy, transmission dosimetry, the development and measurement of tissue air ratios and the subsequent derivation of scatter air ratios (SARs), and differential SARs and the associated algorithms for treatment planning based on the separation of primary and secondary radiation. More recently, Poffenbarger and Podgorsak [15] have investigated the possibility of using an iso-centric unit for stereotactic radiosurgery, and Warrington and Adams [16] have shown that conformal therapy, and even IMRT, could be adequately delivered with a cobalt-60 unit except for the most deep-seated tumors [5].

2.2.2 Basic Construction and Features

A major advantage of cobalt units is the basic simplicity of their design and construction that generally makes them inherently reliable. Nevertheless, care must be taken to ensure that they are robustly built and carefully maintained to minimize the potential hazards from the high activity source and the associated

University of Ghana http://ugspace.ug.edu.gh

heavy shielding. A sectional drawing of a modern cobalt unit treatment head is shown in Figure 2.1. The complete cobalt-60 teletherapy machine consists of various components including the head, which contains the source and it is attached to the gantry. It also has a couch on which the patient due for treatment is placed. The following sub-sections look at the major components of the cobalt-60 machine.

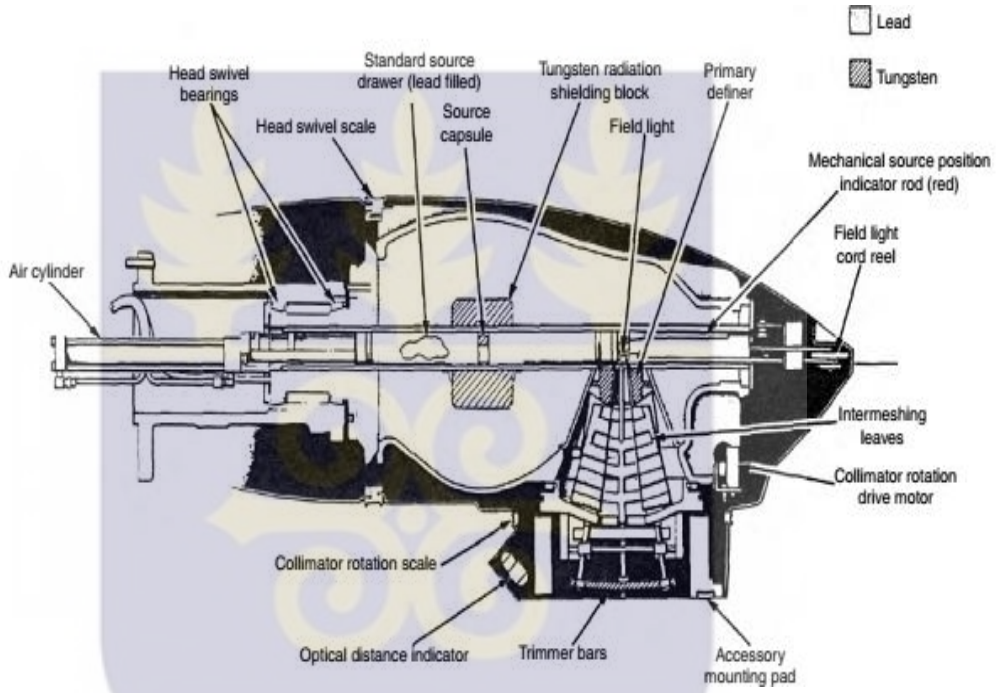

Figure 2.1: Diagram of the head of a Theratron 780 treatment unit showing the source drawer mechanism, collimator and shielding (ref. 5)

2.2.2.1 The Head

The head of a cobalt unit has three basic functions, these are: to shield the source, to expose the source as required, and to collimate the beam to the correct size [5]. Shielding of the source is achieved by surrounding the source with lead, and in many designs, with alloys of a higher density metal such as tungsten in order to reduce the volume. Depleted uranium alloy (with a high percentage of

University of Ghana http://ugspace.ug.edu.gh

U-238, density approximately $19.0\times10^{3}Kgm^{-3}$) was used in some earlier designs, but this has been discontinued because of the problems with stability of the alloy as some of it became powdery and also because of the difficulties associated with eventual disposal.

The source exposure mechanism is usually one of two types; either the source is moved between a safe and exposed position (as shown in Figure 2.1) or whether the source remains stationary, and a moving shutter opens or closes the beam. The latter solution, implemented on earlier machines is now obsolete. In the former solution, the source movement is either a translation (as in Figure 2.1) or a rotation. Various beam collimator designs exist to give variable rectangular fields with sides ranging in length, typically, from 4cm to 30cm or even up to 40 cm on iso-centric units with a source axis distance (SAD) of 100cm. Each of the four collimator leaves is usually focused on the edge of the source proximal to it so as to avoid cut-off of the primary beam and minimize penumbra. Distances from the source to the far edge of the collimators are typically between 40cm and 50cm for machines designed for 80cm SSD, but this distance may be increased by penumbra trimmers that are particularly desirable when the machine is to be used for 100cm SSD treatment.

With careful design of the collimation system and a 15mm diameter source, a penumbra of no more than 10mm (distance between the 20% and 80% decrement lines) may be achieved at 5cm depth for field sizes with an area of less than $20\times20cm^{2}$ [5].

University of Ghana http://ugspace.ug.edu.gh

2.2.2.2 The Source

The cobalt source usually consists of a series of either millimeter-size cylindrical pellets or thin metallic discs sealed within a double capsule of stainless steel and manufactured to meet certain standards regarding protection from impact, corrosion, and heat [5]. Active source diameters and heights are generally in the region of 10mm to 25mm and 20mm to 25mm respectively, being a compromise between achieving a high or sufficient activity to obtain a reasonable output and keeping the source small enough to minimize the beam penumbra. The source length may be longer than the diameter, but this is not such a critical dimension because the photons from the rear of the source contribute relatively less to the clinical beam than those from the front. About 25% of the primary photons are lost in a typical source due to self-attenuation [5]. The space behind the active cobalt material in the capsule must be tightly packed with blank discs to eliminate movement. The low energy beta ray emission from the source is filtered out by the capsule walls.

2.2.2.3 Gantry

In order to obtain a reasonable compromise between output, depth dose, and clearance around the patient, modern cobalt units are manufactured in a standard iso-centric configuration with a source axis distance of 80cm being the most common [5]. Units with an SAD of 100cm are also practical if high activity sources can be afforded and offer the advantages of greater depth dose, larger field sizes, greater clearance around the patient, and geometrical compatibility with linacs. In order to increase their versatility, iso-centric units have often

University of Ghana http://ugspace.ug.edu.gh

been made with the ability to swivel the head about a horizontal axis through the source.

This swivel motion keeps the beam axis in a vertical plane, and when used with an appropriate gantry angle, may be useful for extended SSD treatments or for treating immobile patients in a bed or chair. Some non iso-centric cobalt units have been manufactured with the head held by a yoke on a vertical stand, and these are particularly useful for giving single field palliative treatments. Where an iso-centric unit has the swivel facility, great care must be taken to ensure that its position is accurately reset before the equipment is used for normal iso-centric use since the slightest angulation of the head swivel will create a large deviation of the beam axis from the mechanical iso-center. Some iso-centric units use slip rings for the supply of all power and control signals to the gantry and this allows continuous gantry rotation. Coupled with the guaranteed constant output from the source as the unit rotates, such a versatile and simple rotation mechanism provides an ideal unit for arc or full rotation therapy when this technique is required [5].

2.2.3 Beam Modifiers

Although beam flattening filters can be successfully used on cobalt units, they are rarely employed in practice because of the consequent reduction in output. Without a flattening filter, the beam homogeneity is relatively poor across a large area beam, especially at greater depths, because of scattering in the tissue and the greater distance from the source to the field edges compared to the center for a constant depth. There are various kinds of beam modifiers which include compensators, spoilers, bolus, (block) tray, and wedges. However trays and

University of Ghana http://ugspace.ug.edu.gh

wedges are those mostly inserted into the head of the cobalt-60 machine, whiles the others are placed on the skin of patients (when needed) for the purpose of uniform dose distribution and/or uniformity.

Other beam modifiers and accessories used on cobalt-60 machines include: the beam-defining light, range finder, accessory tray, laser positioning system, front and back pointers, etc. We take a brief look at some of the mostly used beam modifiers in external beam radiotherapy.

2.2.3.1 Use of wedges as beam modifiers

The use of wedges is mainly to modify the dose distribution in one of the principal planes of the beam so that the isodose lines are rotated relative to their open beam position. This is done by inserting a metal wedge in the beam hence producing additional scatter which will increase with wedge thickness. A number of investigations have shown that the relative amount of the scattered radiation which reaches the patient depends on the wedge position (or wedge angle) and field size as well as treatment depth.

2.2.3.2 Use of blocks and tray as modifies

For some treatments, additional blocks of metal or alloy of high density are used to shape the field to conform to the target volume or to protect organs at risk. These blocks are placed on a tray which attenuates the beam slightly and these blocks also changes the scattered radiation component of the beam by [14]:

- Producing additional photon and electron scatter from the block tray: this is due to electrons ejected from the block tray which increases the

University of Ghana http://ugspace.ug.edu.gh

dose close to the surface. This effect is strongly dependent upon the distance between the tray and the patient.

- Modifying the volume in the patient from which scattered photons are generated; this also changes the dose at the beam axis.
- Partially shielding the head scatter

2.2.3.3 Use of compensators as beam modifiers

When the surface of the patient is very uneven as in the head and neck region, it can be difficult to achieve a uniform dose over the target volume, since the beam is attenuated and scattered differently in different regions. A compensator may be used to counter-balance these affects by interposing various thickness of material in different parts of the beam. Compensators may also be used to modify dose distributions which are adversely affected by internal body structures such as air or bone.

2.2.3.4 Use of spoilers and bolus

The most common technique to increase the superficial dose for high-energy photon beams which shows significant skin-sparing is to place some water equivalent material (such as a bolus) onto the patients skin [14]. The dosimetric consequences are handled by treating this bolus as part of the patient, increasing the treatment depth and decreasing the SSD by the bolus thickness. Also, the skin dose can be increased by adding a "spoiler" to the beam, essentially a block tray without blocks in order to produce secondary electrons which travel onto the patient's surface [14].

University of Ghana http://ugspace.ug.edu.gh

2.3 TREATMENT PARAMETERS IN EBRT

As stated earlier, when an electron or photon beam is incident on a patient or phantom, the absorbed dose varies with depth and depends on energy, field size, SSD or SAD, and beam collimation system. The calculation of dose in the patient affects depth dose distribution with regard to these parameters [8]. In this report, discussion of treatment parameters is going to be in the context of treatment planning; however, the central axis depth dose distribution will not be sufficient to characterize a radiation beam that produces a dose distribution in a three-dimensional volume. In view of this, lines passing through points of equal dose (known as isodose curves) are used to represent volumetric variation in absorbed dose and dose distribution [8]. These curves are usually drawn at regular intervals of absorbed dose and are expressed as a percentage of the dose at a reference point. Thus, the isodose curves represent levels of absorbed dose in tissue.

2.3.1 Beam Energy

Beam energy used in EBRT is usually 6MV, 8MV, 10MV or 15MV for high energy photon beams (such as linacs), cobalt-60 units for low energy photon beams (that is an average of 1.25MV), and 6MeV, 10MeV and 15MeV for electron beams; with each energy producing different central axis depth dose distribution [3]. Thus we can say that the central axis depth dose distribution depends on the beam energy; and as a result, the depth of a given isodose curve increases with beam quality. Beam energy also influences isodose curve shape near the field borders [8]; greater lateral scatter associated with lower-energy

University of Ghana http://ugspace.ug.edu.gh

beams causes the isodose curves outside the field to bulge out (see Figure 2.2). In other words, the absorbed dose in the medium outside the primary beam is greater for low-energy beams than for those of higher energy.

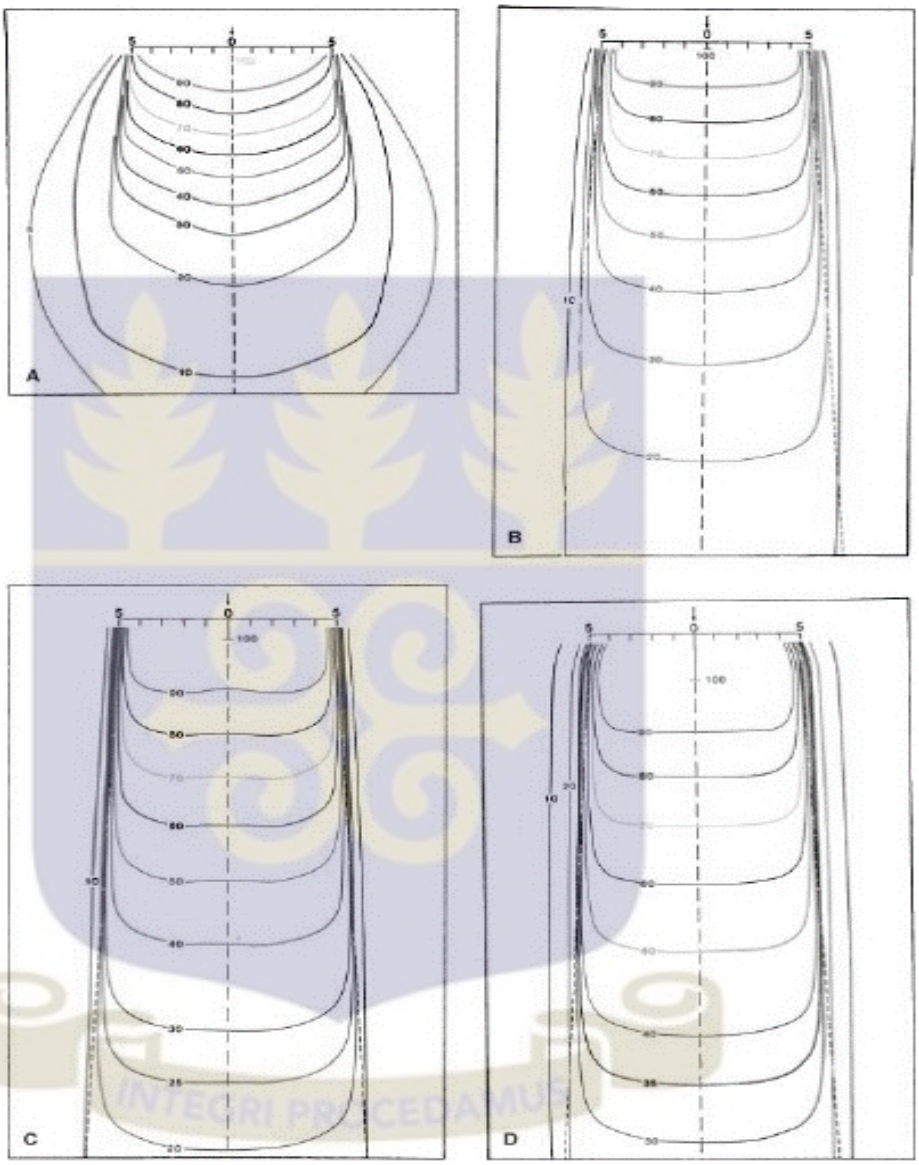

Figure 2.2: Isodose distributions for different-quality radiations.

A: 200 kVp, SSD = 50cm, Half-value layer = 1 mm Cu, field size = 10×10 cm^2.

B: Co-60, SSD = 80cm, field size = 10×10 cm^2.

C: 4-MV x-rays, SSD = 100cm, field size = 10×10 cm^2.

D: 10-MV x-rays, SSD = 100cm, field size = 10×10cm^2.

University of Ghana http://ugspace.ug.edu.gh

Physical penumbra depends on beam quality as illustrated in Figure 2.2. As expected, the isodose curves outside the primary beam (e.g., 10% and 5%) are greatly distended in the case of orthovoltage radiation. Thus, one disadvantage of the orthovoltage beams is the increased scattered dose to tissue outside the treatment region. For megavoltage beams, on the other hand, the scatter outside the field is minimized as a result of predominantly forward scattering and becomes more a function of collimation than energy.

2.3.2 Source to surface distance (SSD) and Source to axis distance (SAD)

Source size, SSD, and SAD all affect the shape of isodose curves by virtue of the geometric penumbra [8]. SSD also affects the percent depth dose and therefore the depth of the isodose curves. Dose variation across the field border is a complex function of geometric penumbra, lateral scatter, and collimation; thus, the field sharpness at depth is not simply determined by the source or focal spot size. For example, by using penumbra trimmers or secondary blocking, the isodose sharpness at depth for cobalt-60 beams with a source size less than 2cm in diameter can be made comparable with higher-energy linac beams, although the focal spot size of these beams is usually less than 2 mm. Comparison of isodose curves for cobalt-60, 4MV, and 10MV in Figure 2.2 illustrates the point that the physical penumbra width for these beams is more or less similar.

It has to be noted that at any normal clinical distance, either SSD or SAD setup can be used; however, the mostly used value of SSD or SAD for clinical practice is about 100cm [17]. When using the SSD setup, the field size is defined at the surface of the phantom, whilst for the SAD setup, the field size is defined at the

University of Ghana http://ugspace.ug.edu.gh

detector position. Figure 2.3 shows a schematic diagram of both the SSD and SAD setup.

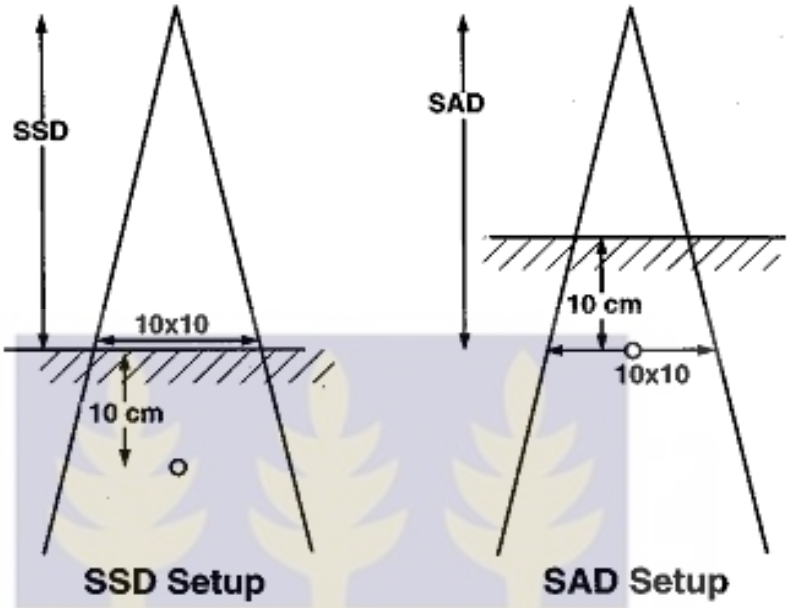

Figure 2.3: Schematic diagram of the SSD or SAD setups which may be used for photon beam reference dosimetry. In both cases the ion chamber is at a water equivalent depth of 10cm in the water phantom.

2.3.3 Beam Collimation System

The term collimation is used here to designate not only the collimator blocks that give shape and size to the beam, but also the flattening filter and other absorbers or scatters in the beam between the target and the patient. Of these, the flattening filter, which is used for megavoltage x-ray beams, has the greatest influence in determining the shape of the isodose curves. Without this filter, the isodose curves will be conical in shape, showing markedly increased x-ray intensity along the central axis and a rapid reduction transversely [8]. The function of the flattening filter is to make the beam intensity distribution

University of Ghana http://ugspace.ug.edu.gh

relatively uniform across the field (i.e., “flat”). Therefore, the filter is thickest in the middle and tapers off toward the edges.

The cross-sectional variation of the filter thickness also causes variation in the photon spectrum or beam quality across the field owing to selective hardening of the beam by the filter. In general, the average energy of the beam is somewhat lower for the peripheral areas compared with the central part of the beam. This change in quality across the beam causes the flatness to change with depth. However, the change in flatness with depth is caused by not only the selective hardening of the beam across the field, but also the changes in the distribution of radiation scatter as the depth increases [8].

2.3.4 Field Size

Field size is one of the most important parameters in treatment planning. Adequate dosimetric coverage of the tumor requires a determination of appropriate field size. This determination must always be made dosimetrically rather than geometrically. In other words, a certain isodose curve (e.g. 93-95%) enclosing the treatment volume should be the guide in choosing a field size rather than the geometric dimensions of the field [6, 8].

Great caution should also be exercised in using field sizes smaller than 6cm in which a relatively large part of the field is in the penumbra region. Depending on the source size, collimation, and design of the flattening filter, the isodose curves for small field sizes, in general, tend to be bell shaped. Thus, treatment planning with isodose curves should be mandatory for small field sizes. The isodose curvature for Cobalt-60 increases as the field size becomes overly large

University of Ghana http://ugspace.ug.edu.gh

unless the beam is flattened by a flattening filter [8]. The reason for this effect is the progressive reduction of scattered radiation with increasing distance from the central axis as well as the obliquity of the primary rays. The effect becomes particularly severe with elongated fields such as cranial spinal fields used in the treatment of medulloblastoma. In these cases, one needs to calculate doses at several off-axis points or use a beam-flattening compensator [6].

2.4 REVIEW ON WEDGE TRANSMISSION FACTORS

2.4.1 Background

The wedge factor TF is defined as the ratio of dose at a specified depth (usually d_{max}) on the central axis with the wedge in the beam to the dose under the same conditions without the wedge [6]. Although the presence of the wedge will affect several other dosimetric quantities, these effects are incorporated into the wedge factor. This approach eliminates the need for separate wedge-field data tables, but may require field size and depth dependent wedge factors. Since wedge field isodose plans are calculated using a treatment-planning system, it is important that the physicist fully understands how field weights are handled in the presence of a wedge. In some cases it is possible to mistakenly apply a "double-wedge factor." This occurs when the treatment planning computer assigns a beam weight that builds in the wedge TF, and the physicist in turn uses this filtered weight to calculate monitor units, and then once again accounts for the wedge TF.

Wedge TFs for both physical and nonphysical wedges depend on the selection of wedge angle and energy; however, the main difference is the dependence on field size and depth of calculation. The field-size dependence is highly

University of Ghana http://ugspace.ug.edu.gh

dependent on the software that drives the filter-less wedge, whereas the depth dependence is nearly eliminated due to the removal of the physical filter beam hardening [13].

2.4.2 Wedge filters

Traditional wedge filters are simply wedge-shaped pieces of brass, aluminum, or lead that are placed in front of the collimators. Filters of different maximum thickness are used to provide different wedge angles; commonly, 15°, 30°, 45°, and 60°. Currently, there are three types of wedge filters, namely: physical (or manual) wedges, motorized (or mechanically fixed) wedges, and dynamic wedges.

- Physical wedges are angled pieces of lead or steel that are placed in the beam to produce a gradient in radiation intensity. Manual intervention is required to place the physical wedges on the treatment unit's collimator assembly.
- A motorized or mechanically fixed wedge (which is similar to the physical wedge), is a physical wedge integrated into the head of the unit and controlled remotely.
- Dynamic wedges produce the same wedged intensity gradient by having one jaw close gradually while the beam is on.

In general all wedges have a thick end called the heel (where the dose is lowest) and the other is called the toe. Also they have the wedge angle which is defined as the angle between the 50% isodose line and the perpendicular to the beam central axis [6]. Most wedges have wedge angles ranging from 10° to 60°. A typical isodose distribution for a wedged beam is shown is Figure 2.4.

University of Ghana http://ugspace.ug.edu.gh

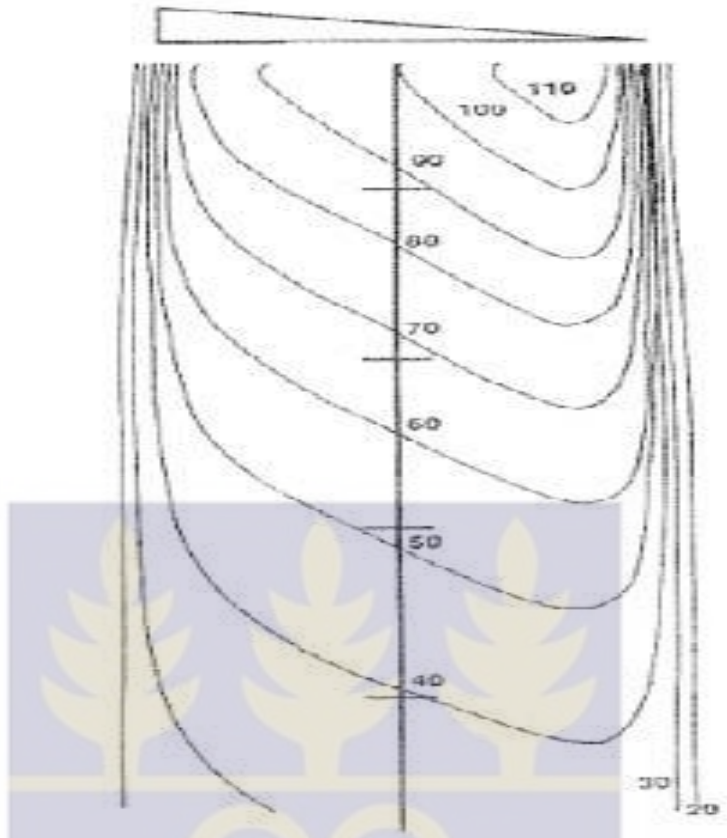

Figure 2.4: Isodose curves for a wedged 6 MV photon beam. The isodose have been normalized to d_{max} with the wedge in place.

2.4.2.1 Uses of wedges

According to a Podgorsak [6], there are two main uses of wedges:

i. Wedges can be used to compensate for a sloping surface, as for example, in nasopharyngeal treatments where wedges are used to compensate for decreased thickness anteriorly, as shown in Figures 2.5 and 2.6.

   Figure 2.5 shows two wedged beams in a parallel-opposed configuration with the wedges used to compensate for missing tissue; whiles Figure 2.6 shows two wedged beams at 90^{o} to one another with the wedges compensating for the hot spot near the surface.

University of Ghana http://ugspace.ug.edu.gh

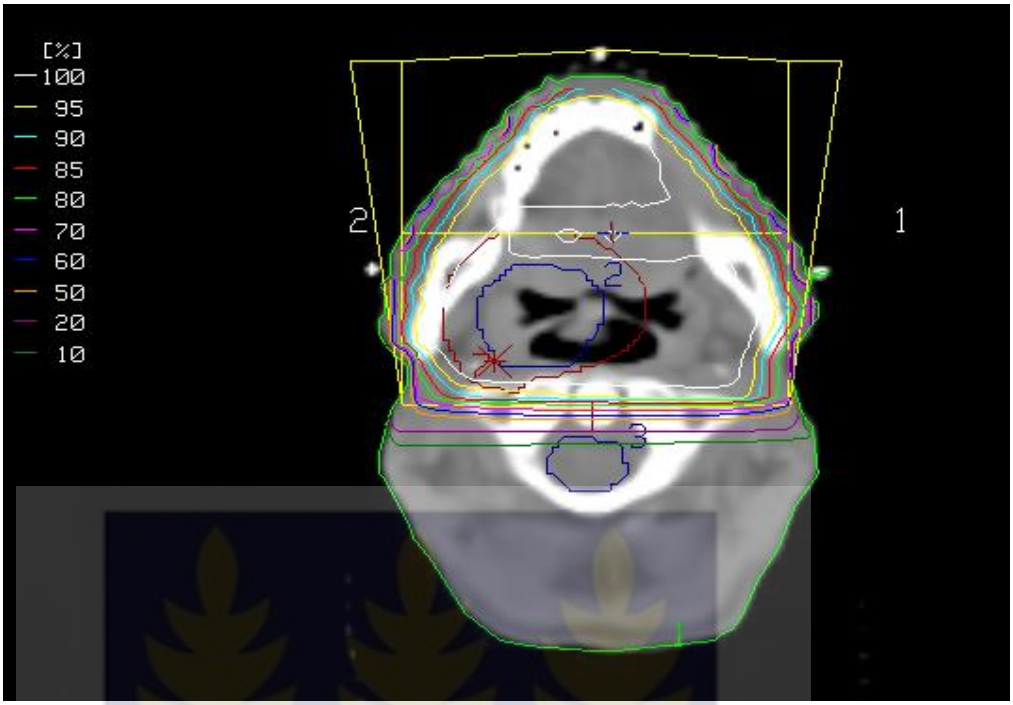

Figure 2.5: Treatment plans illustrating the use of wedge filters in two 15° wedges used to compensate for the decreased thickness anteriorly (Ref. [6]).

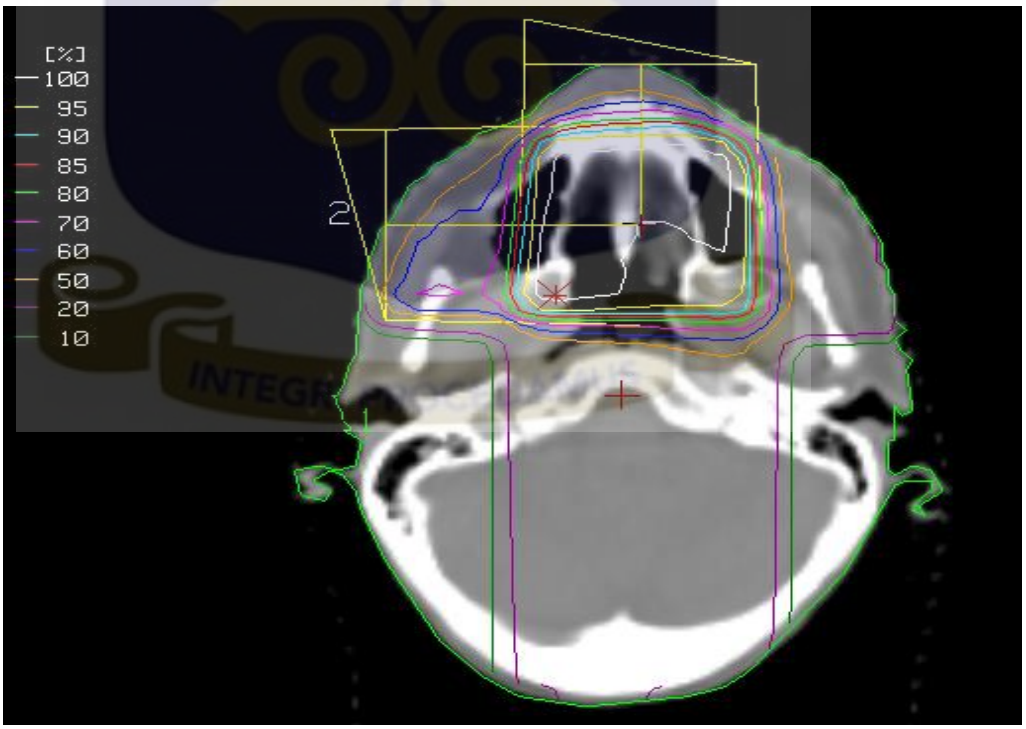

Figure 2.6: Treatment plans illustrating the use of wedge filters in a wedged pair of beams used to compensate for the hot spot that would be produced with a pair of open beams at 90^{o} to each other. (Ref. [6])

University of Ghana http://ugspace.ug.edu.gh

ii. A pair wedged of beams is also useful in the treatment of relatively low lying lesions where two beams are placed at an angle less than 180° called the hinge angle (see Figure 2.7). The optimal wedge angle (assuming a flat patient surface) may be estimated from: 90° minus half the hinge angle (90° - $^1/_2$ (hinge angle)).

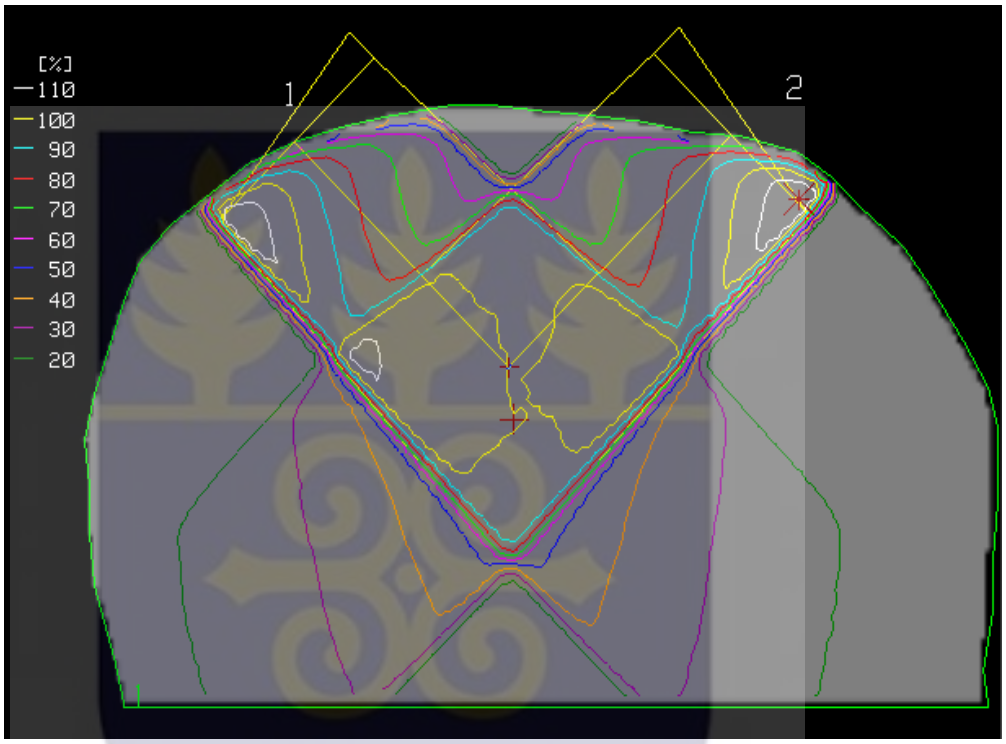

Figure 2.7: A wedge pair of 6 MV beams incident on a patient. The hinge angle is 90° (orthogonal beams) for which the optimal wedge angle would be 45°. However, the additional obliquity of the surface requires the use of a higher wedge angle of 60° (Ref. [6]).

2.4.3 Physical wedges

Physical wedges may be classified into two types, distinguished by their placement relative to the secondary collimating jaws [13]. Internal wedges (sometimes called motorized wedges or universal wedges), located above the collimating jaws are designed using a single wedge with a large wedge angle of

University of Ghana http://ugspace.ug.edu.gh

60°. The internal wedge is inserted into the field using a motorized drive within the accelerator. Wedged isodose distributions with smaller wedge angles are produced by combining the internal wedge field with a corresponding open field with appropriate relative weighting. In contrast, external wedges are placed below the collimating jaws. External wedges are manually inserted into the collimator assembly, and are located much closer to the patient, with source-wedge distances ranging from 40% to 70% of the SAD [13].

2.4.3.1 Motorized (mechanically fixed) wedges

Mechanically fixed wedges may be inserted into the beam below the end of the collimator assembly to give a range of wedge angles, typically between 15° and 60°. These wedges will usually incorporate a certain amount of beam flattening, giving a somewhat straighter isodose curve within the central portion of the beam than for an open field. These wedge filters just like any other wedge filter reduces the dose rate at the center of the beam and this is more of a problem with a cobalt machine than with a linear accelerator [5]. The reduction in output may be minimized by making the wedge shape always begin at the field edge by linking the toe end of the wedge to the collimator so that wedging always begins at the edge of the beam.

With this system, the wedge TF will be different for each field size, so modern units usually have a fixed relationship between the center of the wedge and the center of the field with perhaps different wedges for different ranges of field size [5]. In principle, there is no reason why a virtual wedge could not be created (in the case of a cobalt-60 machine) by dynamically moving one collimator during treatment in a similar fashion to that employed on linacs. Such a system

University of Ghana http://ugspace.ug.edu.gh

has not yet been commercially produced and would probably require a different design for the collimators to allow them to travel across the beam axis, but it would have the advantage of minimizing the increase in treatment time associated with the use of a wedge [5].

2.4.3.2 Investigations and recommendation on wedge factors using physical wedges

A number of investigators have studied the field size and depth dependence of internal and external WFs. The field size dependency appears to originate from a wedge-induced increase in collimator scatter [18]. Heukelom et al. [18] accurately predicted the field-size dependence of internal wedges, which demonstrate a larger variation with field size. A field-size dependence may also be necessary for external wedges, particularly for higher wedge angles [19].

The depth dependence of wedge TF has been attributed both to beam hardening as well as "dose-gradient" effects, i.e., changes in depth dose due to the dose gradient across the field [12]. McCullough et al. [20] demonstrated that for depths less than 10 cm, an error of less than 2% is made if this quantity is ignored. Nevertheless, the increased use of wedged fields for depths beyond 10 cm has necessitated the inclusion of this dependency in clinical calculations [19].

Gibbon et al [13] recommended that physical wedge TFs be measured as a function of both field size and depth. With the chamber axis perpendicular to the gradient direction of the wedge, two sets of measurements should be made with the wedge in opposite orientations to accommodate uncertainties in the

University of Ghana http://ugspace.ug.edu.gh

chamber position and wedge mounting. They also recommended that measurements be made with the chamber at the iso-center.

Wedge TF are most often considered independent of SSD; however, for treatments at extended distances (e.g., SSD > 120cm), it would be prudent to confirm the accuracy of the wedge TF determined at iso-center, as investigators have noted a slight dependence on SSD [13]. For these calculations, it is also necessary to account for the field size divergence with distance whiles for calculations at an off-axis point within a physically wedged field, the wedge TF will change significantly.

For off-axis points along the principal axis in the gradient direction of the wedge, Khan [21] proposed that wedge TF may be approximated by the product of the central-axis wedge TF and the corresponding off axis profile value measured for the largest available wedged-field. This method agreed within 3% with 6MV measurements for calculation points positioned in the geometric center of the asymmetric field for an external wedge. A few years later, Georg [22] proposed two alternative methods consistent with the ESTRO protocol. Each of these methods employed a primary wedge factor measured in a mini-phantom, as well as wedged-field output ratios and tissue-phantom ratios (TPRs).

Both Smulders et al. [23] and Mihailidis et al [24] have proposed methods for off-axis wedged calculations which use open field dosimetry parameters combined with wedged-field off-axis ratios (OAR). The method of Smulders et al. [23] used a product of off-axis wedge TFs for distances parallel to and perpendicular to the gradient direction of the wedge. Wedged OARs were taken as the ratio of measured doses in phantom for symmetric fields centered off and

University of Ghana http://ugspace.ug.edu.gh

on the central axis. The measured OARs for both 6 and 18MV beams on an Elekta internal wedge showed only a small field size dependence, whereas the 18MV results demonstrated a large depth dependence. Mihailidis et al [24] equated wedged OARs to primary OARs measured using techniques employed for open fields. Their results also demonstrated good agreement (that is within 2%) with measured doses for 6 and 18MV beams with 15^{o} and 45^{o} external wedges [13].

For calculations at off-axis points along the principal axis in the non-gradient direction, additional corrections may be necessary in addition to open field OARs. Chui and LoSasso [25] first demonstrated differences between off-axis wedged and open field profiles, measured for external wedged-fields. Storchi and Woudstra [26] proposed using open field OARs in this direction, but at a depth increased by the water equivalent thickness of the wedge at that point. Myler and Szabo [27] obtained agreement within 1% by multiplying central axis wedge TFs with off-axis correction factors. These factors were determined by measuring the effective wedge attenuation coefficient as a function of off-axis position.

2.4.4 Nonphysical (or Dynamic) wedges

The automatic or dynamic wedge has the potential disadvantage that it increases the distance between the source and the front face of the accelerator head [5]. This is a particular disadvantage for machines that use either an in-line accelerator tube or a 270^{o} bending system. Because of the inconvenience of having to enter the treatment room to insert a manual wedge, there was a need to provide some form of automation without decreasing the clearance between

University of Ghana http://ugspace.ug.edu.gh

the machine and the patient. Varian was the first to solve this problem by developing the dynamic wedge that is now available from other manufacturers as well [5, 13]. Both the Varian dynamic wedge and its successor, the enhanced dynamic wedge (EDW) takes advantage of a collimation jaw moving in conjunction with adjustment of the dose rate over the course of one treatment [13].

To achieve a wedged beam profile, one of the jaws is kept stationary, and the other is moved during the treatment. This technique is potentially more flexible than fixed wedges because, in principle, it is possible to design any shape of beam profile that is required, but it is most often limited to one jaw pair because of the requirement for the jaw (or leaf) to cross the central axis of the beam [5]. Wedge factors for nonphysical, or dynamic wedges represent the fractional change in dose per MU at the calculation depth after the treatment field is completed [13]. The variation of jaw position and dose rate is driven by a segmented treatment table (STT), which is unique for each energy, wedge angle, and field size. The basis for the EDW generation is a "golden" STT (GSTT) for a 60^0, 30cm wedge, from which the treatment STTs for other wedge angles are calculated [13].

2.4.4.1 Investigations and recommendation on wedge factors using nonphysical wedges

According to Gibbon et al [13], in contrast to physical wedges, Varian dynamic wedges have very steep field-size dependencies. Thus, it is critical that the input field size be correct for the calculation. Also they stated in their report that, the wedge TF for EDW is primarily dependent on the position of the fixed Y jaw,

University of Ghana http://ugspace.ug.edu.gh

and is virtually independent of the X collimator setting, the initial moving Y jaw position, and the MLC or blocked field size.

A number of researchers have derived methods to predict the wedge TF for Varian's EDW treatment fields. Liu et al. [28] extended their method adopted for DW to EDW. In this effort, they remove the majority of the field-size dependence by defining a normalization function determined from the STT value for the final moving jaw position. They then calculate a normalized wedge TF according to the output for the EDW and the normalized golden STT value for the final jaw position. In a follow-up publication, however, Liu et al. [29] used both an additional normalization function, as well as an in-air output ratio determined within the EDW field to determine the wedge TF.

Additional methods have been proposed to determine the wedge TF from the MU fraction model for EDW. Papatheodorou et al. [30] determined the wedge TF using an exponential model of the GSTT for the 60º EDW. Klein et al. [31] derived a more complex method according to a technique that utilizes the manufacturer's method of constructing a STT by a fitting polynomial. The algorithm for the wedge TF depends on the fixed-jaw position and energy-dependent correction factors. Although the MU fraction model accurately predicts wedge TF for most clinical cases, differences of ~4% exist between wedge TF measured for larger field size and wedge angles [13, 32].

A number of papers have been published to improve agreement between calculated and measured data. Using an exponential model of dose outside the field, Gibbons [32] formulated an analytic algorithm for the wedge TF that demonstrated agreement within 2% to measured data in the center of symmetric and asymmetric fields. Prado et al. [33] used an empirical formula to determine

University of Ghana http://ugspace.ug.edu.gh

the dose to arbitrary points within the field. Miften et al. [34] determined a scatter dose correction determined from the differences between measured and calculated wedge TF for a 60^{o} EDW.

The methods above also apply for calculations to points along the principal axis in the wedge gradient direction. In these cases, the MU fraction model equates the wedge TF to the fraction of MUs delivered, while the off-axis calculation point is in the direct beam [13]. The one comforting aspect of using either an algorithm or fixed tables is that a wedge TF for a given energy is independent of treatment machine [13] as shown below. Therefore, one algorithm or one table can be used for a single energy. Klein et al. [31] compared the measured wedge TFs for three accelerators and found differences of less than 0.5% on average, with no difference more than 1.5% (see Figure 2.8).

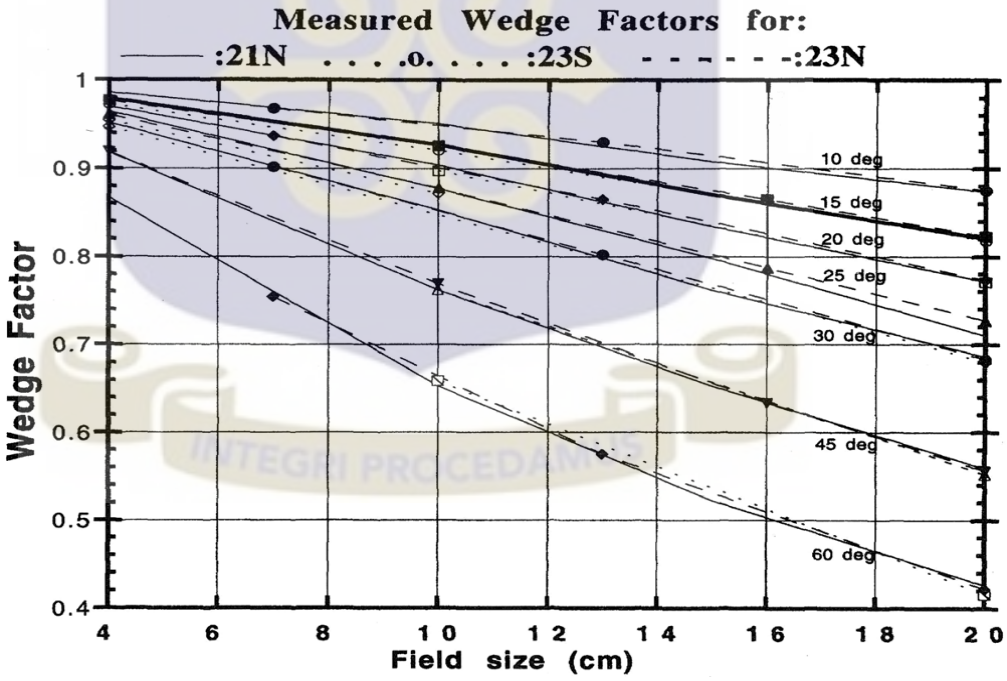

Figure 2.8: Measured 6MV EDW wedge factors for three different Varian machines represented by solid, dashed, and dotted lines. The close agreement between multiple machines allows a common wedge factor table for use in MU calculations (Ref. 13, 31).

University of Ghana http://ugspace.ug.edu.gh

Also according to Alkhatib et al [42] and Misbah et al [43] it has become a common knowledge that wedge TFs are definitely a function of both the beam field size and also a function of the treatment depth. They both defined the field size dependent to be the ratio of ionization readings measured with and without the wedge at the normalization depth for the same field size. Also Tailor et al [19] and Misbah et al [43] who both investigated into dependence of wedge TFs on the field size and depth said their data suggested that the dependence of the wedge TF on field-size and depth in the first approximation, depends on the absolute value of the transmission under reference conditions. Tailor et al [19] added that for wedges with a transmission value greater than 0.65%, field-size dependence and change in depth dose are typically less than 2%, however, for wedges with transmission values less than 0.65%, field-size dependence increases with decreasing reference wedge transmission. Misbah et al [43] in their report stated that the change in wedge transmission with depth is significant (> 2%) only for photon energies less than or equal to 10 MV and can exceed 5% for thick wedges.

2.5 REVIEW ON TRAY TRANSMISSION FACTORS

2.5.1 Fields with a tray

Tray(s) are routinely placed in the primary beam of teletherapy machine to either shield vital structures within the beam (e.g. lung shield) or to optimize dose distributions**.** The radiation output in the presence of tray is characterized by the tray transmission factor and open beam field size factors. In clinical practice, irradiation fields are often partially shielded with customized blocks from high density materials positioned on a tray which in turn, is mounted below

University of Ghana http://ugspace.ug.edu.gh

the collimation jaws of the treatment machine. Usually in this set-up, the source-to-tray distance is approximately two-thirds of the SAD [11]. Block trays are also used to customize the radiation beam so that it will fit the intended treatment area shape and field size. According to Mijnheer et al. [10], to understand the changes in the output factor due to the presence of a tray in the beam path, it is useful to separate the origin of these changes into two parts:

i. The influence of photon attenuation and scatter in the material of the block support (or tray), on the energy fluence at the point of interest, and

ii. The energy fluence reduction due to partial shielding of the flattering filter by additional customized block.

The attenuation can be taken into account by the tray TFs determined at the reference distance and the reference depth; hence the variation in dose with field size due to insertion of 10mm thick PMMA tray in the beam, can amount up to 1.5%, while the attenuation of a 10cmx10cm square field is in the range of 4-5% [9, 10]. However, the influence of the presence of the tray on beam quality is almost negligible [10].

2.5.1.1 The effect of a tray on the dose

When the photons from the treatment machine interacts with the tray material, there is attenuation in the energy fluence of the primary radiation in the beam as well as scattering of photons in the tray material contributing to the dose at a point of interest [35]. The relative importance of this effect depends on the beam quality, the thickness and material of the tray, the actual size of the irradiated tray surface and the distance between the tray and the phantom (or patient)

University of Ghana http://ugspace.ug.edu.gh

surface [11]; and thus, it can be expected that the tray transmission factor will vary with the collimator setting (field size), the source to surface distance (SSD) and with the distance from the tray to the measuring point [6]. It should be noted that the presence of the tray in the photon beam will not result in appreciable amount of backscattered photons into the monitor chamber due to their large mutual distance; however, the effects of the dose distribution will essentially be the same as for wedges and compensators [11, 14].

The effect of the tray on the amount of dose delivered to the point of interest is usually taken into account by applying the tray TF which is defined as the ratio of the dose measured at the reference depth with and without the tray in the beam path for the same number of MUs. According to Van Gasteren et al. [11], two comments can be made on the effect of tray on the dose delivered with respect to the tray TF:

- Firstly, for a particular quality of the photon beam and tray design, the influence of the tray on the energy fluence varies with the actual field size projected on the tray (trays field size) taking the blocked area into account. The magnitude of this depends on the tray-phantom distance and therefore on the source to surface distance (SSD), since the tray is mounted at a fixed point below the head of the treatment machine. In this case, the tray TF can be written as the product of the reference tray TF and a relative tray TF which takes into account the field size and SSD dependence.

  It should be noted that the reference tray TF is the transmission factor measured in the reference irradiation set-up whiles the relative tray TF

University of Ghana http://ugspace.ug.edu.gh

can be found from the ratio of collimator scatter correction factors measured with and without a tray in the beam.

- Secondly, they said that the relative tray TF is close to unity when nearly water equivalent materials (for example polymethylmethacrylate (PMMA), with thickness up to 10mm) are applied. They also stated that the relative tray TF varies less than 2% for field sizes varying from 4cm×4cm to 40cm×40cm; however, there is a more pronounced variation (> 2%) for larger thickness of the tray material and/or for shorter tray to phantom distances (TPDs). They further stated that unless extreme blocking is applied, one may replace the 'tray field size' with the collimator setting (field size) due to the relatively small effects found experimentally for PMMA thickness less than or equal to 10mm.

From these two observations, Van Gasteren et al. [11] concluded that the tray transmission factor can be measured with the mini-phantom as well as in a full scatter phantom; and the values of the relative tray TF have to be obtained for a number of square field sizes covering the full range of clinically used fields and a number of tray-phantom distances. They also recommended that measurements should be repeated at two other SSDs (80cm and 120cm).

2.5.1.2 Influence of a tray on the Relative Depth Dose (RDD)

It has to be noted that for short distances between the tray and phantom surface, electron contamination will substantially increase the surface dose. This effect will not influence readings resulting from the choice of d_{ref} at a depth larger than the range of the contaminating electrons. The variation in the amount of

University of Ghana http://ugspace.ug.edu.gh

contaminating electrons, however, will affect the RDD of the open beam in the first few meters. If clinically relevant, these deviations could be determined by measurement and incorporated in a blocked RDD [11].

2.5.2 Investigations and recommendation on tray factors

Several authors such as Huang et al. [37], Islam and Van Dy [35], Yu Mk and Sloboda [36], Sharma and Johnson [38] have all investigated the effect on the output factor of beam by the presence of beam modifiers such as (block) trays. The influence of field size on the tray TF was reported to be negligible by Sharma and Johnson [38], however the data used in their work were limited to fields within equivalent squares of only 15cm x 15cm. Tatcher and Biarngard [39], studied fields up to 20cmx20cm using a 0.97g/cm^2 acrylic block tray, but found a negligible contribution to head scatter from the block tray and the shielding blocks. Van Dam et al. [40] pointed out that in cases where the field of view on the flattening filter from the point of measurement is shielded by the blocks, the primary photon fluence can be modified, it is noted that for such cases rather extreme blocking close to the collimator rotation axis must be applied.

In the latter part of the 20th century, Jursinic [9], studied the change in the incident primary photon fluence in 6MV and 18MV beams caused by blocks and block trays and found that the total block tray factor can be as much as 3% larger than the single value tray factor that is obtained from measurements in the reference field, depending on the geometry due to the block on the tray. Schaeken and Van Loon [41], also suggested quantifying the influence of the tray on depth–dose data by separate measurements in open field and in fields

University of Ghana http://ugspace.ug.edu.gh

with tray to be able to include differences in depth-dose in dose calculations, especially in the first few centimeters below the surface. They observed a considerable loss of skin sparing and shift of d_{max} due to increased electron contamination in beam with tray.

University of Ghana http://ugspace.ug.edu.gh

CHAPTER THREE

MATERIALS AND METHODS

3.1 MATERIALS

The experimental study and/or data collection was done at the NCRNM of the KBTH. The Center has one Cobalt-60 teletherapy machine (Theratron Equinox 100 cobalt-60 teletherapy unit) which was used in this research. In the measurement of TFs, two main beam modifiers (physical wedge of four different angles and a block tray) shown in Figures 3.1a and 3.1b were used. The experiment was performed using a full scatter large plastic water phantom which mimicked the human tissue(s). Also, a system ion chamber connected to an electrometer (serial number T10005-50316, PTW, Freiburg, Germany) was used to take the readings of the radiation charges interacting with the phantom. These readings were corrected for environmental conditions (Temperature and Pressure) using a barometer and a digital thermometer (Figure 3.2).

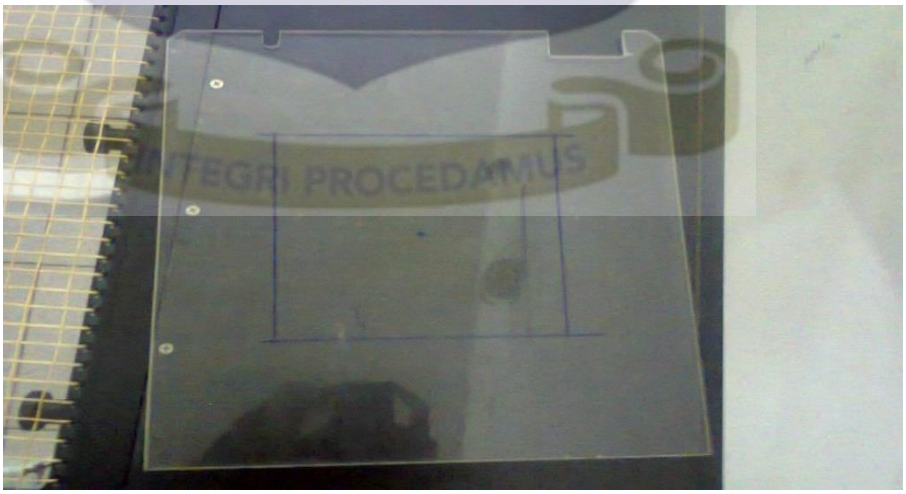

Figure 3.1a: A 6mm thick block tray

University of Ghana http://ugspace.ug.edu.gh

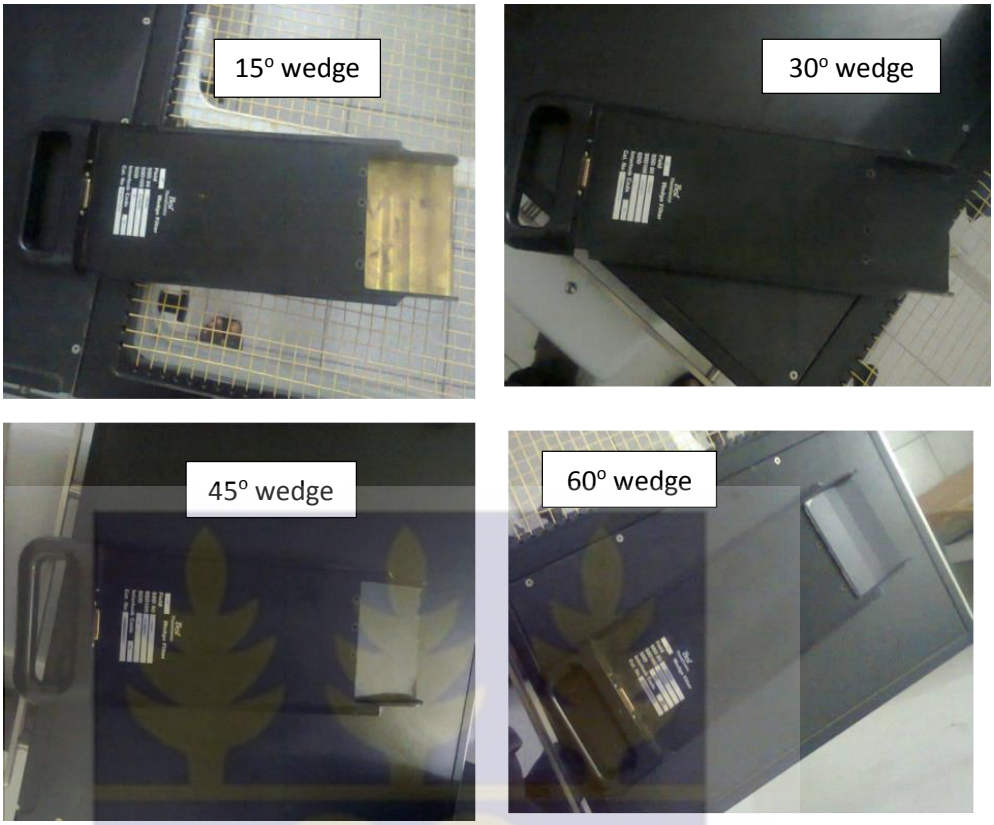

Figure 3.1b: A pictorial view of the physical wedges used in this work

Figure 3.1 Beam modifiers used during this work

a) Digital thermometer b) Barometer

Figure 3.2: Materials used to check environmental conditions during this work

The following sections take a brief look at the specifications of some of the materials used in this work.

University of Ghana http://ugspace.ug.edu.gh

3.1.1 The Theratron Equinox 100 Co-60 teletherapy machine

Theratron Equinox is a teletherapy treatment machine manufactured in Canada with model number 2117 and is owned by NCRNM at KBTH. It consists of a rotatable gantry and collimator, unit head panel, hand control and control console with display monitor as shown in Figure 3.3.

The radiation source is a radioisotope of Co-60 with half-life 5.27 years. The activity of the source and dose rate during measurement on Feb 22, 2014 were 370.4 TBq and 184.63 cGy/min respectively. The Co-60 is sealed inside double layer stainless steel capsule such that the diameter of the whole source assembly is 2.0 cm and 3.0 cm long. The Co-60 atoms spontaneously decay to Ni-60 while emitting two gamma radiations of energies 1.17 MV and 1.33 MV. The energy of the cobalt 60 source is taken as the mean of the two stipulated energies above, which is 1.25 MV.

The Equinox 100 is a fully computerized teletherapy machine, which may be operated either in fixed or arc mode. The following accessories are available: motorized wedge system, physical wedge filters, asymmetrical collimation, and accessories holder system for the support of beam modifying devices such as block trays and compensators. The gantry of the teletherapy machine is mounted iso-centrically.

University of Ghana http://ugspace.ug.edu.gh

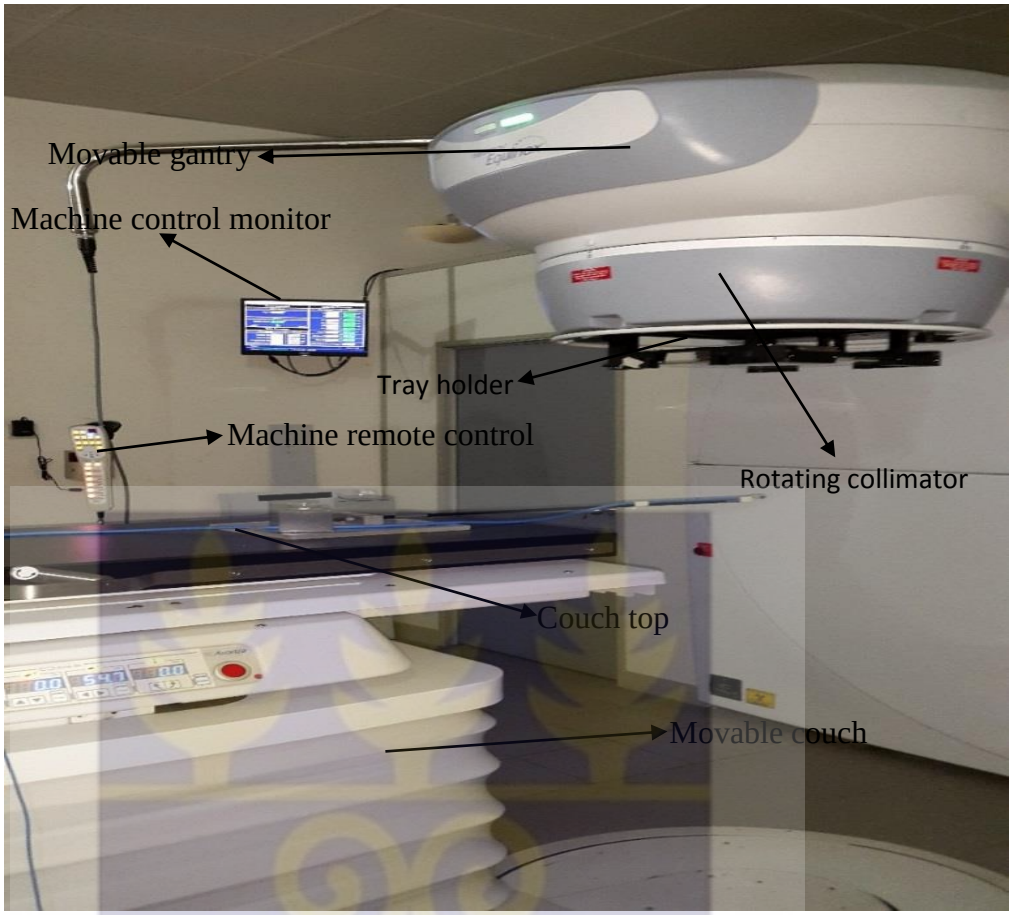

Figure 3.3: The Theratron Equinox 100 Co-60 teletherapy machine

3.1.2 System Ionization chamber

An ion chamber is made up of a collecting electrode and a polarizing electrode between which there is a gas filled cavity. A potential difference is applied between the two electrodes resulting in an electric field inside the cavity. When the chamber is irradiated, secondary electrons are produced thus ionizing the gas within the cavity. The resulting positive and negative ions will move to their respective electrodes due to the presence of the electric field. The total charge collected, or the current produced at the collecting electrode is measured and displayed using an electrometer. The potential difference between the two

University of Ghana http://ugspace.ug.edu.gh

electrodes must be set at a value low enough to minimize charge amplification whilst being large enough to avoid charge recombination.

There are different types of ionization chambers, but in this work a 0.04cc ion chamber manufactured by PTW Freiburg, Germany (model TNC 0503-00, serial number of 11026), is used. The ionization chamber used was calibrated against a source of known beam quality at the IAEA Secondary Standard Dosimetry Laboratory (SSDL). The calibration was done with a bias voltage of 400 V at the temperature of 293K (20^0C), pressure of 101.325kPa and humidity of 50%. Figure 3.4 shows the 0.04cc ionization chamber.

Figure 3.4: A pictorial view of a 0.04cc ion chamber without build up cap

University of Ghana http://ugspace.ug.edu.gh

3.1.3 The PTW UNIDOS Electrometer

There are various kinds of electrometers and with special kinds of functions; however, the electrometer used for measurements during this work is the PTW UNIDOS electrometer (serial number T10005-50316, PTW, Freiburg, Germany).

The PTW UNIDOS electrometer is a high performance secondary standard and reference class dosimeter or electrometer used universally for either radiological or electrical measurements. UNIDOS as a reference class and secondary standard dosimeter is calibrated at the PTW calibration laboratory. PTW-Freiburg is an accredited secondary standard dosimetry laboratory of the German Calibration Service for radiological quantities and a member of the SSDL network organized by the IAEA. Consequently, calibration is based directly on the primary standards of the German Federal Institute of Physics and Metrology (PTB-Braunschweig) and the Bureau International de Poids et Mesure, Paris (BIPM). Ion chambers and solid-state detectors can be connected to the electrometer. The electrometer displays the measured values of dose, dose rate, electric charges and electric currents. Values of dose and dose rates are measured in gray (Gy), Sievert (Sv), Rontgen (R), gray per minute (Gy/min), Sievert per hour (Sv/hr), Rontgen per minute (R/min) or Gy·m; whiles those of electrical charges and currents are measured in coulomb (C) and ampere (A) respectively. The device includes an automatic leakage compensation, an automatic built-in system test and an RS232 interface. It features both on mains (power supply) and battery operation. Figure 3.5 shows the PTW UNIDOS electrometer used during this work.

University of Ghana http://ugspace.ug.edu.gh

Figure 3.5: The PTW UNIDOS electrometer used during this work

3.1.4 Large plastic water phantom

The water phantom used in this work is a locally manufactured water phantom which was made of a 6mm thick clear Perspex glass sides and a 10mm thick clear Perspex glass bottom with a plastic pipe fixed to its side. The clear bottom allows for easy viewing of the chamber and cross hair shadows. The water phantom is a full scatter phantom with size: length = 80cm, width = 70cm and height = 60cm; and it has a volume capacity of about 300L (Figure 3.6)

University of Ghana http://ugspace.ug.edu.gh

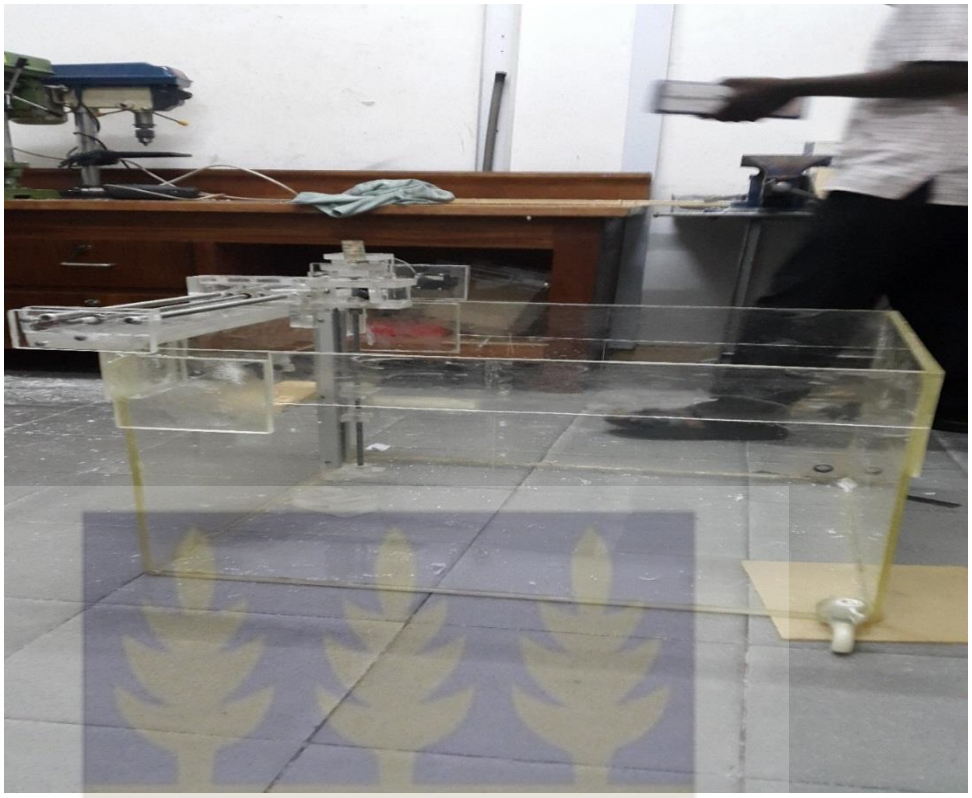

Figure 3.6: A locally manufactured large water phantom

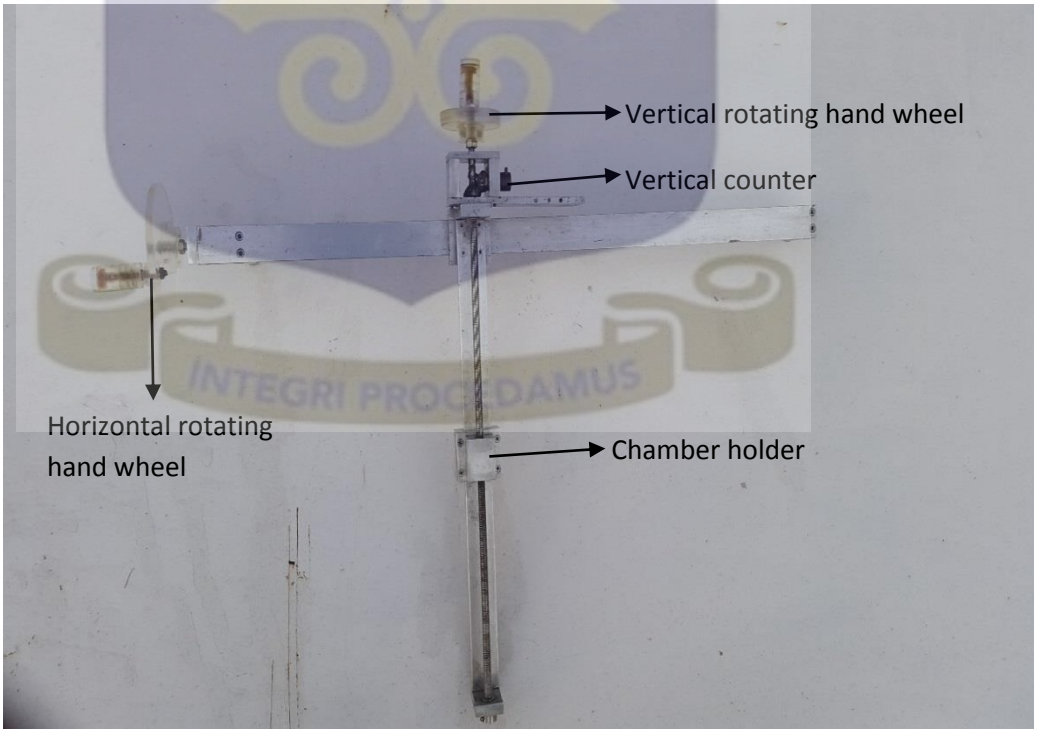

Figure 3.7: The rod with the chamber holder, counter and rotating hand wheel attached to the phantom

University of Ghana http://ugspace.ug.edu.gh

A 70cm long and a 50cm aluminum depth scale with a chamber 'holder' made of a Perspex rod attached to it is fixed to the water phantom at one side (Figure 3.6). The 70cm aluminum 'scaled' bar is placed horizontally on one side of the phantom and is used for off axis ratio (OAR) calculations. The 50cm depth scaled bar which has the chamber holder attached to it, is used in depth measurements and it is fixed on the horizontal aluminum scaled bar. A hand wheel and a mechanical counter is attached to these rods at one end to move the chamber horizontally and/or vertically. The counter was calibrated and it was found that 70counts on the counter was equal to a 1cm shift or travel both horizontally and vertically. One other feature of the mechanical counter is that it can be reset to zero at any position by pressing the reset knob (located on the side of the counter). When using the manual drive large water phantom (as used in this work), the ion chamber placed in the chamber holder (on the vertical aluminum rod) and the preferred hand wheel is used to adjust the chamber to the preferred position (horizontally) and/or depth. The maximum vertical travel is 40cm and that for the horizontal is 60cm.

3.2 METHODOLOGY

This work involves the determination of two main transmission factors (TFs) namely wedge and tray TFs and their dependence on treatment depth and field size using both the source to axis distance (SAD) and source to surface distance (SSD) techniques for both measurements. Physical wedges of four different angles (15^0, 30^0, 45^0, and 60^0; shown in Figure 3.1a-d) were used during this work as well as a 0.6cm thick block tray(Figure 3.1e) which is a plastic plate transparent to light from the light localizer.

University of Ghana http://ugspace.ug.edu.gh

3.2.1 General Procedure and Experimental Set-up

A locally manufactured large water phantom (Figure 3.6) of about 300L in volume is filled with water to simulate the human body and placed on a treatment bed as shown in Figures 3.8 and 3.10. An ionization chamber (Figure 3.4) connected to an electrometer (Figure 3.5) is then placed in the phantom via the 'chamber holder' on the phantom. The ion chamber is then adjusted and its tip ensured to be at the iso-center of the phantom with the aid of fixed lasers (in the treatment room). This is to enable the chamber detect most interacting charges since the most sensitive region where the radiation is felt is the iso-centric region. In order to obtain the exact iso-center of the phantom (or treatment area), three sides of the phantom were vertically marked at their mid portions and the lasers were aligned onto the marks. The intersection (or cross) of the laser is observed and considered to be the iso-center. The ion chamber is thus adjusted and it is ensured that its tip is positioned exactly at the point where the lasers intersect.

University of Ghana http://ugspace.ug.edu.gh

Figure 3.8: A pictorial view of the general experimental set-up

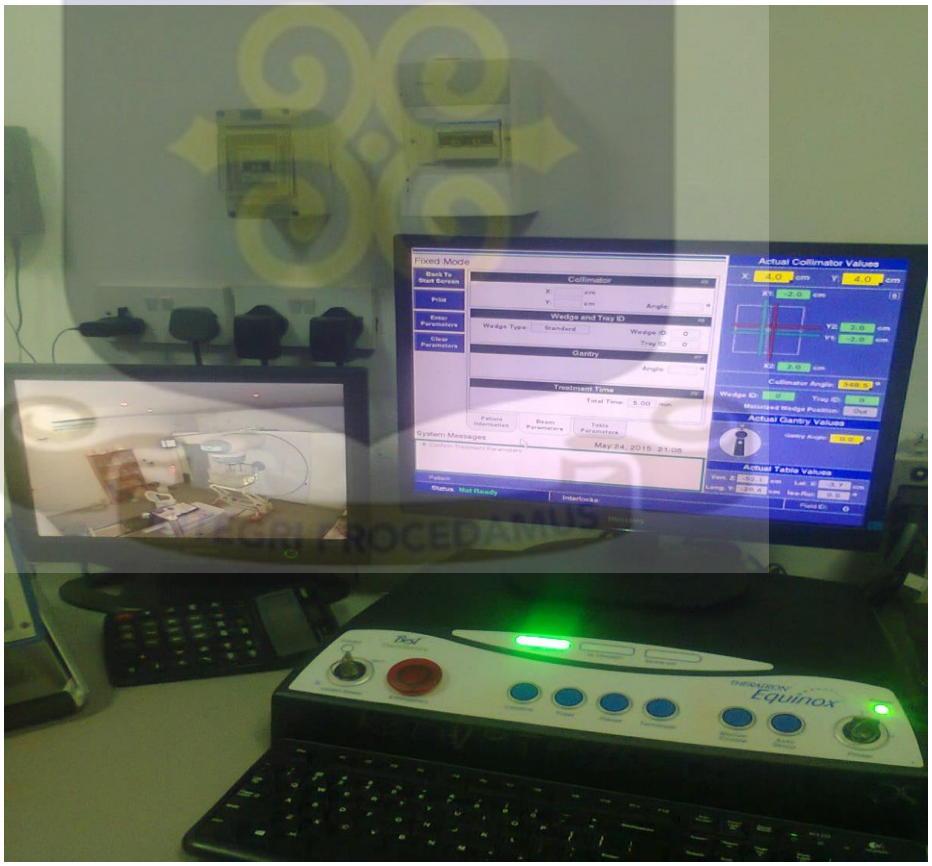

Figure 3.9: Control ‘console’ or computer used in setting the beam parameters before irradiations

University of Ghana http://ugspace.ug.edu.gh

After the set-up, beam parameters are set for irradiation using the 'control console' or computer (shown in Figure 3.9 above) in the control room and the machine's 'remote control' in the treatment room used to confirm these parameters. Throughout the experiment, the gantry angle and collimator angles are set at 0^0; whiles we vary the asymmetric field size from 2x2cm^2 to 18x18cm^2 (for wedge TF measurements) and 4x4cm^2 to 30x30cm^2 (for tray TF measurements). This was done for five different depths of 0.5cm, 6cm, 10cm, 15cm, and 20cm (as recommended by Sharma and Johnson [38]) using both SAD and SSD techniques. A treatment time of 5minutes (300 seconds) is selected for each irradiation for a particular field size chosen and readings are recorded after every 60s for 3minutes and the average taken. These readings are then corrected for temperature and pressure using the formula:

$$\text{corrected reading [nC]} = \frac{273.2+T}{273.2+20} x \frac{101.325}{P} \; x \; Average\; reading\; [nC] \quad (3.1)$$

Where T = Average temperature for each measurement

P = Average pressure during measurement

3.2.1.1 SAD setup for wedge and tray TF measurements

This technique (or setup) takes into consideration the source to axis distance (i.e. the distance from the source to the detector or point of measurement within the phantom) as shown in Figure 2.3. In setting up this technique, the ion chamber is positioned at the iso-center and the phantom is filled with water to the iso-centric region. Using the 'scale' from the control console ('remote control') of the Co-60 machine, a distance of 100cm is set on the surface of the

University of Ghana http://ugspace.ug.edu.gh

water. The tip of the ion chamber is adjusted and ensured to be at the center of the phantom or the point where the lasers intersect in the phantom. Water is then gently added gently added until the scale reads 80cm at the center of the field on the surface of the water. This represents a 20cm depth since the chamber is positioned at a distance of 20cm beneath the surface; thus to vary the depth we drain the water via the plastic tap attached to the phantom and with the use of the 'scale' and field we set the center of the field to the mark (or value) on the scale that sums up with the preferred depth to give 100cm. The difference between this mark and 100 gives us the new treatment depth. The diagram below shows the SAD setup used in this work which was set at 100cm SAD.

Figure 3.10: A pictorial view of the SAD setup used in this work (set at 100cm)

University of Ghana http://ugspace.ug.edu.gh

3.2.1.2 SSD setup for wedge and tray TF measurements

This setup deals with the distance from the source to the surface of the patient or phantom (as shown in Figure 2.3) and not necessarily the point of measurement. In this setup, the tank is placed on the treatment bed and filled almost to capacity. The tank is then adjusted so that the distance from the source to the surface equals 100cm; which is observed by using the scale and field from the machine's remote console. When the 100cm mark on the scale falls exactly on the center of the field, we say we have a 100cm SSD setup. The ionization chamber is then fixed into its holder and positioned right on the surface of the phantom and thus adjusted so that its sensitive area is positioned exactly at the center of the phantom. This center position is obtained by aligning the lasers in the treatment room to the marks lines of the phantom.

In this setup, the treatment depth is varied by moving the rotating hand wheel fixed to the vertical rod that has the chamber attached to it. Connected to the hand wheel is a counter which has been calibrated and found to have 70counts being equivalent to a 1cm shift. Therefore for the TF measurements at a depth of 0.5cm (d_{max}), and with the chamber just on the surface of the phantom (or water), we zero the counter and then rotate the hand wheel until the counter reads 35counts. In like manner for other depths, the chamber is moved by rotating the wheel until the desired counts are obtained. Figure 3.11 shows a physicist undertaking some measurements using the SSD setup or technique.

University of Ghana http://ugspace.ug.edu.gh

Figure 3.11: A physicist undertaking some measurements using the SSD setup

3.2.2 Determination of Wedge and Tray TFs

To determine the wedge and tray TFs, measurement has to be taken for both open field, wedge in beam and tray in beam path. This is because the wedge and tray TF is calculated based on the definition of transmission factor, which says that the TF is expressed as the ratio of the radiation dose with a beam modifier (or device in beam path) to the radiation dose without a beam modifier (or an open field); that is

University of Ghana http://ugspace.ug.edu.gh

$$TF = \frac{radiation\ dose\ with\ a\ beam\ modifier}{\text{radiation dose without a beam modifier}} \quad (3.2)$$

Thus to calculate for the wedge TF we use the formula:

$$Wedge\ TF = \frac{radiation\ dose\ with\ a\ wedge\ in\ beam\ path}{\text{radiation dose for an open field}} \quad (3.3)$$

And for the tray TF we use the formula:

$$Tray\ TF = \frac{radiation\ dose\ with\ a\ tray\ in\ beam\ path}{\text{radiation dose for an open field}} \quad (3.4)$$

As stated earlier both the SAD and SSD setups were used in this work and thus the procedure to determine these two factors for both setups have been outlined in sections 3.2.2.1. After obtaining the measurements from any of the setups, the wedge and tray TF can be determined using equations 3.3 and 3.4 respectively for the various field sizes and treatment depths.

3.2.2.1 Measurement of wedge and tray TFs using either the SAD or SSD technique

After the setup is done (either SAD or SSD) and the phantom is conditioned to attain room temperature, irradiation is then performed for varying field sizes at particular depths for both open field, with wedge in beam path and tray in beam path. This is done by first setting the beam parameters as stated in section 3.2.1 and confirming them (by setting the treatment machine to match those parameters) in the treatment room using the machine's 'remote control'. In the case of the wedge in beam path, the wedge ID was set to correspond to the wedge angle that was being inserted into the machine whiles the tray ID was set at '0' throughout the experiment.

University of Ghana http://ugspace.ug.edu.gh

Before measurements are taken, the system is 'warmed up' by irradiating the phantom for 10minutes. During this time the ion chamber is also checked for consistency as readings are observed after every 60s on the electrometer. After the warm up, readings are now taken by irradiating the phantom for 5minutes within which after every 60s for 3minutes, the readings (in nanoCoulombs (nC)) observed from the electrometer are recorded and the average taken. This is first done at the 20cm depth (in the case of the SAD technique) and d_{max} or 0.5cm (in the case of the SSD technique); for field sizes ranging from $2x2cm^2$ to $30x30cm^2$ (for open field), $2x2cm^2$ to $18x18cm^2$ (for each of the four different angled wedges in beam path) and $4x4cm^2$ to $30x30cm^2$ (for the tray in beam path). At each field size, starting from the smallest to the largest, irradiation is done for open field, followed by the four wedged angles (15^0, 30^0, 45^0, and 60^0) and then the block tray in that order before we move to the next field size. It has to be noted that for each reading at a particular field size, the temperature of the phantom (or water) before and after the irradiation is noted and recorded and the average calculated. Also the pressure of the (treatment) room before irradiation began and that after irradiation was recorded and averaged. These two later readings (temperature and pressure) are used to correct the electrometer readings by using equation 3.1.

The procedure above is repeated for four other depths of 15cm, 10cm, 6cm and 0.5cm; however it has to be noted that, if measurements of various depths are taken on the same day there is no need 'rewarming' the system. Also when using the SAD setup, these depths (15cm, 10cm, 6cm and 0.5cm) are obtained by draining the water in the phantom and using the 'scale' and field on the machine as explained earlier. These depths corresponds to the scale readings of 85cm,

University of Ghana http://ugspace.ug.edu.gh

90cm, 94cm, and 99.5cm respectively which are seen exactly at the center of the field. However, when using the SSD technique or setup, we use the rotating hand wheel to move the ion chamber beneath the water. The hand wheel is moved till the counter reads 420, 700, 1050, and 1400counts which is equivalent to 6cm, 10cm, 15cm, and 20cm respectively.

3.3 DATA ANALYSIS

Due to the large number of data obtained, the Excel programming software was used to analyze the results obtained from the measurement. The version used was that of Microsoft word 2013 plus; and this was used to calculate the average temperature, pressure and electrometer readings throughout the work. The software program was also used to calculate for the corrected readings and the various transmission factors of concern using equations 3.1, 3.3 and 3.4 .Also the Excel program was used to plot various graphs in order to analyze the data obtained from the measurements.

In order to determine the dependence (or variation) of both the wedge and tray TFs on field size and treatment depth, the normalization method was employed to give a fairer and clearer relationship (or variation) between the TFs and the field sizes/treatment depths. In this case, the TF is now referred to as the normalized transmission factor (NTF) and it is defined as the ratio of TF at a given depth and field size to the TF at the normalization point. Mathematically the NTF can be expressed for both depth and field size dependence as in equations (3.5) and (3.6) respectively:

University of Ghana http://ugspace.ug.edu.gh

$$\text{NTF}\ (FS_{ref}, \text{d}) = \frac{TF\ (FS_{ref}, d)}{\text{TF}\ (FS_{ref}, d_{nor})} \quad (3.5)$$

$$\text{NTF}\ (\text{FS}, d_{ref}) = \frac{TF\ (FS, d_{ref})}{\text{TF}\ (FS_{nor}, d_{ref})} \quad (3.6)$$

Where: FS = field size under consideration, FS_{ref} = reference field size, FS_{nor} = normalized field size, d = treatment depth under consideration, d_{ref} = reference depth and d_{nor} = normalized depth.

University of Ghana http://ugspace.ug.edu.gh

CHAPTER FOUR

RESULTS AND DISCUSSION

4.1 INTRODUCTION

This chapter discusses the results obtained from the measurements carried out in this work. TFs for the four physical wedges and block tray used at the NCRNM at the KBTH were obtained and their dependence on treatment depth and field sizes analyzed.

4.2 THE WEDGE TRANSMISSION FACTOR

From the measurements carried out, the wedge TF for each of the physical wedges used was obtained for various field sizes at different treatment depths. These TFs can be seen in Appendix D and F1 for both the SAD and SSD set-ups respectively. In order to obtain a single wedge TF that can be incorporated into dose calculation during treatment planning, the mean wedge TF (for each of the four wedges) with their deviation was calculated for each depth and this is shown in Table 4.1 (SAD set-up) and Table 4.2 (SSD set-up).

University of Ghana http://ugspace.ug.edu.gh

Table 4.1: Mean wedge TFs at various treatment depths for the SAD set-up.

Depth/cm	15º wedge	30º wedge	45º wedge	60º wedge
0.5	0.770±0.003	0.642±0.002	0.497±0.003	0.269±0.004
6	0.771±0.002	0.644±0.003	0.498±0.004	0.270±0.004
10	0.773±0.002	0.646±0.002	0.502±0.003	0.274±0.004
15	0.774±0.001	0.653±0.002	0.508±0.003	0.279±0.004
20	0.777±0.003	0.658±0.002	0.514±0.002	0.285±0.003

Table 4.2: Mean wedge TFs at various treatment depths for the SSD set-up

Depth/cm	15º wedge	30º wedge	45º wedge	60º wedge
0.5	0.768±0.003	0.638±0.002	0.493±0.003	0.266±0.004
6	0.771±0.002	0.645±0.003	0.499±0.003	0.273±0.003
10	0.775±0.003	0.652±0.004	0.504±0.004	0.279±0.004
15	0.777±0.002	0.657±0.004	0.512±0.003	0.286±0.004
20	0.783±0.003	0.666±0.005	0.520±0.002	0.295±0.003

It can be observed from the Tables 4.1 and 4.2 tables that, the amount of attenuation offered by the 15^{o} wedge is least and thus it had the highest TF whiles the 60^{o} attenuated most of the beam and thus had the least TF. The difference in the level of attenuation can be attributed to the thickness of the wedge; since the 15^{o} wedge has a thin edge as compared to the 30^{o}, 45^{o}, and 60^{o} wedges, whose thickness increase in the order.

University of Ghana http://ugspace.ug.edu.gh

Also from Tables 4.1 and 4.2, it can be observed that an increase in the treatment depth showed a slight increase in transmission (that is the amount of radiation reaching the detector with wedge beam in path increased slightly as the depth increased). This shows that with the use of wedges there is an appreciable skin sparing effect. When wedges are used during treatment the doses delivered to the skin is less however deeper tissues tend to receive more dose, this is mainly due to beam hardening as well as the beam pattern and scatter. The dependence on the wedge TF on treatment will be discussed into details in the latter sections.

It has to be noted that the beam hardening effect is dependent on two parameters: the wedge material and angle; and photon energy. From tables 4.1 and 4.2, the 45° and 60° wedges showed larger variation in the wedge TF as thicker materials attenuate the photon flux much more than thinner material which lead to an increased variation in the wedge TF. From the mean TFs obtained at the various depths, it can be deduced that the wedge TF for the 15^{o} wedge is 0.775±0.005, whiles that for the 30^{o} wedge is 0.650±0.010, and that for the 45^{o} wedge is 0.505±0.015 and finally that for the 60^{o} wedge is 0.280±0.015. It can be seen that the deviation increased with increasing wedge angle with the percentage deviation varying from 0.64% for the 15^{o} wedge, to 1.54% for the 30^{o} wedge, to 2.97% for the 45^{o} wedge and then to 5.36% for the 60^{o} wedge. This variation mostly occurred at depths of 15cm and 20cm with slightly higher TFs occurring for the SSD set-up.

University of Ghana http://ugspace.ug.edu.gh

4.2.1 Dependence of the Wedge TF on Treatment Depth

As many researches have opined, the effect of treatment depth on TFs cannot be neglected in today's radiation therapy in order to give optimum treatment to patients. As observed earlier in Table 4.1 and 4.2, the mean wedge TFs were not the same at the various depths; and thus in order to know the dependence of the wedge TF on the treatment depth equation (3.5) was employed, using a reference field size (FS_{ref}) of 10cm×10cm and a normalized depth (d_{nor}) of 0.5cm (for both the SAD and SSD techniques). These choices of the FS_{ref} and d_{nor} were based on recommendations made by Tailor et al. [19], Sharma et al. [38] and Misbah et al. [43]. In view of this the normalized wedge TF for both techniques were calculated using the equation:

$$\text{Normalised Wedge TF}\,(10\text{cm}\times 10\text{cm}, \text{d}) = \frac{wedge\ TF\ (10cm\times 10cm, d)}{\text{wedge TF}\,(10\text{cm}\times 10\text{cm}, 0.5cm)} \quad (4.1)$$

Where d = treatment depth under consideration

From this equation, a table (each for the SAD and SSD techniques) was obtained showing the variation of the normalized wedge TFs with the various treatment depths. Also, a graph of the normalized wedge TF was plotted against the various treatment depths to show the relation between the two.

University of Ghana http://ugspace.ug.edu.gh

Table 4.3: Normalized wedge TFs for different wedge angles at various treatment depth using the SAD set-up

Depth/cm	15º wedge	30º wedge	45º wedge	60º wedge
0.5	1	1	1	1
6	1.0008991	1.00255325	1.00452147	1.0084149
10	1.0039217	1.00881038	1.01242768	1.0218731
15	1.0061996	1.01788582	1.02348354	1.0358158
20	1.0109812	1.02402691	1.03568241	1.0625614

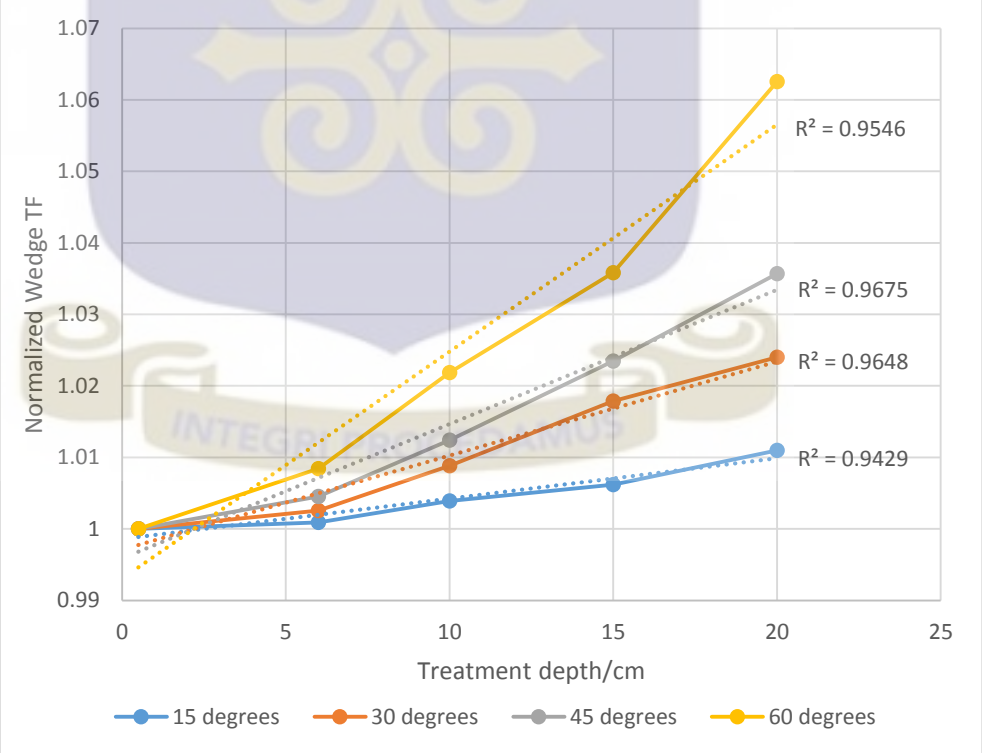

Figure 4.1: A graph showing the dependence of wedge TFs for different wedge angles on treatment depth using SAD set-up

University of Ghana http://ugspace.ug.edu.gh

Table 4.4: Normalized wedge TFs for different wedge angles at various treatment depth using the SSD set-up

Depth/cm	15º wedge	30º wedge	45º wedge	60º wedge
0.5	1	1	1	1
6	1.00338	1.007148	1.011158	1.0161109
10	1.005897	1.0163265	1.0239305	1.038598
15	1.010482	1.0243656	1.0348521	1.0614133
20	1.015951	1.0355182	1.0523395	1.1203931

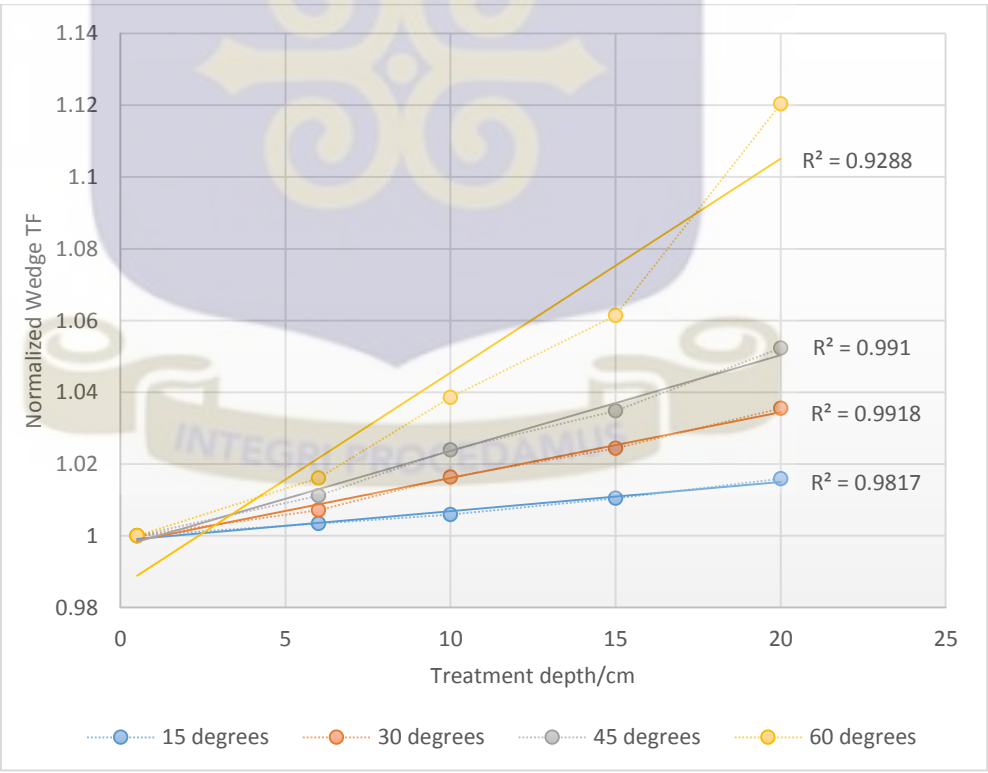

Figure 4.2: A graph showing the dependence of wedge TFs for different wedge angles on treatment depth using SSD set-up

University of Ghana http://ugspace.ug.edu.gh

From both tables (Tables 4.3 and 4.4), it can be observed that the normalized wedge TF increases significantly with treatment depth. However in both set-ups the dependence of the 60° wedge looks stronger followed by the 45° wedge, then the 30° wedge, with the 15° wedge showing the least dependence. This can clearly be observed in Figures 4.1 and 4.2. Also in comparing the two setups using Tables 4.3 and 4.4, it can be seen that the percentage difference (or variation) in wedge TF from d_{max} at the various depths (6cm, 10cm, 15cm and 20cm) is higher for the SSD set-up than the SAD set-up. The percentage difference (or variation) using the SAD set-up ranges from 0.09% to 1.10% for the 15° wedge, 0.25% to 2.40% for the 30° wedge, 0.45% to 3.57% for the 45° wedge and 0.84% to 6.25% for the 60° wedge; whiles for the SSD set-up it ranges from 0.34% to 1.59% for the 15° wedge, 0.71% to 3.55% for the 30° wedge, 1.12% to 5.23% for 45° wedge and 1.61% to 12.04% for the 60° wedge.

The increase in wedge TF with treatment depth mainly arises from beam hardening through the wedge filter which absorbs and/or scatters the low energy photon beams. The beam hardening effect leads to a change in the beam quality and consequently to a modification of the depth dose distribution. The magnitude of this modification is dependent on the composition and thickness of the wedge material as well as the photon beam energy. Since the photon energy in this case is constant (an average of 1.25MeV), it implies that the beam hardening effect is mainly dependent on the wedge material. From Figure 4.1 and 4.2 and the percentage differences, the 45° and 60° wedges showed larger variation in the wedge TF as the thicker (or high density) materials attenuate the photon flux much more than the thinner (or low density materials as in the 15° and 30° wedges) such that it causes an increased variation in the wedge TF. The

University of Ghana http://ugspace.ug.edu.gh

findings from this work agrees with what Misbah et al [43] and Tailor et al [19] reported in their work that at larger depths the ratio of the dose values for wedge and open beam increases with depth. Also Tailor et al [19] and McCullough et al [20] had suggested in their respective reports that for energies equal to or less than 10 MV the depth dependence of the wedge TF is strongly significant (greater than 2%) and can even exceed 5% for 45° and 60° wedges . However, the results from this work also showed a significant variation (greater than 2%) in wedge TF of the 30° wedge with treatment depth (especially for the SSD set-up). This may possibly be due to two reasons: first, the wedge material used in their study was different from what was used in this study and secondly these values are machine specific and slightly dependent on the set-up used [20, 43].

4.2.2 Dependence of the Wedge TF on Field Size

Just as the dependence of the wedge TF on treatment depth cannot be neglected in today's radiotherapy, research has shown that the field size dependence is also equally important. This section tends to look at how the wedge TF of the physical wedges used at the radiotherapy center of the KBTH depends on field size. As stated earlier in order to do this we employ equation (3.6) using a reference depth (d_{ref}) of 0.5cm and a normalized field size (FS_{nor}) of 10cm×10cm for both techniques. Therefore the equation becomes:

$$\text{Normalized wedge TF}\,(FS, 0.5\text{cm}) = \frac{wedge\ TF\ (FS, 0.5cm)}{\text{wedge TF}\,(10\text{cm}\times 10\text{cm}, 0.5cm)} \qquad (4.2)$$

Where FS = field size under consideration

University of Ghana http://ugspace.ug.edu.gh

From equation 4.4, the normalize wedge TFs were obtained for the each of the wedge angles at the various field size. This is shown in Tables 4.5 and 4.6 for both the SAD and SSD set-ups respectively. A graph of the normalized wedge TFs was then plotted against field size for both techniques to see the dependence of the wedge TF on field size. This is shown in Figure 4.3 (SAD technique) and Figure 4.4 (SSD technique)

Table 4.5: Normalized wedge TFs for different wedge angles at various field sizes using the SAD set-up

Field size/cm^2	15^o wedge	30^o wedge	45^o wedge	60^o wedge
2×2	1.0026461	1.00355089	1.0048413	0.99403349
4×4	0.9988376	0.99774039	0.9963341	0.99122864
6×6	0.9984890	0.99925564	0.99733516	0.98845203
10×10	1	1	1	1
14×14	1.0032131	1.00295205	1.0063783	1.01227511
18×18	1.0059619	1.00529813	1.00979204	1.02220278

University of Ghana http://ugspace.ug.edu.gh

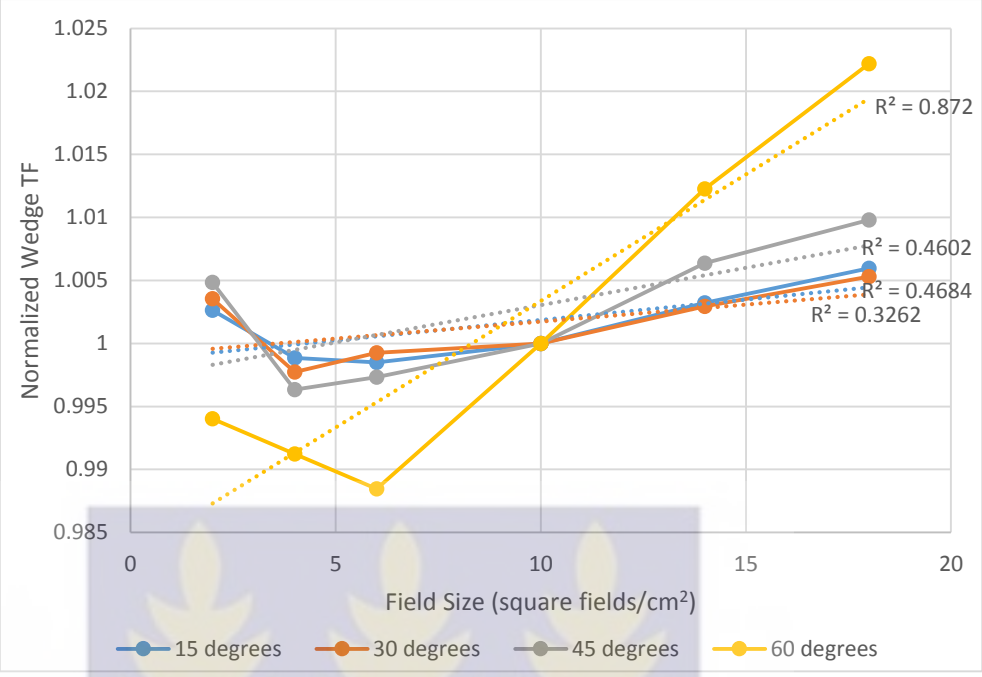

Figure 4.3: A graph showing the dependence of wedge TFs for different wedge angles on field size using SAD technique

Table 4.6: Normalized wedge TFs for different wedge angles at various field sizes using the SSD set-up

Field size/cm^2	15º wedge	30º wedge	45º wedge	60º wedge
2×2	1.000119	1.0018418	1.0030919	0.9930774
4×4	0.996812	0.9934613	0.9898475	0.9834885
6×6	0.998474	0.9968963	0.9945647	0.9895873
10×10	1	1	1	1
14×14	1.002725	1.0004984	1.0039019	1.0106522
18×18	1.007140	1.0038545	1.009931	1.0288161

University of Ghana http://ugspace.ug.edu.gh

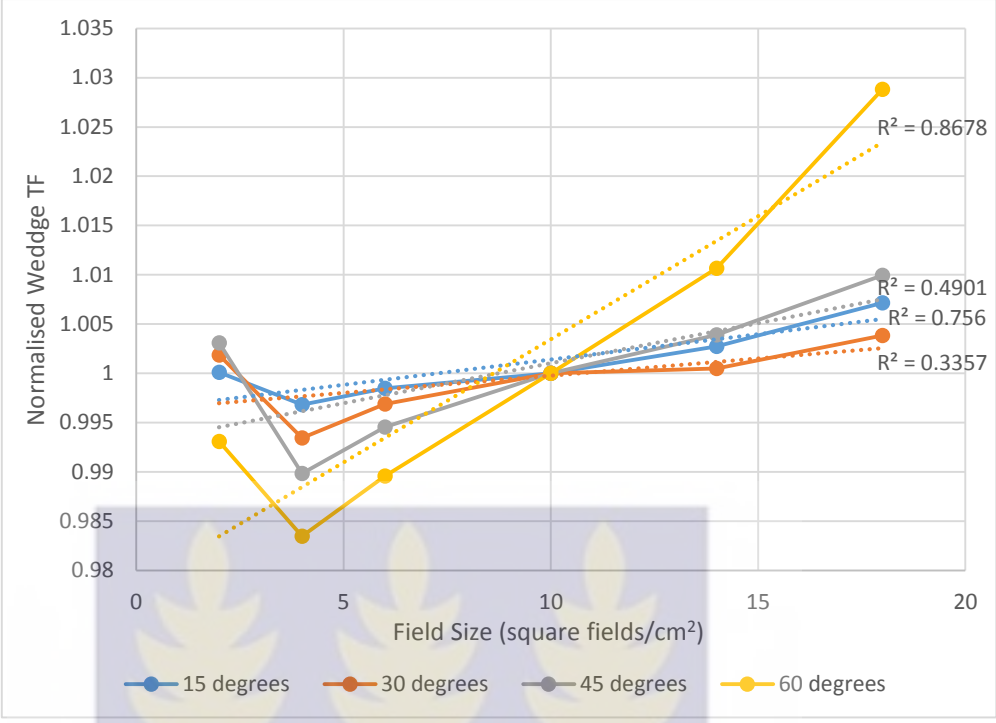

Figure 4.4: A graph showing the dependence of wedge TFs for different wedge angles on field size using SSD set-up

From Figures 4.3 and 4.4 it can be seen that there was a decrease in the wedge TF as the field size was increased from 2×2cm^2 to 4×4cm^2; however as the field size was further increased up to 18×18cm^2, the wedge TF was seen to be increasing slightly. Another interesting trend observed from both graphs is that at field sizes less than the normalized field size (10×10cm^2), the 60^o wedge recorded the least TF (attenuation was high), followed by the 45^o wedge, then the 30^o wedge with the 15^o wedge recording the highest TF (less attenuation). However at field sizes greater than 10×10cm^2, the 60^o wedge produced higher TFs, followed by the 45^o wedge, then the 15^o wedge and 30^o wedge in that order (for the SSD set-up); however in the SAD set-up, the 30^o and 15^o wedges recorded almost the same TFs with the 15^o wedge slightly higher.

University of Ghana http://ugspace.ug.edu.gh

Also from Table 4.5 and 4.6 it can be seen that the percentage variation (or difference) in wedge TF from the normalized field size at the various field sizes is less than or equal to 1% for the 15°, 30° and 45° wedges. Considering the SAD, the percentage variation for the 15°, 30° and 45° wedges rises to a maximum of 0.60%, 0.53%, and 0.98% respectively; whiles for the SSD technique they the percentage variation rises to a maximum of 0.71%, 0.65%, and 1.02% respectively. However the percentage variation for the 60° wedge rises to maximum of 2.22% and 2.88% for the SAD and SSD techniques respectively. In view of this it can be concluded that the dependence of the wedge TF of the 15°, 30° and 45° wedges on field size is less significant (less than 2%) and thus no obvious increasing trend was observed with increasing field size compared to the depth dependency. However, the 60° wedge shows a significant variation as an increase in field size is accompanied by an increase in its wedge TF.

It has to be noted that the variation of the wedge TF with field size may be due to the introduction of non-uniform scattering of photons in the presence of the wedges and/or the filtration of the scattered radiation from the treatment head by the wedge filter. In other words the dependence of wedge TF on field size is mainly due to change in the phantom and collimator scattering due to the presence of physical wedges. Also, the scattered photon fluence increases with the irradiated wedge volume that increases with the field size. However, the nonlinearity with field size may be due to the fact that the scattering is not from a point, rather from within the wedge volume.

University of Ghana http://ugspace.ug.edu.gh

4.3 THE TRAY TRANSMISSION FACTOR

In this work, the tray TF for a 6mm thick block tray (made of Perspex glass which is a tissue equivalent material) was measured at various field sizes and different treatments depths using both the SAD and SSD setups respectively; this is shown in Appendix C and F2. In order to obtain a single tray TF that can be incorporated into dose calculation during treatment planning, the mean tray TF was calculated at each depth for both the SAD and SSD technique and this is shown in Table 4.7.

Table 4.7: Mean tray TFs at various treatment depths for both SAD and SSD set-ups.

	Mean tray transmission factors	
Depth/cm	**SAD set-up**	**SSD set-up**
0.5	0.961±0.004	0.957±0.001
6	0.964±0.002	0.958±0.001
10	0.960±0.001	0.958±0.001
15	0.965±0.002	0.957±0.001
20	0.962±0.003	0.958±0.001

It can be observed from Table 4.7 that the tray TF for the SAD set-up was higher than that obtained from the SSD set-up at all the treatment depths and also the TFs recorded for the SSD set-up seems constant at all the depth whiles that for the SAD varies slightly. This can be attributed to the change in tray-phantom

University of Ghana http://ugspace.ug.edu.gh

distance (TPD) for the SAD technique. For a particular photon beam energy and tray design (or thickness), the magnitude of variation on the influence of the tray on the energy fluence (in terms of attenuation) depends on the TPD [11]. Therefore since for the SSD set-up the distance from the source to the surface of the phantom is kept constant (thus constant TPD), the magnitude of attenuation (hence TF) is also constant whiles that for the SAD varies due to varying distance from source to phantom surface (varying TPD).

Also from Table 4.7, it can be deduced that the 6mm thick tray (made of Perspex glass) has a mean TF of 0.960 with a standard deviation of ±0.003 representing 0.31%. This TF is close to unity (1.0) and agrees with a number of works carried out by other researchers. Van Gasteren et al [11] for instance indicated in their work that the tray TF is close to unity when nearly water (or tissue) equivalent materials with thickness less than or equal to 10mm are applied.

4.3.1 Dependence of the Tray TF on Treatment Depth

Just as in the case of the wedge TF, equation (3.5) was used to generate the dependence of the tray TF on treatment depth. Using a normalized depth (d_{nor}) of 10cm (based on the recommendations made in various reports such as Mijnheer et al [10], Van Gasteren et al [11] and Gibbon et al [13]) and a reference field size (FS_{ref}) of 10cm×10cm, the normalized tray TF at various depths for both SAD and SSD technique was calculated using the equation:

$$\text{Normalised tray TF}\,(10\text{cm}\times 10\text{cm}, \text{d}) = \frac{tray\ TF\ (10cm\times 10cm, d)}{\text{tray TF}\,(10\text{cm}\times 10\text{cm}, 10cm)} \quad (4.3)$$

Where d = treatment depth under consideration

University of Ghana http://ugspace.ug.edu.gh

From this calculation, the variation of the normalized tray TFs with the various treatment depths was obtained (Table 4.8), and a graph of the normalized tray TFs was plotted against treatment depth to show the relationship between the two.

Table 4.8: Normalized tray TFs at various treatment depths for both SAD and SSD set-ups

	Normalized tray transmission factors	
depth/cm	**SAD set-up**	**SSD set-up**
0.5	0.995033	0.999411
6	1.000972	1.000235
10	1	1
15	1.005036	1.000812
20	1.005974	1.001236

University of Ghana http://ugspace.ug.edu.gh

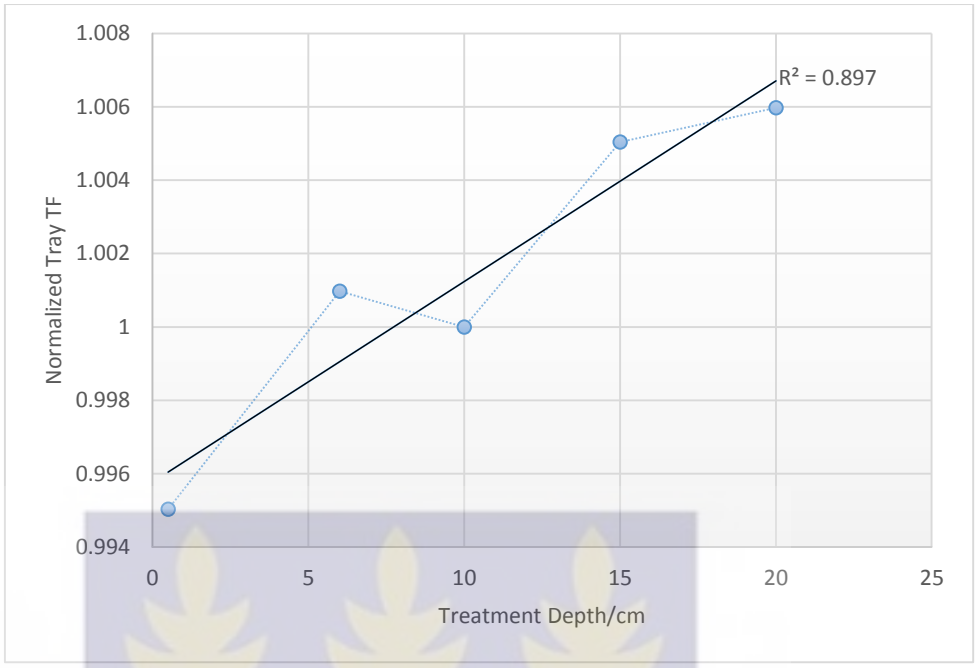

Figure 4.5: A graph showing the dependence of tray TFs on treatment depth using the SAD set-up

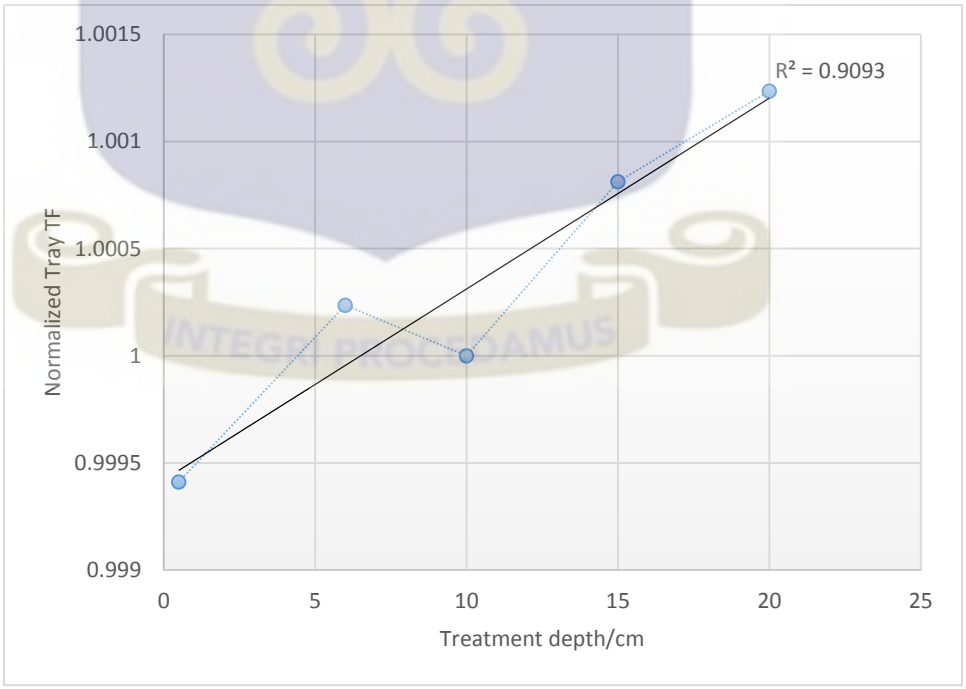

Figure 4.6: A graph showing the dependence of tray TFs on treatment depth using the SSD set-up.

University of Ghana http://ugspace.ug.edu.gh

From Table 4.8, it can be observed that the normalized tray TF increases significantly with treatment depth for both the SAD and SSD technique. Also Figures 4.5 and 4.6 show a strong linear dependence of the tray TF on treatment depth. However the percentage difference (or variation) of the tray TF at the various depths from the normalized depth (d_{nor} = 10cm) ranges from 0.10% to 0.60% for the SAD technique and 0.02% to 0.12% for the SSD technique. Thus the graphs show a strong linear dependence with less significant variation (less than 2%). This agrees with the findings of Mijnheer et al [10], who stated in their report that the variation of the tray TF at various depths has been found to be less than 1% for 10cm×10cm and 20cm×20cm field sizes both in cobalt-60 beams and 18MV x-ray beams; and thus a single tray TF can be used for all treatment depths. Also it can be seen that the percentage variation in the SAD set-up is higher than that in the SSD set-up, this can be attributed to the varying TPD in the SAD set-up.

4.3.2 Dependence of the Tray TF on Field Size

Concerning the field size dependency of tray TFs, equation (3.6) was used to generate the relationship between the tray TF and field size. A normalized depth (d_{nor}) of 10cm and a reference field size (FS_{ref}) of 10cm×10cm was used to modify the equation and therefore the normalized tray TF at various field sizes (FS) for both SAD and SSD techniques was calculated using the equation:

$$\text{Normalized tray TF (FS, 10cm)} = \frac{tray\ TF\ (FS,10cm)}{\text{tray TF (10cm×10cm,10}cm)} \qquad (4.4)$$

Where FS = field size under consideration

University of Ghana http://ugspace.ug.edu.gh

From this calculation, the normalized tray TFs at the various field sizes was obtained (this is shown in Table 4.9), after which a graph of the normalized tray TFs was plotted against field size in order to determine the relationship between the two.

Table 4.9: Normalized tray TFs at various field sizes for both SAD and SSD set-ups

	Normalized tray transmission factor	
Field size/cm^2	**SAD set-up**	**SSD set-up**
4×4	1.0004129	1.0003884
6×6	0.9988798	0.999415
8×8	1.0005981	-
10×10	1	1
14×14	1.0001602	1.0010356
18×18	1.0008312	1.0015082
22×22	1.0013792	1.0017617
26×26	1.0026008	-
30×30	1.0029375	-

University of Ghana http://ugspace.ug.edu.gh

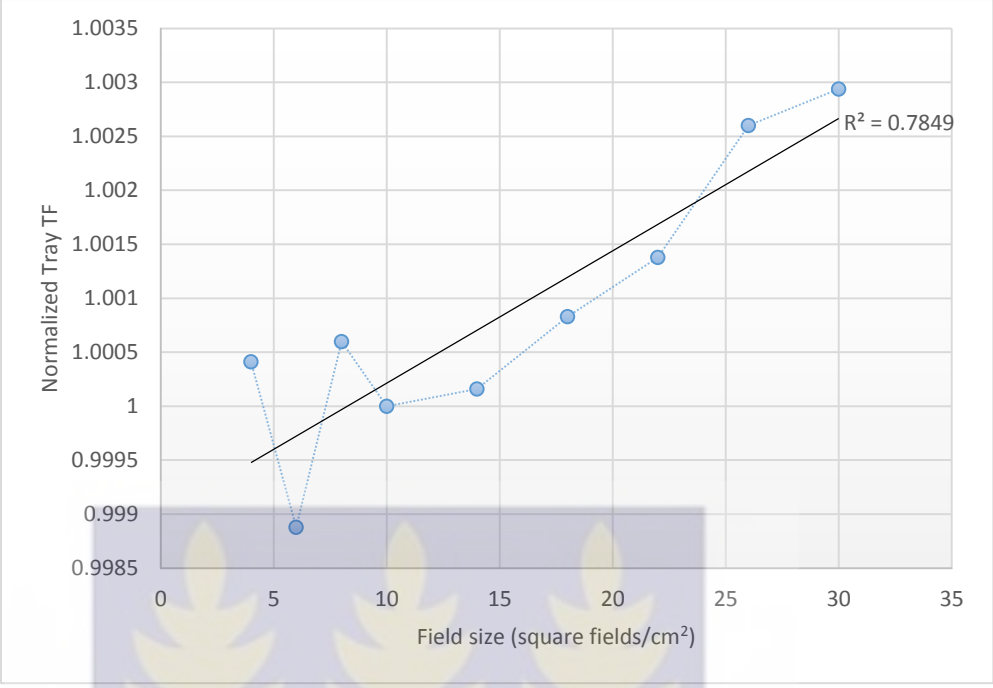

Figure 4.7: A graph showing the dependence of tray TFs on field size using the SAD set-up

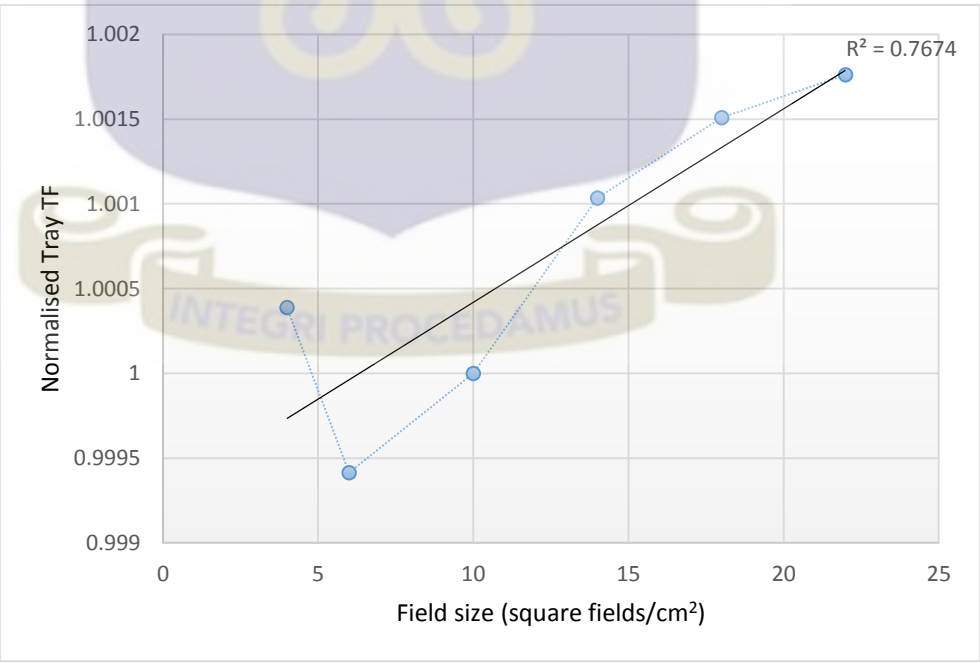

Figure 4.8: A graph showing the dependence of tray TFs on field size using the SSD set-up

University of Ghana http://ugspace.ug.edu.gh

Although Figures 4.7 and 4.8 show a linear dependence of the tray TF on field size for both SAD and SSD set-ups respectively, it can be observed that for field sizes less than 10cm×10cm, the normalized tray TF does not show any particular trend in its dependence on field size. However above the 10cm×10cm field size, an increase in field size is accompanied with an increase in the normalize tray TF. This increase may be due to the scatter from the tray, which is a maximum source of secondary electrons, generated by the primary radiations. These electrons will travel in the forward direction so when the field size increases (from 10cm×10cm to 30cm×30cm), the irradiated area of the tray increases and this results in an increase of the tray TF.

Also from Table 4.9, the percentage difference (or variation) of the tray TF at the various field sizes from the normalized field size (10cm×10cm) was obtained, and this was found to be ranging from 0.02% to 0.29% for the SAD technique and 0.03% to 0.18% for the SSD technique. Therefore though the graphs in Figures 4.7 and 4.8 show a strong linear dependence of the tray TF on field size, the percentage variation shows only a slight dependence. And thus, since the maximum percentage difference for both set-ups is far less than 1%, the field size dependence is almost negligible. This agrees with the conclusion made by Sharma and Johnson [38] in their report that: the influence of field size on the tray transmission factor negligible. Also Tatcher and Biarngard [39] in their work found a negligible contribution to head scatter from the block tray and thus a negligible variation of tray TF with increasing field size. It can therefore be concluded that the variation of the tray TF with increase in field size is far less significant (less than 2%) and thus a single tray TF can be used for all field sizes.

University of Ghana http://ugspace.ug.edu.gh

4.4 THE SAD SET-UP VERSUS THE SSD SET-UP

Most researches carried out in determining TFs focused on using the SSD set-up (most often set at 100cm) with a few using the SAD set-up. In this work however, both the SAD and SSD set-ups were used both set at 100cm as described in the previous chapter. With insufficient literature about the use of both the SAD and SSD set-ups and/or techniques in a 'single' TF determination; comparison, verification and an in-depth discussion of the results obtained in this work becomes difficult. However considering the theory behind both techniques some deductions can be made and thus have an idea of what to expect from the results obtained.

Fixed SSD setup requires moving the patient such that the skin is at the correct distance (nominal SSD) for each beam orientation whiles the iso-centric (SAD) technique require placing the patient such that the target is at the iso-center and thus the machine gantry is then rotated around the patient for each treatment field. The SSD is therefore defined as the distance from the source to the surface of the patient (or phantom) whiles the SAD is defined as the distance from the source to the point of detection. Dosimetrically, there is little difference between these two techniques: fixed SSD arrangements are usually used at a greater SSD than iso-centric (SAD) beams and therefore have a slightly higher percentage depth dose (PDD) at higher depths [6]. Additionally, beam divergence is smaller with SSD due to the larger distance. These advantages are small and, with the exception of very large fields exceeding $40\times40cm^2$, the advantages of the SAD technique greatly outweigh the dosimetric advantage of the SSD technique [6].

University of Ghana http://ugspace.ug.edu.gh

4.4.1 Effect of Depth Variation on both SAD and SSD Techniques

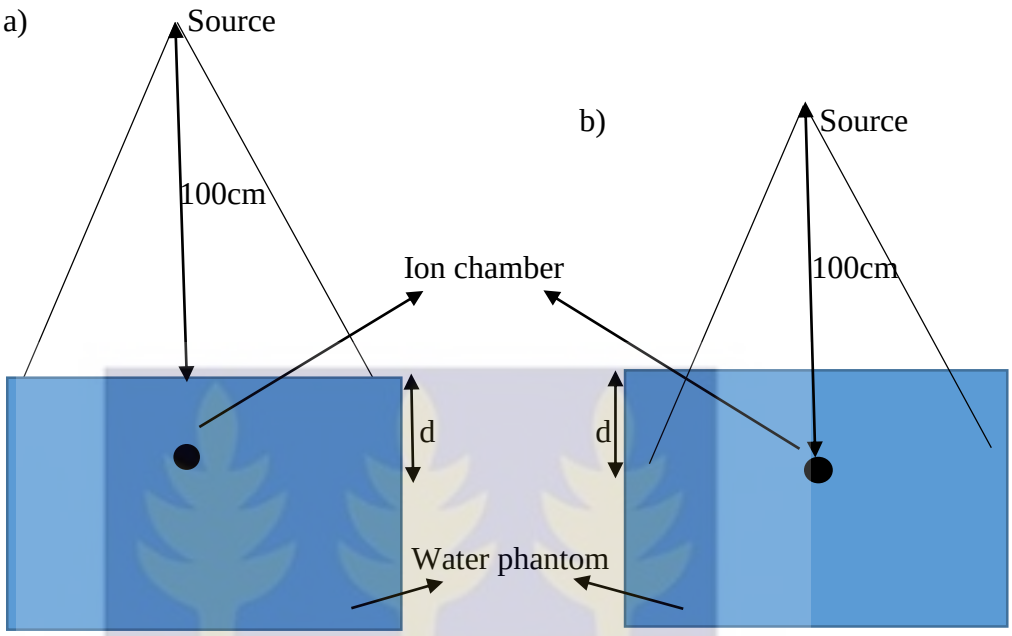

Figure 4.9: Schematic diagram of the a) SSD and b) SAD techniques both set at 100cm from the source. In both cases the ion chamber is at a depth, d in the water phantom.

It has to be noted that an increase in depth, d (or tissue thickness) increases the distance from source to detector in the SSD set-up whiles that for the SAD remains the same. Also the distance from the source to the surface of the phantom (SSD), in the SSD technique is kept constant whiles that of the SAD decreases with increase in depth. This is illustrated in the Figure above. It can clearly be observed from the Figure that during measurement at a cretain depth d, the distance from the source to the detector in the SSD set-up is '100cm+d' whiles that in the SAD set-up is 100cm. Also at a certain depth d, the distance from the source to the surface of the phantom in the SAD becomes '100cm-d' whiles that of the SSD remains at 100cm. This is because in the SSD set-up the ion chamber (detector) is moved down the phantom in order to vary the depth

University of Ghana http://ugspace.ug.edu.gh

whiles in the SAD set-up the chamber's position is maintained and depth is varied by the addition/removal of water.

The difference in distance from the source to the detector in both techniques can attribute to a variation or difference in the amount of radiation detected by the ion chamber in the set-ups. This difference can be as a attributed to the inverse square law (ISL) since all other parameters (beam energy, treatment depth, and field size) are the same thus scattering and attenuation would be the same in both set-ups. The ISL states that the intensity of radiation from a point source decreases as the square of the distannce from the source in a non-absorbing medium increases. This means that for the same tissue thickness (or treatment depth), field size and beam energy, a greater distance from the source should have lesser amount of radiation reaching or being detectored by the ion chamber and vice versa. This agrees with what Podgorsak [6] wrote in his book: as distance increases, relative change in dose rate decreases which results in an increase in PDD (since there is less of a dose decrease due to distance), although the actual dose rate decreases. It can therefore be concluded that for the two set-ups shown in Figure 4.9 the SAD technique should have more charges (or radiation doses) reaching the ion chamber than for the SSD technique.

University of Ghana http://ugspace.ug.edu.gh

4.4.2 Wedge in beam path

From the results obtained for both set-ups with wedge in beam path (considering the mean wedge TFs in Table 4.1 and 4.2), there were slight differences in the transmission factors obtained at particular depths. These differences have been shown in Table 4.10 below where the mean wedge TFs for the SSD set-up was subtracted from the mean wedge TFs for the SAD set-up.

Table 4.10: Quantitative difference between mean wedge TFs obtained from both SAD and SSD techniques.

Depth/cm	15° wedge	30° wedge	45° wedge	60° wedge
0.5	0.002	0.004	0.004	0.003
6	0.000	-0.001	-0.001	-0.003
10	-0.002	-0.006	-0.002	-0.005
15	-0.003	-0.004	-0.004	-0.007
20	-0.006	-0.008	-0.006	-0.010

From the above table, it can be observed that at the 0.5cm depth, for all the wedge angles, the wedge TF for the SAD set-up was slightly higher than that of the SSD set-up (that is the amount of radiation reaching the detector with wedge in beam path was higher for the SAD set-up as compared to the SSD set-up). However, as the treatment depth increased that is for the 6cm, 10cm, 15cm and 20cm depths, the wedge TFs for the SSD technique was slightly higher than that of the SAD technique. This shows that the SSD technique produced slightly higher TFs than the SAD technique at all depths except the 0.5cm depth (which

University of Ghana http://ugspace.ug.edu.gh

is sometimes referred to as d_{max}, which is the depth of maximum dose for the cobalt-60 teletherapy unit).

This findings, most particularly for the depths higher than 0.5cm, contradicts the theoretical deductions made in section 4.4. This is because from the ISL with all other parameters the same (that is same beam energy, tissue thickness or depth, field size and beam modifier in beam path), the amount of radiation reaching the detector (ion chamber) must decrease with increasing distance. Therefore it was expected that the SAD technique records slightly higher TFs than that of the SSD technique. In view of this it would be recommended that further research be carried out to ascertain the findings of this work or otherwise with wedge in beam path most especially for depths greater than d_{max}.

4.4.3 Tray in beam path

Just like the wedge in beam path, the results obtained for both SAD and SSD set-ups with tray in beam path showed slight differences in the transmission factors obtained at the various depths. These differences have been shown in Table 4.11 below where the mean tray TFs for the SSD set-up was subtracted from the mean tray TFs for the SAD set-up at particular depths.

University of Ghana http://ugspace.ug.edu.gh

Table 4.11: Quantitative difference between mean tray TFs obtained from both SAD and SSD techniques

Depth/cm	SAD-SSD for tray TF
0.5	0.004
6	0.006
10	0.002
15	0.008
20	0.004

These differences unlike the wedge in beam path showed that the mean tray TFs for the SAD technique was higher than that of the SSD technique at all depths. This observation or findings agrees with the theoretical deductions made in section 4.4. It however has to be noted that the variation (or difference) was not constant and didn't follow any particular trend; and thus just as with the wedge in beam path further studies into the use of both the SAD and SSD technique and their variation thereof in tray TF determination would be recommended.

University of Ghana http://ugspace.ug.edu.gh

CHAPTER FIVE

CONCLUSSION AND RECOMMENDATION

5.1 CONCLUSSION

From the research carried out the wedge TF for the various wedge angles was found to be as follows: 0.775±0.005 for the 15^o wedge, 0.650±0.010 for the 30^o wedge, 0.505±0.015 for the 45^o wedge, and 0.280±0.015 for the 60^o wedge. The wedge TF increases significantly with treatment depth; with the 60^o wedge showing the strongest variation (or dependence), followed by the 45^o wedge, then the 30^o wedge. The 15^o wedge showing the least dependence. In terms of the field size dependency, the wedge TF was seen to be increasing slightly with an increase in field size; however the percentage variations obtained for the 15^o, 30^o and 45^o wedges were less significant and thus no obvious increasing trend in the wedge TF was observed with increasing field size as compared to the depth dependency. However, the 60^o wedge showed a significant variation of 2.22% and 2.88% for the SAD and SSD techniques respectively. An interesting trend was also observed as the 60^o wedge recorded the least TF, followed by the 45^o wedge, then the 30^o wedge with the 15^o wedge recording the highest TF at field sizes less than 10×10cm^2. However at field sizes greater than 10×10cm^2, the 60^o wedge was found to produce higher TFs, followed by the 45^o wedge, then the 15^o wedge and 30^o wedge in that order (for the SSD set-up); however for the SAD set-up, the 30^o and 15^o wedges recorded almost the same TFs with the 15^o wedge slightly higher. It can therefore be concluded that the wedge TF (for all wedge angles) depends on the treatment depth whilst only the 60^o wedge shows a significant variation with field size.

University of Ghana http://ugspace.ug.edu.gh

The TF of the tray used in this work was also found to be 0.96±0.003. It was realized that the tray TF increases slightly with increasing depth, however the percentage variation of the tray TF with treatment depth was less significant (0.10% to 0.60% for the SAD technique and 0.02% to 0.12% for the SSD technique). This was not much different from the field size dependency as an increase in field size (from $10\times10cm^2$ upwards) was accompanied with a slight increase in the tray TF. However, the percentage variation of the tray TF with field size was found to be ranging from 0.02% to 0.29% for the SAD technique and 0.03% to 0.18% for the SSD technique. These variations were far less than 1% and therefore it can be concluded that the dependence of the tray TF on field size and treatment depth is almost negligible and thus a single tray TF can be used for all treatment depths and field sizes.

Comparing the two set-up techniques used, it was observed that they recorded almost the same transmission values. However, the SAD technique recorded slightly higher tray TFs than that of the SSD technique whiles the SSD technique recorded slightly higher wedge TFs than that of the SAD technique (except at d_{max}). It can therefore be said the theory behind both techniques was obeyed during tray TF measurements.

Based on the findings from this work, it can be concluded that most of the results observed agreed with literature and thus these findings/results can serve as guideline values that can be incorporated into the treatment planning of patients undergoing radiotherapy in order to address any discrepancies in dose delivery at the NCRNM of the KBTH.

University of Ghana http://ugspace.ug.edu.gh

5.2 RECOMMENDATION

The following are the recommendations made to the various stake holders in the treatment of cancer at the NCRNM of the KBTH as well as regulatory bodies and the research community.

5.2.1 Clinical Community

Since it has been reported that most centers ignore the depth and field size dependence of most TFs, it is recommended that the depth and field size dependence of the TFs all beam modifiers used for treatment be considered and incorporated into treatment planning in order to deliver accurate (optimal) doses to patients. Also it is recommended that the findings and/or results of this work be used as guideline values that can be incorporated into the treatment planning of patients undergoing radiotherapy in order to address any discrepancies in dose delivery at the NCRNM of the KBTH.

5.2.2 Policy Makers and Regulators

It is recommended that policy makers and regulators ensure that all radiotherapy centers have a protocol on the dependence of transmission factors of beam modifiers (such as wedges, block tray, compensators and table couch) used for treatment on the various beam parameters.

University of Ghana http://ugspace.ug.edu.gh

5.2.3 Research community

As stated by Podgorsak [6] and Khan [8], when electron or photon beam is incident on a patient or phantom, the absorbed dose in the patient or phantom varies with depth and depends on beam energy, field size, beam collimation system and SSD/SAD. In view of this, and the findings of this research, a further extension of this work is recommended for the investigation of the variations of wedge and tray TFs as a function of other treatment parameters such as beam energy and SSD/SAD. Since the NCRNM at the KBTH is preparing to receive a linac machine which operates with different beam energies, it would be expedient to know the dependence of these TFs on varying beam energies beforehand. Also, it is recommended that research be carried out on the combined use of block tray and wedge in order to determine the effective TF of these beam modifiers.

Finally, it was observed from this work that due to insufficient literature about the use of both the SAD and SSD technique in a 'single' transmission factor determination, comparing their results and drawing vivid conclusions was difficult. It is therefore recommended that further studies be done using both SAD and SSD set-ups in TF determination in order to verify the theory behind both set-ups.

University of Ghana http://ugspace.ug.edu.gh

REFERENCES

[1] Fontenla D. P., Napoli J. J., Hunt M., Fass D., McCormick B. et al., (1994), "Effects of beam modifiers and immobilization devices on the dose in the build-up region". Int J Radiat Oncol Bio Phys. Vol. 30: 211-219.

[2] Gerbi B. J. and Khan F. M., (1990), "Measurement of dose in the buildup region using fixed-separation plane-parallel ionization chambers", Med Phys., Vol. 17: 17-26

[3] Ravikumar M. and Ravichandran R., (2000) "Dose measurements in the build-up region for the photon beams from Clinac-1800 dual energy medical linear accelerator". Strahlentherapie and Onkologie, Vol. 176: 223-228.

[4] Bilge H., Ozbek N., Okutan M., Cakir A., and Acar H., (2010) "Surface dose and build-up region measurements with wedge filters for 6 and 18 MV photon beams". Japanese Journal of Radiology, Vol. 28: 110-116.

[5] Mayles P., Nahum A., and Rosenwald J. C., 2007, "Handbook of Radiotherapy Physics: Theory and Practice", Published by Taylor and Francis Group, LLC; Vol. 12: 225-244.

[6] Podgorsak E. B., (2005), "Radiation Oncology Physics: A Handbook for Teachers and Students", Sponsored by IAEA; 161-271

[7] ICRU Report No. 50, (1994) "Prescribing, Recording and Reporting Photon Beam Therapy," Washington, DC: International Commission on Radiation Units and measurements.

University of Ghana http://ugspace.ug.edu.gh

[8] Khan F. M., (2010), "The Physics of Radiation Therapy", 4th Edition; 235-245.

[9] Jursinic P. A., (1999), "Changes in Incident Photon Fluence of 6 and 18MV X-rays Caused by Block and Block Trays", Med Phys., Vol. 26; 2092-2098.

[10] Mijnheer B., Brider A., Garibaldi C., Torzsok K., and Vernelaar J., (2001), "Monitor Unit Calculation for High Energy Photon Beams – Practical Examples", Physics for Clinical Radiotherapy, ESTRO Booklet 6; 18-20

[11] Van Gasteren J. J. M., Heukelom S., Jager H. N., Mijnheer B., Van der Laarse R., Van Kleffens H. J., Venselaar J. L. M., and Westernmann C. F., (1998), "Determination and Use of Scatter Correction Factors of Mega Voltage Photon Beams", Report 12, Netherlands Commission on Rdiation Dosimetry; 32-43.

[12] International Commission on Radiation Units and Measurements (ICRU), (1976), "Determination of Absorbed Doses in a Patient Irradiated by Beams of X or Gamma Rays in Radiotherapy Procedures, Report 24, ICRU Publication, Washington, DC.

[13] Gibbon J. P., Antolak J. A., Followill D. S., Huq M. S., Klein E. E., Lam K. L., Palta J. R., Roback D. M., Reid M. and Kahn F. M., (2014) "Monitor Unit Calculations for External Photon and Electron Beams", Report of the AAPM Therapy Physics Committee Task Group No. 71, Med Phys. Vol. 41(3), 3-20.

University of Ghana http://ugspace.ug.edu.gh

[14] Dutreix A., Bjarngard B. E., Mijnheer B., Brider A., Shaw J. E., and Svensson H., (2001), "Monitor Unit Calculation for High Energy Photon Beams", Physics for Clinical Radiotherapy, ESTRO Booklet 3; 11-18.

[15] Poffenbarger B. A. and Podgorsak E. B., (1998), "Viability of an iso-centric cobalt-60 teletherapy unit for stereotactic radiosurgery", Med. Phys., Vol. 25; 1935–1943.

[16] Warrington, A. P. and Adams, E. J., (2001), Conformal and intensity modulated radiotherapy using cobalt-60 and 6 MV x-ray beams: A treatment planning comparison of different sites, Radiotherapy Oncology, vol. 61; (Suppl. 1); S73–S74.

[17] Almond P. R., Biggs P. J., Coursey B. M., Hanson W. F., Huq M. S., Math R., Rogers D. W. O., (1999), "AAPM's TG 51 Protocol for Clinical Reference Dosimetry of High-Energy Photon and Electron Beams, Med Phys. 26 (9); 1848 - 1860.

[18] Heukelom S., Lanson J. H., and Mijnheer B. J., (1994) "Wedge factor constituents of high energy photon beams: Field size and depth dependence," J. Eur. Soc. Therap. Radiol. Oncology, Vol. 30; 66–73.

[19] Tailor R. C., Followill D. S., and Hanson W. F., (1998), "A first order approximation of field-size and depth dependence of wedge transmission," Med. Phys., Vol. 25 (2); 241–244.

[20] McCullough E. C., Gortney J., and Blackwell C. R., (1988) "A depth dependence determination of the wedge transmission factor for 4–10 MV photon beams," Med. Phys., Vol. 15 (4); 621–623.

[21] Khan F. M., (1993), "Dosimetry of wedged fields with asymmetric collimation," Med. Phys., Vol. 20; 1447–1451.

University of Ghana http://ugspace.ug.edu.gh

[22] Georg D., (1999), "Monitor unit calculation on the beam axis of open and wedged asymmetric high-energy photon beams," Phys. Med. Biol. 44; 2987–3007.

[23] Smulders B.,Bruinvis I. A., and Mijnheer B. J., (2002), "Monitor unit calculations for wedged asymmetric photon beams," Phys. Med. Biol. 47; 2013–2030.

[24] Mihailidis D. N., Tomara P. D., and Gibbons J. P., (2005) "Measurements of primary off-axis ratios in wedged asymmetric photon fields: A formalism for dose and monitor unit calculations," Phys. Med. Biol. 50; 2003–2014.

[25] Chui C. S. and LoSasso T., (1994), "Beam profiles along the non-wedged direction for large wedged fields," Med. Phys. 21; 1685–1690.

[26] Storchi P. and Woudstra E., (1995), "Calculation models for determining the absorbed dose in water phantoms in off-axis planes of rectangular fields of open and wedged photon beams," Phys. Med. Biol. 40; 511–527

[27] Myler U. and Szabo J. J., (2002) "Dose calculation along the non-wedged direction for externally wedged beams: Improvement of dosimetric accuracy with comparatively moderate effort," Med. Phys. 29; 748–754.

[28] Liu C., Li Z., and Palta J. R., (1998) "Characterizing output for the Varian enhanced dynamic wedge field," Med. Phys. 25 (1); 64–70.

[29] Liu C., Kim S., Kahler D. L., and Palta J. R., (2003) "Generalized monitor unit calculation for the Varian enhanced dynamic wedge field," Med. Phys. 30; 1891–1896.

University of Ghana http://ugspace.ug.edu.gh

[30] Papatheodorou S., Zefkili S., and Rosenwald J. C., (1999), "The 'equivalent wedge' implementation of the Varian enhanced dynamic wedge (EDW) into a treatment planning system," Phys. Med. Biol. 44; 509–524.

[31] Klein E. E., Gerber R., Zhu X. R., Oehmke F., and Purdy J. A., (1998), "Multiple machine implementation of enhanced dynamic wedge," Int. J. Radiat., Oncol., Biol., Phys. Vol. 40; 977-985.

[32] Gibbons J. P., (1998), "Calculation of enhanced dynamic wedge factors for symmetric and asymmetric photon fields," Med. Phys. 25; 1411–1418.

[33] Prado K. L., Kirsner S. M., Kudchadker R. J., Steadham R. E, and Lane R. G., (2003), "Enhanced dynamic wedge factors at off-axis points in asymmetric fields," J. Appl. Clin. Med. Phys. Vol. 4; 75–84.

[34] Miften M., Wiesmeyer M., Beavis A., Takahashi K., and Broad S., (2000), "Implementation of enhanced dynamic wedge in the focus rtp system," Med. Dosim. Vol. 25; 81–86.

[35] Islam M. K. and Van Dy K. J., (1995), "Effects of Scatter Generated by Beam Modifying Absorbers in Megavoltage Photon Beams". Med. Phys. Vol. 22; 2075-2081.

[36] Yu M. K. and Sloboda R. S., (1997), "Effect of Beam Blocking on LINAC Head Scatter Factor". Int. J. Radiat. Oncol. Biol. Phys. Vol. 37; 465-268.

[37] Huang P.H., Chin L.M. and Bjarngard B.E., (1986), "Scattered Photons Produced by Beam Modifying Filters". Med. Phys. Vol. 13; 57-63.

University of Ghana http://ugspace.ug.edu.gh

[38] Sharma S. C. and Johnson, M. W., (1994) "Recommendations for Measurement of Tray and Wedge Factors for High Energy Photons", Med. phys. Vol. 21 (4); 573-575.

[39] Tatcher M. and Biarngard B. E., (1999) "Head Scatter in Blocked Photon Fields". Radiother. Oncol. Vol. 33; 64-67.

[40] Van Dam J., Bridier A., Lasselin C., Blanckaret N. and Dutreix A., (1992) "Influence of Shielding Blocks on the Output of Photon Beams as a Function of Energy and Type of Treatment Unit." Radiother. Oncol. Vol. 24; 55-59.

[41] Schaeken B. and Van Loon R., (1988) "Influence of Tray on Patient Dosimetry". In: proc. ESTRO 7th Annual Meeting; 165.

[42] Alkhatib H., Higgins P. D., Mihailidis D. N., Gerbi B. J., Gibbons J. P., (2000), "Dependence of Wedge Transmission Factors on Blocking in High Energy Beams", Annual Int. Conf., IEEE Eng. in Medicine and Biology; 4, 2542-2543.

[43] Misbah A., Amjad H., Wazir M., Syed Q. A. R., Matiullah, (2010), "Studying Wedge Factors and Beam Profiles for Physical and Enhanced Dynamic Wedges", Journal of Med Phys., vol. 35(1), 33-41

University of Ghana http://ugspace.ug.edu.gh

APPENDICES

APPENDIX A Raw data measurements showing average Temperature, Pressure and Corrected ion chamber readings for Wedge TF using the SAD setup

APPENDIX A1 Treatment depth of 0.5cm

Open Field								
		P1	P2	Av. Pressure				
		101.05	101.1	101.075				
Field size /cm²	RD1	RD2	RD3	Av. Reading /nC	T1	T2	Av. Temp. /°C	Corrected readings /nC
2×2	1.364	1.364	1.364	1.364	23.3	23.3	23.3	1.382764
4×4	1.545	1.545	1.545	1.545	23.2	23.2	23.2	1.565725
6×6	1.583	1.583	1.583	1.583	23.2	23.1	23.15	1.603964
10×10	1.650	1.650	1.650	1.650	23.0	22.9	22.95	1.670723
14×14	1.704	1.704	1.704	1.704	22.9	22.9	22.9	1.72511
18×18	1.750	1.750	1.750	1.750	22.8	22.7	22.75	1.770783
15° wedge								
		P1	P2	Av. Pressure				
		101.05	101.1	101.075				
Field size /cm²	RD1	RD2	RD3	Av. Reading /nC	T1	T2	Av. Temp. /°C	Corrected readings /nC
2×2	1.053	1.053	1.053	1.053	23.3	23.2	23.25	1.067305
4×4	1.188	1.188	1.188	1.188	23.2	23.2	23.2	1.203936
6×6	1.217	1.217	1.217	1.217	23.1	23.1	23.1	1.232909
10×10	1.270	1.270	1.270	1.27	23.0	23.0	23.0	1.286168
14×14	1.316	1.316	1.316	1.316	22.9	22.9	22.9	1.332304
18×18	1.355	1.355	1.355	1.355	22.8	22.8	22.8	1.371323
30° wedge								
		P1	P2	Av. pressure				
		101.05	101.1	101.075				
Field size /cm²	RD1	RD2	RD3	Av. Reading /nC	T1	T2	Av. Temp. /°C	Corrected readings/nC
2×2	0.877	0.878	0.877	0.877333	23.2	23.2	23.2	0.889102
4×4	0.987	0.988	0.988	0.987667	23.2	23.2	23.2	1.000916
6×6	1.013	1.014	1.014	1.013667	23.1	23.1	23.1	1.026918
10×10	1.057	1.057	1.057	1.057000	23	23	23	1.070456
14×14	1.095	1.095	1.095	1.095000	22.9	22.9	22.9	1.108566
18×18	1.127	1.127	1.127	1.127000	22.8	22.8	22.8	1.140577

University of Ghana http://ugspace.ug.edu.gh

APPENDIX A1 continued

45° wedge								
		P1	P2	Average pressure				
		101.05	101.1	101.075				
Field size /cm^2	RD1	RD2	RD3	Av. Reading /nC	T1	T2	Av. Temp. /°C	Corrected readings/nC
2×2	0.679	0.679	0.679	0.679	23.2	23.2	23.2	0.688108
4×4	0.763	0.762	0.762	0.762333	23.2	23.2	23.2	0.77256
6×6	0.782	0.782	0.782	0.782	23.1	23.1	23.1	0.792223
10×10	0.817	0.817	0.817	0.817	23	23	23	0.827401
14×14	0.847	0.847	0.847	0.847	22.9	22.9	22.9	0.857493
18×18	0.875	0.875	0.875	0.875	22.8	22.8	22.8	0.885541
60° wedge								
		P1	P2	Average Pressure				
		101.05	101.1	101.075				
Field size /cm^2	RD1	RD2	RD3	Av. Reading /nC	T1	T2	Av. Temp. /°C	Corrected readings /nC
2×2	0.364	0.364	0.364	0.364	23.2	23.2	23.2	0.368883
4×4	0.411	0.411	0.411	0.411	23.2	23.2	23.2	0.416513
6×6	0.420	0.420	0.420	0.42	23.1	23.1	23.1	0.42549
10×10	0.442	0.443	0.443	0.442667	23.1	23	23.05	0.448378
14×14	0.463	0.463	0.463	0.463	22.9	22.8	22.85	0.468657
18×18	0.480	0.480	0.480	0.48	22.8	22.8	22.8	0.485782

APPENDIX A2 Treatment depth of 6cm

Open Field								
		P1	P2	Average pressure				
		101	101	101				
Field size /cm^2	RD1	RD2	RD3	Av. Reading /nC	T1	T2	Av. Temp. /°C	Corrected readings/nC
2×2	1.050	1.050	1.050	1.05	23.6	23.6	23.6	1.066312
4×4	1.219	1.219	1.219	1.219	23.7	23.6	23.65	1.238146
6×6	1.290	1.290	1.290	1.29	23.7	23.7	23.7	1.310482
10×10	1.392	1.393	1.392	1.392333	23.9	23.8	23.85	1.415155
14×14	1.467	1.467	1.467	1.467	23.9	23.9	23.9	1.491297
18×18	1.524	1.524	1.524	1.524	24	24	24	1.549762

University of Ghana http://ugspace.ug.edu.gh

APPENDIX A2 continued

15° wedge								
		P1	P2	Average Pressure				
		101	101	101				
Field size /cm²	RD1	RD2	RD3	Av. Reading /nC	T1	T2	Av. Temp. /°C	Corrected readings/nC
2×2	0.81	0.81	0.81	0.81	23.6	23.6	23.6	0.822584
4×4	0.937	0.937	0.937	0.937	23.6	23.6	23.6	0.951557
6×6	0.992	0.992	0.992	0.992	23.7	23.7	23.7	1.007751
10×10	1.073	1.073	1.073	1.073	23.8	23.8	23.8	1.090404
14×14	1.134	1.134	1.134	1.134	23.9	23.9	23.9	1.152781
18×18	1.18	1.18	1.18	1.18	24	24	24	1.199947
30° wedge								
		P1	P2	Average pressure				
		101	101	101				
Field size /cm²	RD1	RD2	RD3	Av. Reading /nC	T1	T2	Av. Temp. /°C	Corrected readings/nC
2×2	0.681	0.681	0.681	0.681	23.6	23.6	23.6	0.69158
4×4	0.78	0.781	0.78	0.780333	23.6	23.6	23.6	0.792456
6×6	0.827	0.827	0.827	0.827	23.7	23.7	23.7	0.840131
10×10	0.894	0.895	0.895	0.894667	23.8	23.7	23.75	0.909025
14×14	0.945	0.945	0.945	0.945	23.9	23.9	23.9	0.960651
18×18	0.986	0.986	0.986	0.986	24	24	24	1.002668
45° wedge								
		P1	P2	Average pressure				
		101	101	101				
Field size /cm²	RD1	RD2	RD3	Av. Reading /nC	T1	T2	Av. Temp. /°C	Corrected readings/nC
2×2	0.527	0.527	0.527	0.527	23.6	23.6	23.6	0.535187
4×4	0.601	0.601	0.601	0.601	23.6	23.6	23.6	0.610337
6×6	0.637	0.637	0.637	0.637	23.7	23.7	23.7	0.647114
10×10	0.693	0.693	0.693	0.693	23.7	23.7	23.7	0.704003
14×14	0.731	0.731	0.731	0.731	23.9	23.9	23.9	0.743107
18×18	0.765	0.765	0.765	0.765	24	24	24	0.777932
60° wedge								
		P1	P2	Average pressure				
		101	101	101				
Field size /cm²	RD1	RD2	RD3	Av. Reading /nC	T1	T2	Av. Temp. /°C	Corrected readings/nC
2×2	0.281	0.281	0.281	0.281	23.6	23.6	23.6	0.285366
4×4	0.323	0.323	0.323	0.323	23.6	23.6	23.6	0.328018
6×6	0.343	0.343	0.343	0.343	23.7	23.7	23.7	0.348446
10×10	0.377	0.377	0.377	0.377	23.7	23.7	23.7	0.382986
14×14	0.401	0.401	0.401	0.401	23.9	23.9	23.9	0.407641
18×18	0.419	0.419	0.419	0.419	24	23.9	23.95	0.426011

University of Ghana http://ugspace.ug.edu.gh

APPENDIX A3 Treatment depth of 10cm

Open Field								
		P1	P2	Average Pressure				
		101	101	101				
Field size/cm²	RD1	RD2	RD3	Av. Readings/ nC	T1	T2	Av. Temp./ °C	Corrected readings/nC
2×2	0.803	0.803	0.803	0.803	24.6	24.6	24.6	0.818223
4×4	0.958	0.958	0.958	0.958	24.5	24.5	24.5	0.975833
6×6	1.032	1.032	1.032	1.032	24.5	24.5	24.5	1.051211
10×10	1.149	1.149	1.149	1.149	24.3	24.3	24.3	1.169602
14×14	1.236	1.237	1.236	1.236333	24.3	24.3	24.3	1.258502
18×18	1.304	1.304	1.304	1.304	24.2	24.2	24.2	1.326936
15° wedge								
		P1	P2	Average pressure				
		101	101	101				
Field size/cm²	RD1	RD2	RD3	Av. Reading/nC	T1	T2	Av. Temp/°C	Corrected readings/nC
2×2	0.621	0.621	0.621	0.621	24.6	24.6	24.6	0.632772
4×4	0.738	0.738	0.738	0.738	24.5	24.5	24.5	0.751738
6×6	0.796	0.796	0.796	0.796	24.5	24.5	24.5	0.810818
10×10	0.888	0.888	0.888	0.888	24.3	24.3	24.3	0.903923
14×14	0.958	0.958	0.958	0.958	24.3	24.3	24.3	0.975178
18×18	1.010	1.010	1.010	1.01	24.2	24.2	24.2	1.027764
30° wedge								
		P1	P2	Average pressure				
		101	101	101				
Field size/cm²	RD1	RD2	RD3	Av. Reading/nC	T1	T2	Av. Temp./°C	Corrected readings/nC
2×2	0.52	0.52	0.52	0.52	24.6	24.6	24.6	0.529858
4×4	0.617	0.617	0.617	0.617	24.5	24.5	24.5	0.628486
6×6	0.665	0.665	0.665	0.665	24.5	24.4	24.45	0.677265
10×10	0.743	0.742	0.743	0.742667	24.3	24.3	24.3	0.755983
14×14	0.801	0.801	0.801	0.801	24.3	24.2	24.25	0.815226
18×18	0.845	0.846	0.845	0.845333	24.2	24.2	24.2	0.860202
45° wedge								
		P1	P2	Average Pressure				
		101	101	101				
Field size/cm²	RD1	RD2	RD3	Av. Reading/nC	T1	T2	Av. Temp/°C	Corrected readings/nC
2×2	0.405	0.405	0.405	0.405	24.6	24.5	24.55	0.412608
4×4	0.478	0.478	0.478	0.478	24.5	24.5	24.5	0.486898
6×6	0.516	0.516	0.516	0.516	24.4	24.4	24.4	0.525429
10×10	0.576	0.576	0.576	0.576	24.4	24.3	24.35	0.586427
14×14	0.622	0.622	0.622	0.622	24.2	24.2	24.2	0.63294
18×18	0.659	0.659	0.659	0.659	24.2	24.2	24.2	0.670591

University of Ghana http://ugspace.ug.edu.gh

APPENDIX A3 continued

60° wedge								
		P1	P2	Average pressure				
		101	101	101				
Field size/cm²	RD1	RD2	RD3	Average reading/nC	T1	T2	Av. Temp/°C	Corrected reading/nC
2×2	0.219	0.219	0.219	0.219	24.5	24.5	24.5	0.223077
4×4	0.258	0.258	0.258	0.258	24.5	24.5	24.5	0.262803
6×6	0.279	0.279	0.279	0.279	24.4	24.4	24.4	0.284098
10×10	0.315	0.315	0.315	0.315	24.4	24.4	24.4	0.320756
14×14	0.343	0.343	0.343	0.343	24.2	24.2	24.2	0.349033
18×18	0.364	0.364	0.364	0.364	24.2	24.2	24.2	0.370402

APPENDIX A4 Treatment depth of 15cm

Open Field								
		P1	P2	Average pressure				
		101.15	101.05	101.1				
Field size/cm²	RD1	RD2	RD3	Average reading/nC	T1	T2	Av. Temp/°C	Corrected reading/nC
2×2	0.581	0.581	0.581	0.581	24.7	24.7	24.7	0.591627
4×4	0.699	0.699	0.699	0.699	24.8	24.8	24.8	0.712024
6×6	0.762	0.762	0.762	0.762	24.8	24.8	24.8	0.776198
10×10	0.874	0.874	0.874	0.874	25	25	25	0.890883
14×14	0.962	0.962	0.962	0.962	25	25	25	0.980583
18×18	1.033	1.033	1.033	1.033	25.2	25.2	25.2	1.05366
15° wedge								
		P1	P2	Average pressure				
		101.15	101.05	101.1				
Field size/cm²	RD1	RD2	RD3	Average reading/nC	T1	T2	Av. Temp/°C	Corrected readings/nC
2×2	0.450	0.450	0.450	0.45	24.7	24.7	24.7	0.458231
4×4	0.54	0.54	0.54	0.54	24.8	24.7	24.75	0.54997
6×6	0.589	0.589	0.589	0.589	24.8	24.8	24.8	0.599975
10×10	0.677	0.677	0.677	0.677	25	25	25	0.690077
14×14	0.746	0.746	0.746	0.746	25	25	25	0.76041
18×18	0.801	0.801	0.801	0.801	25.2	25.2	25.2	0.81702
30° wedge								
		P1	P2	Average pressure				
		101.15	101.05	101.1				
Field size/cm²	RD1	RD2	RD3	Average reading/nC	T1	T2	Av. Temp/°C	Corrected readings/nC
2×2	0.382	0.382	0.382	0.382	24.7	24.7	24.7	0.388987
4×4	0.456	0.456	0.456	0.456	24.7	24.7	24.7	0.464341
6×6	0.497	0.497	0.497	0.497	24.8	24.8	24.8	0.506261
10×10	0.570	0.570	0.570	0.57	25	25	25	0.581011
14×14	0.627	0.627	0.627	0.627	25	25	25	0.639112
18×18	0.676	0.675	0.676	0.675667	25.2	25.1	25.15	0.689065

University of Ghana http://ugspace.ug.edu.gh

APPENDIX A4 continued

45° wedge								
		P1	P2	Average pressure				
		101.15	101.05	101.1				
Field size/cm²	RD1	RD2	RD3	Average reading/nC	T1	T2	Av. Temp/°C	Corrected reading/nC
2×2	0.296	0.296	0.296	0.296	24.7	24.7	24.7	0.301414
4×4	0.354	0.354	0.354	0.354	24.7	24.7	24.7	0.360475
6×6	0.384	0.384	0.384	0.384	24.9	24.8	24.85	0.391221
10×10	0.443	0.443	0.443	0.443	25	25	25	0.451557
14×14	0.488	0.488	0.488	0.488	25.1	25	25.05	0.49751
18×18	0.528	0.529	0.529	0.528667	25.1	25.1	25.1	0.539059
60° wedge								
		P1	P2	Average pressure				
		101.15	101.05	101.1				
Field size/cm²	RD1	RD2	RD3	Average reading/nC	T1	T2	Av. Temp/°C	Corrected reading/nC
2×2	0.162	0.162	0.162	0.162	24.7	24.7	24.7	0.164963
4×4	0.192	0.192	0.192	0.192	24.7	24.7	24.7	0.195512
6×6	0.210	0.210	0.210	0.21	24.9	24.9	24.9	0.213985
10×10	0.243	0.243	0.243	0.243	25	24.9	24.95	0.247652
14×14	0.273	0.273	0.273	0.273	25.1	25.1	25.1	0.278367
18×18	0.294	0.294	0.294	0.294	25.1	25.1	25.1	0.29978

APPENDIX A5 Treatment depth of 20cm

Open Field								
		P1	P2	Average pressure				
		101.2	101.15	101.175				
Field size/cm²	RD1	RD2	RD3	Average reading/nC	T1	T2	Av. Temp/°C	Corrected reading/nC
2×2	0.429	0.429	0.429	0.429	26.1	26.1	26.1	0.438575
4×4	0.518	0.519	0.519	0.518667	26	26	26	0.530065
6×6	0.568	0.568	0.568	0.5685	26	25.9	25.95	0.580897
10×10	0.663	0.663	0.663	0.663	25.7	25.7	25.7	0.676891
14×14	0.745	0.745	0.745	0.745	25.7	25.7	25.7	0.760609
18×18	0.813	0.813	0.813	0.813	25.5	25.5	25.5	0.829479
15° wedge								
		P1	P2	Average pressure				
		101.2	101.15	101.175				
Field size/cm²	RD1	RD2	RD3	Average reading/nC	T1	T2	Av. Temp/°C	Corrected reading/nC
2×2	0.334	0.334	0.334	0.334	26.1	26.1	26.1	0.341454
4×4	0.402	0.402	0.402	0.402	26	26	26	0.410835
6×6	0.44	0.44	0.44	0.44	25.9	25.9	25.9	0.449519
10×10	0.516	0.516	0.516	0.516	25.7	25.7	25.7	0.526811
14×14	0.580	0.580	0.580	0.58	25.7	25.7	25.7	0.592152
18×18	0.634	0.635	0.635	0.634667	25.5	25.5	25.5	0.647531

University of Ghana http://ugspace.ug.edu.gh

APPENDIX A5 continued

30° wedge								
		P1	P2	Av. pressure				
		101.2	101.15	101.175				
Field size/cm²	RD1	RD2	RD3	Average reading/nC	T1	T2	Av. Temp/°C	Corrected reading/nC
2×2	0.284	0.284	0.284	0.284	26.1	26	26.05	0.29029
4×4	0.342	0.342	0.342	0.342	26	26	26	0.349516
6×6	0.373	0.373	0.373	0.373	25.9	25.9	25.9	0.38107
10×10	0.435	0.435	0.435	0.435	25.7	25.7	25.7	0.444114
14×14	0.489	0.489	0.489	0.489	25.7	25.7	25.7	0.499246
18×18	0.535	0.534	0.534	0.534333	25.5	25.5	25.5	0.545164
45° wedge								
		P1	P2	Av. pressure				
		101.2	101.15	101.175				
Field size/cm²	RD1	RD2	RD3	Average reading/nC	T1	T2	Av. Temp/°C	Corrected reading/nC
2×2	0.222	0.222	0.222	0.222	26	26	26	0.226879
4×4	0.266	0.265	0.265	0.26533	26	26	26	0.271165
6×6	0.291	0.291	0.291	0.291	25.9	25.9	25.9	0.297296
10×10	0.340	0.340	0.340	0.34	25.8	25.7	25.75	0.347182
14×14	0.383	0.383	0.383	0.383	25.7	25.6	25.65	0.390959
18×18	0.42	0.42	0.42	0.42	25.6	25.5	25.55	0.428585
60° wedge								
		P1	P2	Av. Pressure				
		101.2	101.15	101.175				
Field size/cm²	RD1	RD2	RD3	Average readings/nC	T1	T2	Av. temp/°C	Corrected readings/nC
2×2	0.123	0.123	0.123	0.123	26	26	26	0.125703
4×4	0.147	0.147	0.147	0.147	26	26	26	0.150231
6×6	0.159	0.159	0.159	0.159	25.9	25.8	25.85	0.162413
10×10	0.189	0.189	0.189	0.189	25.8	25.8	25.8	0.193024
14×14	0.214	0.214	0.214	0.214	25.6	25.6	25.6	0.218411
18×18	0.234	0.234	0.234	0.234	25.6	25.6	25.6	0.238823

INTEGRI PROCEDAMUS

University of Ghana http://ugspace.ug.edu.gh

APPENDIX B Raw data measurements showing average Temperature, Pressure and Corrected ion chamber readings for Tray TF using the SAD setup

APPENDIX B1 Treatment depth of 0.5cm

Open Field								
		P1	P2	Av. pressure				
Field size/cm^2		101.05	101.1	101.075				
	RD1	RD2	RD3	Av. Reading/nC	T1	T2	Av. Temp/^{o}C	Corrected reading/nC
4×4	1.545	1.545	1.545	1.545	23.2	23.2	23.2	1.565725
6×6	1.583	1.583	1.583	1.583	23.2	23.2	23.2	1.604235
8×8	1.617	1.617	1.617	1.617	23	23	23	1.637585
10×10	1.650	1.650	1.650	1.65	23	22.9	22.95	1.670723
14×14	1.704	1.704	1.704	1.704	22.9	22.9	22.9	1.72511
18×18	1.75	1.75	1.75	1.75	22.8	22.7	22.75	1.770783
22×22	1.787	1.787	1.787	1.787	22.7	22.7	22.7	1.807917
26×26	1.816	1.816	1.816	1.816	22.7	22.7	22.7	1.837256
30×30	1.836	1.836	1.836	1.836	22.7	22.7	22.7	1.85749

Tray in beam path								
		P1	P2	Av. pressure				
Field size/cm^2		101	101.05	101.025				
	RD1	RD2	RD3	Av. Reading/nC	T1	T1	Av. Temp/^{o}C	Corrected reading/nC
4×4	1.482	1.482	1.482	1.482	22.1	22.1	22.1	1.497047
6×6	1.522	1.522	1.522	1.522	22	22	22	1.536932
8×8	1.557	1.557	1.557	1.557	22	22	22	1.572276
10×10	1.581	1.581	1.581	1.581	21.8	21.8	21.8	1.59543
14×14	1.642	1.642	1.642	1.642	21.8	21.8	21.8	1.656986
18×18	1.689	1.689	1.689	1.689	21.7	21.7	21.7	1.703838
22×22	1.726	1.726	1.726	1.726	21.7	21.7	21.7	1.741163
26×26	1.757	1.757	1.757	1.757	21.6	21.6	21.6	1.771834
30×30	1.78	1.78	1.78	1.78	21.6	21.6	21.6	1.795028

University of Ghana http://ugspace.ug.edu.gh

APPENDIX B2 Treatment depth of 6cm

Open Field								
		P1	P2	Av. pressure				
Field size/cm^2		101	101	101				
	RD1	RD2	RD3	Av. Reading/nC	T1	T2	Av. Temp/^{o}C	Corrected readings/nC
4×4	1.219	1.219	1.219	1.219	23.6	23.6	23.6	1.237938
6×6	1.29	1.29	1.29	1.29	23.7	23.7	23.7	1.310482
8×8	1.342	1.342	1.342	1.342	23.7	23.7	23.7	1.363308
10×10	1.393	1.393	1.393	1.393	23.9	23.9	23.9	1.416071
14×14	1.467	1.467	1.467	1.467	23.9	23.9	23.9	1.491297
18×18	1.524	1.524	1.524	1.524	24	24	24	1.549762
22×22	1.572	1.572	1.572	1.572	24	24	24	1.598574
26×26	1.606	1.606	1.606	1.606	24	24	24	1.633148
30×30	1.633	1.633	1.633	1.633	24.1	24	24.05	1.660884

Tray in beam path								
		P1	P2	Av. pressure				
Field size/cm^2		101.3	101.25	101.275				
	RD1	RD2	RD3	Av. Readings/nC	T1	T1	Av. Temp/^{o}C	Corrected readings/nC
4×4	1.182	1.182	1.182	1.182	23.7	23.7	23.7	1.197507
6×6	1.248	1.248	1.248	1.248	23.5	23.5	23.5	1.263521
8×8	1.303	1.303	1.303	1.303	23.5	23.5	23.5	1.319205
10×10	1.344	1.344	1.344	1.344	23.4	23.4	23.4	1.360257
14×14	1.419	1.419	1.419	1.419	23.4	23.4	23.4	1.436164
18×18	1.477	1.477	1.477	1.477	23.2	23.2	23.2	1.493857
22×22	1.523	1.523	1.523	1.523	23.2	23.2	23.2	1.540382
26×26	1.558	1.558	1.558	1.558	23.1	23.1	23.1	1.57525
30×30	1.586	1.586	1.586	1.586	23.1	23	23.05	1.603289

University of Ghana http://ugspace.ug.edu.gh

APPENDIX B3 Treatment depth of 10cm

Open Field								
		P1	P2	Av. pressure				
Field size/cm^2		101	101	101				
	RD1	RD2	RD3	Av. Readings/nC	T1	T2	Av. Temp/^{o}C	Corrected readings/nC
4×4	0.958	0.958	0.958	0.958	24.5	24.5	24.5	0.975833
6×6	1.032	1.032	1.032	1.032	24.5	24.5	24.5	1.051211
8×8	1.091	1.091	1.091	1.091	24.3	24.3	24.3	1.110562
10×10	1.149	1.149	1.149	1.149	24.3	24.3	24.3	1.169602
14×14	1.236	1.236	1.236	1.236	24.3	24.3	24.3	1.258162
18×18	1.304	1.304	1.304	1.304	24.2	24.2	24.2	1.326936
22×22	1.356	1.356	1.356	1.356	24.2	24.2	24.2	1.37985
26×26	1.396	1.396	1.396	1.396	24.2	24.1	24.15	1.420315
30×30	1.428	1.428	1.428	1.428	24.1	24.1	24.1	1.452628

Tray in beam path								
		P1	P2	Av. pressure				
Field size/cm^2		101.2	101.15	101.175				
	RD1	RD2	RD3	Av. Reading/nC	T1	T1	Av. Temp/^{o}C	Corrected readings/nC
4×4	0.926	0.926	0.926	0.926	23	23	23	0.936862
6×6	0.996	0.996	0.996	0.996	23	23	23	1.007683
8×8	1.054	1.053	1.053	1.053333	23.2	23.2	23.2	1.066408
10×10	1.108	1.109	1.109	1.108667	23.2	23.2	23.2	1.122428
14×14	1.192	1.192	1.192	1.192	23.4	23.4	23.4	1.20761
18×18	1.258	1.258	1.258	1.258	23.4	23.4	23.4	1.274475
22×22	1.308	1.308	1.308	1.308	23.6	23.6	23.6	1.326023
26×26	1.348	1.348	1.348	1.348	23.6	23.6	23.6	1.366574
30×30	1.378	1.379	1.379	1.378667	23.7	23.7	23.7	1.398134

University of Ghana http://ugspace.ug.edu.gh

APPENDIX B4 Treatment depth of 15cm

Open Field								
		P1	P2	Av. pressure				
Field size/cm²		101.1	101.05	101.075				
	RD1	RD2	RD3	Av. Readings/nC	T1	T2	Av. Temp/°C	Corrected readings/nC
4×4	0.699	0.699	0.699	0.699	24.8	24.8	24.8	0.712201
6×6	0.762	0.762	0.762	0.762	24.8	24.8	24.8	0.77639
8×8	0.818	0.818	0.818	0.818	24.8	24.8	24.8	0.833448
10×10	0.874	0.874	0.874	0.874	25	25	25	0.891103
14×14	0.962	0.962	0.962	0.962	25	25	25	0.980825
18×18	1.033	1.033	1.033	1.033	25.2	25.2	25.2	1.053921
22×22	1.089	1.089	1.089	1.089	25.2	25.2	25.2	1.111055
26×26	1.133	1.133	1.133	1.133	25.2	25.2	25.2	1.155946
30×30	1.166	1.166	1.166	1.166	25.2	25.2	25.2	1.189615

Tray in beam path								
		P1	P2	Av. pressure				
Field size/cm²		101.15	101.15	101.15				
	RD1	RD2	RD3	Av. Reading/nC	T1	T1	Av. Temp/°C	Corrected readings/nC
4×4	0.672	0.672	0.672	0.672	25	25	25	0.684642
6×6	0.735	0.735	0.735	0.735	24.6	24.6	24.6	0.747823
8×8	0.791	0.791	0.791	0.791	24.6	24.6	24.6	0.8048
10×10	0.845	0.845	0.845	0.845	24.5	24.5	24.5	0.859453
14×14	0.93	0.93	0.93	0.93	24.5	24.4	24.45	0.945748
18×18	1.001	1.001	1.001	1.001	24.2	24.2	24.2	1.017096
22×22	1.055	1.055	1.055	1.055	24.2	24.2	24.2	1.071964
26×26	1.101	1.101	1.101	1.101	24	24	24	1.117951
30×30	1.135	1.135	1.135	1.135	24	24	24	1.152475

INTEGRI PROCEDAMUS

University of Ghana http://ugspace.ug.edu.gh

APPENDIX B5 Treatment depth of 20cm

Open Field								
		P1	P2	Av. pressure				
Field size/cm^2		101.2	101.15	101.175				
	RD1	RD2	RD3	Av. Reading/nC	T1	T2	Av. Temp/^{o}C	Corrected readings/nC
4×4	0.518	0.518	0.518	0.518	26	26	26	0.529384
6×6	0.569	0.569	0.569	0.569	26	25.9	25.95	0.581408
8×8	0.616	0.616	0.616	0.616	25.9	25.9	25.9	0.629327
10×10	0.663	0.663	0.663	0.663	25.7	25.7	25.7	0.676891
14×14	0.745	0.745	0.745	0.745	25.7	25.5	25.6	0.760355
18×18	0.813	0.813	0.813	0.813	25.5	25.5	25.5	0.829479
22×22	0.867	0.867	0.867	0.867	25.5	25.5	25.5	0.884573
26×26	0.912	0.912	0.912	0.912	25.5	25.4	25.45	0.930329
30×30	0.947	0.947	0.947	0.947	25.4	25.4	25.4	0.965871

Tray in beam path								
		P1	P2	Av. pressure				
Field size/cm^2		101.25	101.35	101.3				
	RD1	RD2	RD3	Av. Reading/nC	T1	T2	Av. Temp/^{o}C	Corrected readings/nC
4×4	0.493	0.493	0.493	0.493	28	28	28	0.506577
6×6	0.543	0.543	0.543	0.543	28	28	28	0.557953
8×8	0.589	0.589	0.589	0.589	27.9	27.9	27.9	0.605019
10×10	0.637	0.637	0.637	0.637	27.5	27.5	27.5	0.653456
14×14	0.713	0.713	0.713	0.713	27.5	27.5	27.5	0.731419
18×18	0.778	0.778	0.778	0.778	27.1	27.1	27.1	0.797036
22×22	0.834	0.834	0.834	0.834	26.7	26.7	26.7	0.853269
26×26	0.876	0.876	0.876	0.876	26.7	26.7	26.7	0.896239
30×30	0.912	0.912	0.912	0.912	26.4	26.4	26.4	0.932137

INTEGRI PROCEDAMUS

University of Ghana http://ugspace.ug.edu.gh

APPENDIX C Raw data measurements showing average Temperature, Pressure and Corrected ion chamber readings for Wedge and Tray TF using the SSD setup

APPENDIX C1 Treatment depth of 0.5cm

Open Field								
		P1	P2	Average pressure				
Field size/cm²		101.05	101.1	101.075				
	RD1	RD2	RD3	Average Reading/nC	T1	T2	Average Temp/°C	Corrected readings/nC
2×2	0.267	0.267	0.267	0.267	22	22	22	0.269486
4×4	0.354	0.354	0.354	0.354	22	22	22	0.357296
6×6	0.392	0.392	0.392	0.392	22	22	22	0.39565
10×10	0.463	0.463	0.463	0.463	22	22	22	0.467311
14×14	0.520	0.520	0.520	0.52	21.8	21.8	21.8	0.524486
18×18	0.567	0.567	0.567	0.567	21.8	21.8	21.8	0.571892
22×22	0.593	0.593	0.593	0.593	21.7	21.7	21.7	0.597914
15° wedge								
		P1	P2	Average pressure				
Field size/cm²		101.05	101.1	101.075				
	RD1	RD2	RD3	Average Reading/nC	T1	T2	Average Temp/°C	Corrected readings/nC
2×2	0.210	0.210	0.210	0.21	22	22	22	0.211955
4×4	0.277	0.277	0.277	0.277	22	22	22	0.279579
6×6	0.306	0.306	0.306	0.306	22	22	22	0.308849
10×10	0.361	0.361	0.361	0.361	22	22	22	0.364361
14×14	0.408	0.408	0.408	0.408	21.9	21.8	21.85	0.41159
18×18	0.446	0.446	0.446	0.446	21.8	21.8	21.8	0.449848
30° wedge								
		P1	P2	Average pressure				
Field size/cm²		101.05	101.1	101.075				
	RD1	RD2	RD3	Average Reading/nC	T1	T2	Average Temp/°C	Corrected readings/nC
2×2	0.180	0.180	0.180	0.18	22	22	22	0.181676
4×4	0.237	0.237	0.237	0.237	22	22	22	0.239207
6×6	0.261	0.261	0.261	0.261	22	22	22	0.26343
10×10	0.306	0.306	0.306	0.306	22	21.9	21.95	0.308797
14×14	0.345	0.345	0.345	0.345	21.9	21.9	21.9	0.348095
18×18	0.375	0.375	0.375	0.375	21.8	21.8	21.8	0.378235

University of Ghana http://ugspace.ug.edu.gh

APPENDIX C1 continued

45° wedge								
		P1	P2	Average pressure				
Field size/cm²		101.05	101.1	101.075				
	RD1	RD2	RD3	Average readings/nC	T1	T2	Average temp/°C	Corrected reading/nC
2×2	0.14	0.14	0.14	0.14	22	22	22	0.141304
4×4	0.183	0.183	0.183	0.183	22	22	22	0.184704
6×6	0.204	0.204	0.204	0.204	22	22	22	0.2059
10×10	0.240	0.240	0.240	0.24	21.9	21.9	21.9	0.242153
14×14	0.270	0.270	0.270	0.27	21.9	21.9	21.9	0.272422
18×18	0.296	0.296	0.296	0.296	21.8	21.7	21.75	0.298503
60° wedge								
		P1	P2	Average reading/nC				
Field size/cm²		101.05	101.1	101.075				
	RD1	RD2	RD3	Average reading/nC	T1	T2	Average temp/°C	Corrected reading/nC
2×2	0.078	0.078	0.078	0.078	22	22	22.0	0.078726
4×4	0.105	0.105	0.105	0.105	22	22	22.0	0.105978
6×6	0.114	0.114	0.114	0.114	22	22	22.0	0.115062
10×10	0.138	0.138	0.138	0.138	21.9	21.9	21.9	0.139238
14×14	0.155	0.155	0.155	0.155	21.9	21.9	21.9	0.15639
18×18	0.167	0.167	0.167	0.167	21.7	21.7	21.7	0.168384
Tray in beam path								
		P1	P2	Average pressure				
Field size/cm²		101.05	101.1	101.075				
	RD1	RD2	RD3	Average reading/nC	T1	T2	Average Temp/°C	Corrected reading/nC
4×4	0.339	0.339	0.339	0.339	22	22	22	0.342157
6×6	0.375	0.375	0.375	0.375	22	22	22	0.378492
10×10	0.444	0.444	0.444	0.444	21.9	21.9	21.9	0.447983
14×14	0.499	0.498	0.498	0.498333	21.9	21.9	21.9	0.502803
18×18	0.544	0.544	0.544	0.544	21.7	21.7	21.7	0.548507
22×22	0.567	0.568	0.568	0.567667	21.7	21.7	21.7	0.57237

APPENDIX C2 Treatment depth of 6cm

Open Field								
		P1	P2	Average pressure				
Field size/cm²		101.25	101.1	101.175				
	RD1	RD2	RD3	Average reading/nC	T1	T2	Average Temp/°C	Corrected readings/nC
2×2	0.899	0.899	0.899	0.899	23	23	23	0.909545
4×4	1.086	1.086	1.086	1.086	23.1	23.1	23.1	1.099109
6×6	1.149	1.149	1.149	1.149	23.1	23.1	23.1	1.16287
10×10	1.243	1.243	1.243	1.243	23.3	23.2	23.25	1.258641
14×14	1.309	1.309	1.309	1.309	23.3	23.3	23.3	1.325695
18×18	1.361	1.361	1.361	1.361	23.5	23.5	23.5	1.379288
22×22	1.402	1.402	1.402	1.402	23.5	23.5	23.5	1.420839

University of Ghana http://ugspace.ug.edu.gh

APPENDIX C2 continued

15° wedge								
		P1	P2	Average pressure				
Field size/cm²		101.25	101.1	101.175				
	RD1	RD2	RD3	Avearge reading/nC	T1	T2	Average Temp/°C	Corrected reading/nC
2×2	0.694	0.694	0.694	0.694	23	23	23	0.70214
4×4	0.834	0.834	0.834	0.834	23.1	23.1	23.1	0.844067
6×6	0.883	0.883	0.883	0.883	23.1	23.1	23.1	0.893659
10×10	0.957	0.958	0.957	0.957333	23.2	23.2	23.2	0.969217
14×14	1.01	1.01	1.01	1.01	23.3	23.3	23.3	1.022882
18×18	1.055	1.055	1.055	1.055	23.5	23.4	23.45	1.068996
30° wedge								
		P1	P2	Average pressure				
Field size/cm²		101.25	101.1	101.175				
	RD1	RD2	RD3	Average reading/nC	T1	T2	Average Temp/°C	Corrected reading/nC
2×2	0.586	0.585	0.586	0.585667	23	23	23	0.592536
4×4	0.699	0.699	0.699	0.699	23.1	23.1	23.1	0.707438
6×6	0.738	0.738	0.738	0.738	23.1	23.1	23.1	0.746909
10×10	0.799	0.799	0.799	0.799	23.2	23.2	23.2	0.808918
14×14	0.841	0.841	0.841	0.841	23.3	23.3	23.3	0.851726
18×18	0.878	0.878	0.878	0.878	23.4	23.4	23.4	0.889498
45° wedge								
		P1	P2	Average pressure				
Field size/cm²		101.25	101.1	101.175				
	RD1	RD2	RD3	Average reading/nC	T1	T2	Average Temp/°C	Corrected reading/nC
2×2	0.453	0.454	0.453	0.453333	23	23	23	0.458651
4×4	0.539	0.539	0.539	0.539	23.1	23.1	23.1	0.545506
6×6	0.572	0.571	0.571	0.571333	23.1	23.1	23.1	0.57823
10×10	0.619	0.619	0.619	0.619	23.2	23.2	23.2	0.626684
14×14	0.651	0.651	0.651	0.651	23.3	23.3	23.3	0.659303
18×18	0.683	0.683	0.683	0.683	23.4	23.4	23.4	0.691945
60° wedge								
		P1	P2	Average pressure				
Field size/cm²		101.25	101.1	101.175				
	RD1	RD2	RD3	Average reading/nC	T1	T2	Average Temp/°C	Corrected reading/nC
2×2	0.246	0.246	0.246	0.246	23	23	23	0.248885
4×4	0.291	0.291	0.291	0.291	23.1	23.1	23.1	0.294513
6×6	0.314	0.314	0.314	0.314	23.2	23.2	23.2	0.317898
10×10	0.336	0.336	0.336	0.336	23.2	23.1	23.15	0.340113
14×14	0.357	0.357	0.357	0.357	23.3	23.3	23.3	0.361553
18×18	0.378	0.378	0.378	0.378	23.4	23.4	23.4	0.38295

University of Ghana http://ugspace.ug.edu.gh

APPENDIX C2 continued

Tray in beam path								
		P1	P2	Average pressure				
Field size/cm²		101.25	101.1	101.175				
	RD1	RD2	RD3	Average reading/nC	T1	T2	Average Temp/°C	Corrected reading/nC
4×4	1.038	1.038	1.038	1.038	23.1	23.1	23.1	1.05053
6×6	1.100	1.100	1.100	1.1	23.1	23.2	23.15	1.113466
10×10	1.191	1.191	1.191	1.191	23.1	23.1	23.1	1.205377
14×14	1.255	1.255	1.255	1.255	23.4	23.3	23.35	1.271221
18×18	1.305	1.305	1.305	1.305	23.4	23.4	23.4	1.32209
22×22	1.346	1.346	1.346	1.346	23.5	23.5	23.5	1.364087

APPENDIX C3 Treatment depth of 10cm

Open Field								
		P1	P2	Average pressure				
Field size/cm²		101.1	101.05	101.075				
	RD1	RD2	RD3	Average reading/nC	T1	T2	Average Temp/°C	Corrected reading/nC
2×2	0.631	0.631	0.631	0.631	22.9	22.9	22.9	0.638805
4×4	0.782	0.782	0.782	0.782	22.7	22.7	22.7	0.791138
6×6	0.858	0.858	0.858	0.858	22.7	22.7	22.7	0.868026
10×10	0.956	0.956	0.956	0.956	22.6	22.6	22.6	0.966844
14×14	1.026	1.027	1.026	1.026333	22.6	22.6	22.6	1.037975
18×18	1.082	1.082	1.082	1.082	22.6	22.5	22.55	1.094088
22×22	1.125	1.126	1.125	1.125333	22.5	22.5	22.5	1.137713
15° wedge								
		P1	P2	Average pressure				
Field size/cm²		101.1	101.05	101.075				
	RD1	RD2	RD3	Average reading/nC	T1	T2	Average Temp/°C	Corrected reading/nC
2×2	0.489	0.489	0.489	0.489	22.9	22.9	22.9	0.495058
4×4	0.611	0.611	0.611	0.611	22.7	22.7	22.7	0.618152
6×6	0.662	0.662	0.662	0.662	22.7	22.7	22.7	0.669749
10×10	0.738	0.738	0.738	0.738	22.6	22.6	22.6	0.746386
14×14	0.794	0.794	0.794	0.794	22.6	22.6	22.6	0.803022
18×18	0.842	0.842	0.842	0.842	22.6	22.6	22.6	0.851568
30° wedge								
		P1	P2	Average pressure				
Field size/cm²		101.1	101.05	101.075				
	RD1	RD2	RD3	Average reading/nC	T1	T2	Average Temp/°C	Corrected reading/nC
2×2	0.414	0.414	0.414	0.414	22.9	22.8	22.85	0.419058
4×4	0.516	0.516	0.516	0.516	22.7	22.7	22.7	0.52204
6×6	0.557	0.557	0.557	0.557	22.7	22.7	22.7	0.56352
10×10	0.620	0.620	0.620	0.62	22.6	22.6	22.6	0.627045
14×14	0.667	0.667	0.667	0.667	22.6	22.6	22.6	0.674579
18×18	0.704	0.704	0.704	0.704	22.6	22.6	22.6	0.712

University of Ghana http://ugspace.ug.edu.gh

APPENDIX C3 continued

45° wedge								
		P1	P2	Average pressure				
Field size/cm²		101.1	101.05	101.075				
	RD1	RD2	RD3	Average reading/nC	T1	T2	Average Temp/°C	Corrected reading/nC
2×2	0.32	0.32	0.32	0.32	22.8	22.8	22.8	0.323855
4×4	0.396	0.396	0.396	0.396	22.8	22.7	22.75	0.400703
6×6	0.432	0.432	0.432	0.432	22.7	22.7	22.7	0.437057
10×10	0.482	0.482	0.482	0.482	22.6	22.6	22.6	0.487477
14×14	0.519	0.519	0.519	0.519	22.6	22.6	22.6	0.524897
18×18	0.556	0.556	0.556	0.556	22.6		11.3	0.540836

60 degrees wedge								
		P1	P2	Average pressure				
Field size/cm²		101.1	101.05	101.075				
	RD1	RD2	RD3	Average reading/nC	T1	T2	Average Temp/ °C	Corrected reading/nC
2×2	0.176	0.176	0.176	0.176	22.8	22.8	22.8	0.17812
4×4	0.218	0.217	0.217	0.217333	22.8	22.8	22.8	0.219952
6×6	0.235	0.235	0.235	0.235	22.7	22.7	22.7	0.237751
10×10	0.264	0.264	0.264	0.264	22.7	22.6	22.65	0.267045
14×14	0.289	0.289	0.289	0.289	22.6	22.6	22.6	0.292284
18×18	0.309	0.309	0.309	0.309	22.6	22.6	22.6	0.312511

Tray								
		P1	P2	Average pressure				
Field size/cm²		101.1	101.05	101.075				
	RD1	RD2	RD3	Average reading/nC	T1	T2	Average Temp/ °C	Corrected reading/nC
4×4	0.517	0.518	0.518	0.517667	22.8	22.8	22.8	0.757773
6×6	0.821	0.821	0.821	0.821	22.7	22.7	22.7	0.83061
10×10	0.915	0.915	0.915	0.915	22.7	22.7	22.7	0.92571
14×14	0.984	0.983	0.984	0.983667	22.6	22.6	22.6	0.994844
18×18	1.037	1.038	1.037	1.037333	22.6	22.6	22.6	1.049121
22×22	1.08	1.079	1.079	1.079333	22.5	22.5	22.5	1.091229

APPENDIX C4 Treatment depth of 15cm

Open Field								
		P1	P2	Average pressure				
Field size/cm²		101.05	101.05	101.05				
	RD1	RD2	RD3	Average reading/nC	T1	T2	Average Temp/ °C	Corrected reading/nC
2×2	0.415	0.415	0.415	0.415	22.1	22.1	22.1	0.41911
4×4	0.531	0.531	0.531	0.531	22.1	22.1	22.1	0.536259
6×6	0.583	0.583	0.583	0.583	22.2	22.2	22.2	0.588973
10×10	0.673	0.673	0.673	0.673	22.3	22.2	22.25	0.68001
14×14	0.710	0.710	0.710	0.71	22.3	22.3	22.3	0.717517
18×18	0.794	0.794	0.794	0.794	23.5	23.5	23.5	0.805665
22×22	0.837	0.837	0.837	0.837	23.5	23.5	23.5	0.849296

University of Ghana http://ugspace.ug.edu.gh

APPENDIX C4 continued

15 degrees wedge								
		P1	P2	Average pressure				
Field size/cm²		101.05	101.05	101.05				
	RD1	RD2	RD3	Average reading/nC	T1	T2	Average Temp/ °C	Corrected reading/nC
2×2	0.324	0.324	0.324	0.324	22.1	22.1	22.1	0.327209
4×4	0.411	0.411	0.411	0.411	22.1	22.1	22.1	0.41507
6×6	0.452	0.452	0.452	0.452	22.2	22.2	22.2	0.456631
10×10	0.522	0.522	0.522	0.522	22.2	22.2	22.2	0.527348
14×14	0.552	0.552	0.552	0.552	22.3	22.3	22.3	0.557844
18×18	0.620	0.620	0.620	0.62	22.5	22.4	22.45	0.626882
30 degrees wedge								
		P1	P2	Average pressure				
Field size/cm²		101.05	101.05	101.05				
	RD1	RD2	RD3	Average reading/nC	T1	T2	Average Temp/ °C	Corrected reading/nC
2×2	0.276	0.276	0.276	0.276	22.1	22.1	22.1	0.278733
4×4	0.349	0.349	0.349	0.349	22.1	22.1	22.1	0.352456
6×6	0.383	0.383	0.383	0.383	22.2	22.2	22.2	0.386924
10×10	0.44	0.44	0.44	0.44	22.2	22.2	22.2	0.444508
14×14	0.466	0.466	0.466	0.466	22.3	22.3	22.3	0.470934
18×18	0.52	0.52	0.52	0.52	22.4	22.4	22.4	0.525683
45 degrees wedge								
		P1	P2	Average pressure				
Field size/cm²		101.05	101.05	101.05				
	RD1	RD2	RD3	Average reading/nC	T1	T2	Average Temp/ °C	Corrected reading/nC
2×2	0.215	0.215	0.215	0.215	22.1	22.1	22.1	0.217129
4×4	0.271	0.271	0.271	0.271	22.1	22.1	22.1	0.273684
6×6	0.297	0.297	0.297	0.297	22.2	22.2	22.2	0.300043
10×10	0.343	0.343	0.343	0.343	22.2	22.2	22.2	0.346514
14×14	0.364	0.363	0.363	0.363333	22.3	22.3	22.3	0.36718
18×18	0.408	0.408	0.408	0.408	22.4	22.4	22.4	0.412459
60 degrees wedge								
		P1	P2	Average pressure				
Field size/cm²		101.05	101.05	101.05				
	RD1	RD2	RD3	Average reading/nC	T1	T2	Average Temp/ °C	Corrected reading/nC
2×2	0.12	0.12	0.12	0.12	22.1	22.1	22.1	0.121188
4×4	0.15	0.15	0.15	0.15	22.1	22.1	22.1	0.151485
6×6	0.165	0.165	0.165	0.165	22.2	22.2	22.2	0.16669
10×10	0.190	0.190	0.190	0.19	22.2	22.2	22.2	0.191947
14×14	0.204	0.204	0.204	0.204	22.3	22.3	22.3	0.20616
18×18	0.234	0.234	0.234	0.234	22.4	22.4	22.4	0.236557

University of Ghana http://ugspace.ug.edu.gh

APPENDIX C4 continued

Tray								
		P1	P2	Average pressure				
Field size/cm²		101.05	101.05	101.05				
	RD1	RD2	RD3	Average reading/nC	T1	T2	Average Temp/ °C	Corrected reading/nC
4×4	0.508	0.508	0.508	0.508	22.1	22.1	22.1	0.513031
6×6	0.559	0.559	0.559	0.559	22.2	22.2	22.2	0.564727
10×10	0.645	0.645	0.645	0.645	22.2	22.2	22.2	0.651608
14×14	0.680	0.680	0.680	0.68	22.3	22.3	22.3	0.687199
18×18	0.762	0.762	0.762	0.762	22.4	22.3	22.35	0.770198
22×22	0.803	0.803	0.803	0.803	22.5	22.5	22.5	0.812051

APPENDIX C5 Treatment depth of 0.5cm

Open Field								
		P1	P2	Average pressure				
Field size/cm²		101.05	101.1	101.075				
	RD1	RD2	RD3	Average reading/nC	T1	T2	Average Temp/ °C	Corrected reading/nC
2×2	0.267	0.267	0.267	0.267	22	22	22	0.269486
4×4	0.354	0.354	0.354	0.354	22	22	22	0.357296
6×6	0.392	0.392	0.392	0.392	22	22	22	0.39565
10×10	0.463	0.463	0.463	0.463	22	22	22	0.467311
14×14	0.520	0.520	0.520	0.52	21.8	21.8	21.8	0.524486
18×18	0.567	0.567	0.567	0.567	21.8	21.8	21.8	0.571892
22×22	0.593	0.593	0.593	0.593	21.7	21.7	21.7	0.597914
15 degrees wedge								
		P1	P2	Average pressure				
Field size/cm²		101.05	101.1	101.075				
	RD1	RD2	RD3	Average reading/nC	T1	T2	Average Temp/ °C	Corrected reading/nC
2×2	0.210	0.210	0.210	0.21	22	22	22	0.211955
4×4	0.277	0.277	0.277	0.277	22	22	22	0.279579
6×6	0.306	0.306	0.306	0.306	22	22	22	0.308849
10×10	0.361	0.361	0.361	0.361	22	22	22	0.364361
14×14	0.408	0.408	0.408	0.408	21.9	21.8	21.85	0.41159
18×18	0.446	0.446	0.446	0.446	21.8	21.8	21.8	0.449848
30 degrees wedge								
		P1	P2	Average pressure				
Field size/cm²		101.05	101.1	101.075				
	RD1	RD2	RD3	Average reading/nC	T1	T2	Average Temp/ °C	Corrected reading/nC
2×2	0.180	0.180	0.180	0.18	22	22	22	0.181676
4×4	0.237	0.237	0.237	0.237	22	22	22	0.239207
6×6	0.261	0.261	0.261	0.261	22	22	22	0.26343
10×10	0.306	0.306	0.306	0.306	22	21.9	21.95	0.308797
14×14	0.345	0.345	0.345	0.345	21.9	21.9	21.9	0.348095
18×18	0.375	0.375	0.375	0.375	21.8	21.8	21.8	0.378235

University of Ghana http://ugspace.ug.edu.gh

APPENDIX C5 continued

45 degrees wedge								
		P1	P2	Average pressure				
Field size/cm²		101.05	101.1	101.075				
	RD1	RD2	RD3	Average reading/nC	T1	T2	Average Temp/ °C	Corrected reading/nC
2×2	0.14	0.14	0.14	0.14	22	22	22	0.141304
4×4	0.183	0.183	0.183	0.183	22	22	22	0.184704
6×6	0.204	0.204	0.204	0.204	22	22	22	0.2059
10×10	0.240	0.240	0.240	0.24	21.9	21.9	21.9	0.242153
14×14	0.270	0.270	0.270	0.27	21.9	21.9	21.9	0.272422
18×18	0.296	0.296	0.296	0.296	21.8	21.7	21.75	0.298503
60 degrees wedge								
		P1	P2	Average pressure				
Field size/cm²		101.05	101.1	101.075				
	RD1	RD2	RD3	Average reading/nC	T1	T2	Average Temp/ °C	Corrected reading/nC
2×2	0.078	0.078	0.078	0.078	22	22	22.0	0.078726
4×4	0.105	0.105	0.105	0.105	22	22	22.0	0.105978
6×6	0.114	0.114	0.114	0.114	22	22	22.0	0.115062
10×10	0.138	0.138	0.138	0.138	21.9	21.9	21.9	0.139238
14×14	0.155	0.155	0.155	0.155	21.9	21.9	21.9	0.15639
18×18	0.167	0.167	0.167	0.167	21.7	21.7	21.7	0.168384
Tray								
		P1	P2	Average Pressure				
Field size/cm²		101.05	101.1	101.075				
	RD1	RD2	RD3	Average reading/nC	T1	T2	Average Temp/ °C	Corrected reading/nC
4×4	0.339	0.339	0.339	0.339	22	22	22	0.342157
6×6	0.375	0.375	0.375	0.375	22	22	22	0.378492
10×10	0.444	0.444	0.444	0.444	21.9	21.9	21.9	0.447983
14×14	0.499	0.498	0.498	0.498333	21.9	21.9	21.9	0.502803
18×18	0.544	0.544	0.544	0.544	21.7	21.7	21.7	0.548507
22×22	0.567	0.568	0.568	0.567667	21.7	21.7	21.7	0.57237

INTEGRI PROCEDAMUS

University of Ghana http://ugspace.ug.edu.gh

APPENDIX D **Wedge TFs at various field sizes for different wedge angles obtained from measurements using the SAD set-up**

Treatment depth of 0.5cm									
Field size /cm^2	corrected ion chamber readings /nC					Transmission Factors			
	open field	15° wedge	30° wedge	45° wedge	60° wedge	15° wedge	30° wedge	45° wedge	60° wedge
2x2	1.38276368	1.06730544	0.88910228	0.68810842	0.368882863	0.77186395	0.64298932	0.49763269	0.26677217
4x4	1.56572534	1.20393638	1.00091568	0.77255962	0.416513342	0.76893204	0.63926645	0.49341963	0.26601942
6x6	1.60396447	1.23290929	1.02691787	0.79222273	0.425490471	0.76866372	0.64023730	0.49391539	0.26527425
10x10	1.67072349	1.28616792	1.07045629	0.82740093	0.448377773	0.76982692	0.64071422	0.49523511	0.26837342
14x14	1.72511040	1.33230357	1.10856566	0.85749326	0.468656832	0.77230047	0.64260563	0.49706573	0.27166773
18x18	1.77078278	1.37132345	1.14057677	0.88554097	0.485782477	0.77441653	0.64410880	0.50008447	0.27433205
mean TFs						0.771	0.642	0.496	0.269
standard deviation						0.002	0.002	0.003	0.004
Treatment depth of 6cm									
Field Size /cm^2	corrected ion chamber readings/nC					Transmission Factors			
	open field	15° wedge	30° wedge	45° wedge	60° wedge	15° wedge	30° wedge	45° wedge	60° wedge
2X2	1.06631242	0.82258387	0.69157977	0.53518728	0.285365515	0.77142857	0.64857143	0.50190476	0.26761905
4X4	1.23814649	0.95155689	0.79245631	0.61033692	0.328018012	0.76853337	0.64003437	0.49294403	0.26492666
6X6	1.31048236	1.00775078	0.84013094	0.64711416	0.348446086	0.76899225	0.64108527	0.49379845	0.26589147
10X10	1.41515513	1.09040402	0.90902507	0.70400332	0.382985931	0.77051907	0.64235012	0.49747431	0.27063177
14X14	1.49129664	1.15278145	0.96065121	0.74310691	0.407641412	0.77300613	0.64417178	0.49829584	0.27334697
18X18	1.54976213	1.19994706	1.00266763	0.77793178	0.426011213	0.77427822	0.64698163	0.50196850	0.27488813
mean TFs						0.771	0.644	0.498	0.270
standard deviation						0.002	0.003	0.004	0.004

University of Ghana http://ugspace.ug.edu.gh

APPENDIX D continued

treatment depth of 10cm									
Field Size/cm^2	corrected ion chamber readings/nC					Transmission Factors			
	open field	15° wedge	30° wedge	45° wedge	60° wedge	15° wedge	30° wedge	45° wedge	60° wedge
2×2	0.81822268	0.63277246	0.52985777	0.4126084	0.223076706	0.77334994	0.64757161	0.50427397	0.27263569
4×4	0.97583326	0.75173794	0.62848551	0.48689801	0.262802694	0.77035491	0.64405010	0.49895616	0.26931106
6×6	1.05121078	0.81081761	0.67726527	0.52542883	0.284098148	0.77131783	0.64427162	0.49983205	0.27025802
10×10	1.16960246	0.90392252	0.75598325	0.58642667	0.320755974	0.77284595	0.64635915	0.50138974	0.27424359
14×14	1.25850174	0.97517768	0.81522551	0.63294011	0.349032893	0.77487193	0.64777464	0.50293146	0.27734002
18×18	1.32693555	1.0277645	0.86020157	0.67059089	0.370402254	0.77453988	0.64826176	0.50536810	0.27914110
mean TFs						0.773	0.646	0.502	0.274
standard deviation						0.002	0.002	0.003	0.004
Treatment depth of 15cm									
Field Size/cm^2	corrected ion chamber readings/nC					Transmission Factors			
	open field	15° wedge	30° wedge	45° wedge	60° wedge	15° wedge	30° wedge	45° wedge	60° wedge
2×2	0.59162719	0.45823104	0.38898724	0.3014142	0.164963176	0.77452668	0.65748709	0.50946644	0.27882960
4×4	0.71202449	0.54996954	0.46434079	0.36047509	0.195511912	0.77240257	0.65214160	0.50626782	0.27458594
6×6	0.77619837	0.59997486	0.50626062	0.39122071	0.213984719	0.77296588	0.65223097	0.50402156	0.27568303
10×10	0.89088278	0.69007739	0.58101051	0.45155729	0.247652421	0.77459954	0.65217391	0.50686499	0.27798542
14×14	0.98058264	0.76041024	0.63911156	0.49750994	0.278366771	0.77546778	0.65176715	0.50736156	0.28387895
18×18	1.05366033	0.81702026	0.68906474	0.53905946	0.299779599	0.77541142	0.65397236	0.51160649	0.28451256
mean TFs						0.774	0.653	0.508	0.279
standard deviation						0.001	0.002	0.003	0.004

University of Ghana http://ugspace.ug.edu.gh

APPENDIX D continued

Treatment depth of 20cm									
Field Size/cm^2	corrected ion chamber readings/nC					Transmission Factors			
	open field	15° wedge	30° wedge	45° wedge	60° wedge	15° wedge	30° wedge	45° wedge	60° wedge
2×2	0.43857457	0.34145432	0.2902899	0.22687884	0.125703142	0.77855478	0.66189407	0.51730962	0.28661749
4×4	0.53006528	0.41083466	0.34951605	0.2711645	0.150230585	0.77506427	0.65938303	0.51156812	0.28341902
6×6	0.5808967	0.44951949	0.38106993	0.29729584	0.162412841	0.77383722	0.65600291	0.51178780	0.27958988
10×10	0.67689121	0.52681126	0.44411414	0.34718177	0.193024495	0.77828054	0.65610860	0.51290630	0.28516325
14×14	0.76060928	0.59215219	0.49924556	0.39095923	0.218410644	0.77852349	0.65637584	0.51400796	0.28715222
18×18	0.82947863	0.64753067	0.54516369	0.42858467	0.238822854	0.78064781	0.65723657	0.51669164	0.28791924
mean TFs						0.777	0.658	0.514	0.285
standard deviation						0.003	0.002	0.002	0.003

University of Ghana http://ugspace.ug.edu.gh

APPENDIX E Tray TFs at various field sizes obtained from measurements using the SAD set-up

Field size/cm^2	Treatment depth of 0.5cm			Treatment depth of 6.cm			Treatment depth of 10cm			Treatment depth of 15cm			Treatment depth of 20cm		
	Open Field	Tray field	TF	Open Field	Tray	TF	Open Field	Tray field	TF	Open Field	Tray field	TF	Open Field	Tray field	TF
4×4	1.565725	1.497047	0.956136	0.529384	0.506577	0.956917	1.237938	1.197507	0.96734	0.975833	0.936862	0.960063	0.712201	0.684642	0.961305
6×6	1.604235	1.536932	0.958047	0.581408	0.557953	0.95966	1.310482	1.263521	0.964165	1.051211	1.007683	0.958592	0.77639	0.747823	0.963205
8×8	1.637585	1.572276	0.960118	0.629327	0.605019	0.961375	1.363308	1.319205	0.96765	1.110562	1.066408	0.960241	0.833448	0.8048	0.965627
10×10	1.670723	1.59543	0.954933	0.676891	0.653456	0.965378	1.416071	1.360257	0.960585	1.169602	1.122428	0.959667	0.891103	0.859453	0.964482
14×14	1.72511	1.656986	0.96051	0.760355	0.731419	0.961944	1.491297	1.436164	0.96303	1.258162	1.20761	0.959821	0.980825	0.945748	0.964237
18×18	1.770783	1.703838	0.962195	0.829479	0.797036	0.960888	1.549762	1.493857	0.963927	1.326936	1.274475	0.960465	1.053921	1.017096	0.965059
22×22	1.807917	1.741163	0.963077	0.884573	0.853269	0.96461	1.598574	1.540382	0.963598	1.37985	1.326023	0.960991	1.111055	1.071964	0.964816
26×26	1.837256	1.771834	0.964391	0.930329	0.896239	0.963356	1.633148	1.57525	0.964548	1.420315	1.366574	0.962163	1.155946	1.117951	0.967131
30×30	1.85749	1.795028	0.966373	0.965871	0.932137	0.965074	1.660884	1.603289	0.965323	1.452628	1.398134	0.962486	1.189615	1.152475	0.96878
mean TF			0.961			0.962			0.964			0.96			0.965
Standard dev.			0.004			0.003			0.002			0.001			0.002

University of Ghana http://ugspace.ug.edu.gh

APPENDIX F Wedge and Tray TF values at various field sizes obtained from measurements using the SSD set-up

APPENDIX F1 Wedge TFs for the various wedge angles at various field sizes

Treatment depth of 0.5cm									
Field size/cm^2	corrected ion chamber reading/nC					Transmission Factors			
	open field	15° wedge	30° wedge	45° wedge	60° wedge	15° wedge	30° wedge	45° wedge	60° wedge
2×2	1.42011323	1.09000364	0.90788586	0.70144065	0.37504775	0.76754699	0.63930526	0.49393291	0.26409707
4×4	1.56907572	1.20035812	0.99472715	0.76478513	0.41038711	0.765009684	0.63395739	0.48741123	0.26154704
6×6	1.60452933	1.22952694	1.02072033	0.78579263	0.42226228	0.766285115	0.63614937	0.48973404	0.26316894
10×10	1.66778411	1.27995089	1.06426296	0.82123431	0.44352729	0.767455981	0.63812993	0.49241044	0.26593807
14×14	1.72246555	1.32551876	1.09970464	0.85146947	0.46294861	0.769547325	0.63844797	0.49433179	0.2687709
18×18	1.76481855	1.36409141	1.13052439	0.87764529	0.48285675	0.77293578	0.64058959	0.49730058	0.27360136
Mean TF						0.768	0.638	0.493	0.266
standard deviation						0.003	0.002	0.003	0.004

University of Ghana http://ugspace.ug.edu.gh

APPENDIX F1 continued

Treatment depth of 6cm									
Field size/cm^2	corrected ion chamber readings in nC					Transmission Factors			
	open field	15° wedge	30° wedge	45° wedge	60° wedge	15° wedge	30° wedge	45° wedge	60° wedge
2×2	0.90954498	0.70214039	0.59253635	0.45865079	0.2488855	0.771968854	0.65146459	0.504264	0.27363737
4×4	1.09910937	0.84406742	0.7074378	0.5455064	0.29451273	0.767955801	0.64364641	0.49631676	0.2679558
6×6	1.16286986	0.89365891	0.74690858	0.57823004	0.31789762	0.768494343	0.64229765	0.49724398	0.27337335
10×10	1.25864141	0.96921653	0.80891784	0.62668353	0.34011332	0.770049772	0.64269126	0.49790474	0.27022257
14×14	1.32569549	1.02288193	0.85172644	0.6593031	0.36155331	0.77158136	0.64247517	0.49732620	0.27272727
18×18	1.37928847	1.06899641	0.88949825	0.69194454	0.38295027	0.775034688	0.64489646	0.50166775	0.27764335
Mean TF						0.771	0.645	0.499	0.273
standard deviation						0.002	0.003	0.003	0.003

Treatment depth of 10cm									
Field size/cm^2	corrected ion chamber reading/nC					Transmission Factors			
	open field	15° wedge	30° wedge	45° wedge	60° wedge	15° wedge	30° wedge	45° wedge	60° wedge
2×2	0.63880468	0.49505809	0.41905816	0.32385498	0.17812024	0.774975677	0.65600358	0.50697027	0.27883365
4×4	0.79113763	0.61815171	0.52203974	0.40070285	0.21995151	0.781345346	0.65985957	0.50648943	0.27801927
6×6	0.86802569	0.66974866	0.56351964	0.43705653	0.23775066	0.771577001	0.64919696	0.50350644	0.27389818
10×10	0.96684395	0.7463859	0.62704507	0.48747697	0.26704497	0.771981765	0.64854837	0.50419405	0.27620276
14×14	1.03797508	0.80302223	0.67457913	0.5248974	0.29228391	0.773643072	0.64989915	0.50569365	0.28159049
18×18	1.09408821	0.85156766	0.71199956	0.54083646	0.31251117	0.778335465	0.65076979	0.49432619	0.28563617
Mean TF						0.775	0.652	0.504	0.279
standard deviation						0.003	0.004	0.004	0.004

University of Ghana http://ugspace.ug.edu.gh

APPENDIX F1 continued

Treatment depth of 15cm									
Field size/cm^2	corrected ion chamber readings/nC					Transmission Factors			
	open field	15° wedge	30° wedge	45° wedge	60° wedge	15° wedge	30° wedge	45° wedge	60° wedge
2×2	0.41910985	0.32720866	0.2787333	0.2171292	0.12118839	0.780722892	0.66506024	0.51807229	0.28915663
4×4	0.53625863	0.41507024	0.35245624	0.27368378	0.15148549	0.774011299	0.65725047	0.51035782	0.28248588
6×6	0.58897298	0.45663086	0.38692393	0.30004284	0.16669047	0.775300172	0.65694683	0.50943396	0.28301887
10×10	0.68001014	0.52734802	0.44450791	0.34651412	0.1919466	0.775500238	0.65367836	0.509572	0.2822702
14×14	0.71751695	0.55784416	0.47093366	0.36718003	0.2061598	0.777464789	0.65633803	0.51173709	0.28732394
18×18	0.80566478	0.62688215	0.5256832	0.41245913	0.23655744	0.778093028	0.65248379	0.51194882	0.2936177
Mean TF						0.777	0.657	0.512	0.286
standard deviation						0.002	0.004	0.003	0.004
Treatment depth of 20cm									
Field size/cm^2	corrected ion chamber reading/nC					Transmission Factors			
	open field	15° wedge	30° wedge	45° wedge	60° wedge	15° wedge	30° wedge	45° wedge	60° wedge
2×2	0.26948619	0.21195543	0.18167608	0.14130362	0.0787263	0.78651685	0.67415730	0.52434457	0.29213483
4×4	0.35729629	0.2795793	0.23920684	0.18470402	0.10597771	0.78248588	0.66949153	0.51694915	0.29661017
6×6	0.39565013	0.30884934	0.26343032	0.20589956	0.11506152	0.78061224	0.66581633	0.52040816	0.29081633
10×10	0.46731125	0.36436147	0.30879703	0.24215272	0.13923781	0.77969762	0.66079519	0.51818294	0.29795519
14×14	0.52448643	0.41158987	0.34809453	0.27242181	0.1563903	0.78474837	0.66368644	0.51940678	0.29817797
18×18	0.57189193	0.44984798	0.37823541	0.29850321	0.16838374	0.78659612	0.66137566	0.52195737	0.29443279
Mean TF						0.783	0.666	0.520	0.295
Standard deviation						0.003	0.005	0.002	0.003

University of Ghana http://ugspace.ug.edu.gh

APPENDIX F2 Tray TFs for the various wedge angles at various field sizes

Field size/cm^2	depth of 0.5cm			depth of 6cm			depth of 10cm		
	open field	Tray field	TF	open field	Tray field	TF	open field	Tray field	TF
4×4	1.42011323	1.501207	0.956746	0.90954498	1.05053	0.955801	0.63880468	0.757773	0.957827
6×6	1.56907572	1.533106	0.955486	1.09910937	1.113466	0.957516	0.79113763	0.83061	0.956895
10×10	1.60452933	1.595888	0.956891	1.16286986	1.205377	0.957681	0.86802569	0.92571	0.957455
14×14	1.66778411	1.651231	0.958644	1.25864141	1.271221	0.958909	0.96684395	0.994844	0.958447
18×18	1.72246555	1.691517	0.958465	1.32569549	1.32209	0.958531	1.03797508	1.049121	0.958899
22×22	1.76481855	1.727714	0.958637	1.37928847	1.364087	0.960057	1.09408821	1.091229	0.959142
Mean TF			0.957			0.958			0.958111
standard dev.			0.001			0.001			0.00087

University of Ghana http://ugspace.ug.edu.gh

APPENDIX F2 continued

	depth of 20cm			depth of 15cm		
Field size/cm^2	open field	Tray field	TF	open field	Tray field	TF
4×4	0.26948619	0.342157	0.957627	0.41910985	0.513031	0.956686
6×6	0.35729629	0.378492	0.956633	0.53625863	0.564727	0.958834
10×10	0.39565013	0.447983	0.958638	0.58897298	0.651608	0.958233
14×14	0.46731125	0.502803	0.958658	0.68001014	0.687199	0.957746
18×18	0.52448643	0.548507	0.95911	0.71751695	0.770198	0.955978
22×22	0.57189193	0.57237	0.957279	0.80566478	0.812051	0.956145
Mean TF			0.958			0.957
Standard dev.			0.001			0.001